

**DEVELOPMENT OF AN ENERGY EFFICIENT STAND-ALONE
SOLAR PHOTOVOLTAIC DC REFRIGERATOR FOR OFF-GRID COMMUNITIES**

By
KNUST

SOLOMON KOFI ANANE,

(Bsc. Agricultural Engineering)

A Thesis submitted to the

School of Graduate Studies,

Kwame Nkrumah University of Science and Technology, Kumasi, Ghana

In partial fulfillment of the requirements for the Degree of

MASTER OF SCIENCE IN MECHANICAL ENGINEERING

Department of Mechanical Engineering

College of Engineering

OCTOBER, 2015

STUDENT'S DECLARATION

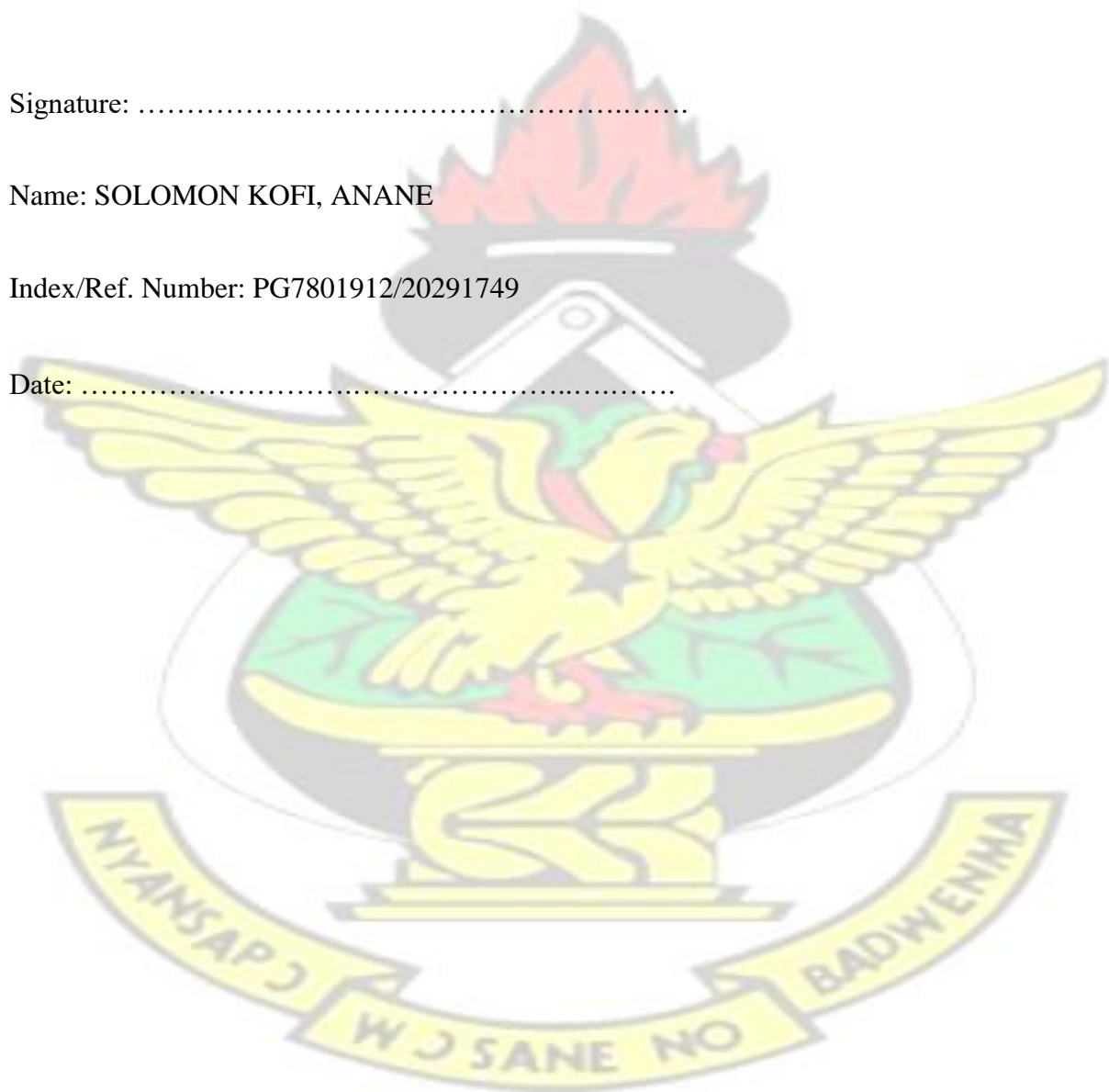
I hereby declare that all information in this document has been obtained and presented in accordance with academic rules and ethical conduct. I also declare that, as required by these rules and conduct, I have fully cited and referenced all material and results that are not original to this work.

Signature:

Name: SOLOMON KOFI, ANANE

Index/Ref. Number: PG7801912/20291749

Date:



KNUST

CERTIFICATION

This is to certify that we have read this thesis and that in our opinion, it is fully adequate, in scope and quality, as a thesis for the degree of Master of Science.

DR. RICHARD OPOKU

(First Supervisor)

Signature

Date

Department of Mechanical Engineering

KNUST

DR. GABRIEL TAKYI

(Second Supervisor)

Signature

Date

Department of Mechanical Engineering

KNUST

I certify that this thesis has been assessed and all corrections have been made in accordance with the comments made by the examiners.

PROF. FRANCIS K.FORSON

(Head of Department)

Signature

Date

Department of Mechanical Engineering

KNUST



KNUST



ABSTRACT

A reliable and energy efficient approach to providing refrigeration needs (both grid connected and off-grid areas) is a major challenge in Ghana and most developing countries due to low energy access and unreliable power supply. Research and development of appropriate and sustainable stand-alone refrigeration technologies are therefore relevant and essential.

In the current study, the methodology of converting an AC refrigerator to serve as a DC refrigerator has been explored. A 92 L stand-alone solar powered DC refrigerator operating with a Variable Speed Direct Current (VSDC) compressor has been developed. The design replaces the single speed alternating current (AC) compressor with a VSDC compressor.

VSDC compressors are strong candidates to be employed in energy-efficient refrigeration systems, especially for renewable energy technologies, as these compressors do not require power inverters that an alternating current compressor would require. Secondly, these compressors present the option of matching the cooling requirements with refrigerator power consumption thereby reducing wastage of energy.

In this study, the DC refrigerator is powered by an installed 170 Watt peak (Wp) solar PV panel, 20 A charge controller and a 100 AH battery bank without an inverter. By using the coefficient of performance and the pull down time as indicating factors, the developed refrigerator has been experimentally optimised with the correct amount of refrigerant charge using ISO test standard. The performance (in terms of evaporator temperature profile and energy consumption) of the DC refrigerator has been evaluated at various speeds of the VSDC compressor.

Similarly, the performance of the solar powered DC refrigerator has been experimentally compared with an identical AC refrigerator operating on the national grid.

The experimental results revealed that the 92 L DC refrigerator performed optimally when charged with 30 g of refrigerant 134a. This yielded an average coefficient of performance of 1.6 W/W and attained a pull down temperature of -12 °C in 20 minutes. Secondly, operating the refrigerator at lower speeds (2000RPM, 2500RPM and 3000RPM) of the VSDC compressor during high (positive) temperature settings presented the potential of saving 19 % to 44 % of the refrigerator's energy consumption. It has also been observed that the AC refrigerator is associated with relatively high power consumption and power surges as compared to the developed DC refrigerator. Finally, an economic assessment conducted between the AC (with inverter) and the developed DC refrigerator (without an inverter) all powered by solar PV system indicates that converting an AC refrigerator to DC has the

potential of reducing the overall system cost (refrigerator, battery, charge controller and solar panel) by 20 %.

Keywords::

Variable Speed, Direct Current, Compressor, Stand-Alone Solar PV, Refrigeration, Energy Savings,



KNUST



ACKNOWLEDGEMENT

I am very grateful to the Almighty God for His strength, the gift of knowledge and perseverance that have made this master's thesis possible.

I also express my heartfelt gratitude to Dr Richard Opoku and Dr Gabriel Takyi my major supervisors for their keen support throughout this study. This work would not have been completed without your patience, encouragement and constructive criticism. In fact, I could

never have wished for a better supervision than what you provided me. I am forever indebted to you.

Thirdly, I wish to express my profound gratitude to Mr Isaac A. Edwin. and Mr Kyere Robert for making the solar lab accessible for me always. Thank you, Mr Edwin for providing me with the various instruments I requested. Thank you for your patience and all that you sacrificed for me. I say may God richly bless you. A big thank you also goes to Dr Tamakloe of Physics Department, Mr Ackarh of Electrical Engineering Department all of KNUST for the support they gave me.

I wish to express my special appreciation to Mr Isaac Badu Amankwah for the financial support and motivation you gave me. I am forever grateful to you.

I am also grateful to the youth wing of Dunwel Methodist Church, Santamaria, Accra, for their continuous prayer and support. Not forgetting my course mates and senior course mates for their guidance and encouragement. I say thank you.

My final thank you goes to my family and friends; Asamoh Yaw, Elizabeth Krah, Doris Kuma, Robert Obour, and Dr and Mrs Effah Ameyaw for their continuous support, love and encouragement. I couldn't have made it this far without you by my side, I am forever grateful to you all. For all who expressed concern and offered help, I say God richly bless you.

KNUST

DEDICATION

I dedicate this master's thesis with the deepest love and respect to my parents, Mr and Mrs Tawiah-Acheampong & my uncle, Mr Isaac Badu Amankwah for their continuous support and encouragement.



TABLE OF CONTENTS

ABSTRACT	vi
ACKNOWLEDGEMENT	ix
DEDICATION.....	xi
LIST OF FIGURES.....	xvi
LIST OF TABLES.....	xx

Chapter 1 INTRODUCTION 1

1.1 BACKGROUND	1
1.2 PROBLEM STATEMENT	2
1.3 THE SPECIFIC OBJECTIVES	3
1.4 JUSTIFICATION	4
1.5 SCOPE OF THESIS	6
1.6 THESIS ORGANIZATION	6

Chapter 2 LITERATURE REVIEW 8

2.0. INTRODUCTION	8
2.1 REFRIGERATION	8
2.2 TYPES OF REFRIGERATION CYCLES	9
2.3 FUNDAMENTALS OF VAPOUR COMPRESSION REFRIGERATION SYSTEM	10
2.3.1 Refrigerator Compressors	11
2.3.2 AC and DC Refrigerator Compressors	11
2.3.3. Capacity Control of Refrigerator Compressors	12
2.3.4. Capacity Control Methods	13

2.3.4.1. ON and OFF Capacity Control (Constant Speed AC Compressors)	13
2.3.4.2. Variable Speed Control (VSDC Compressors)	15
2.4. SOLAR ELECTRIC REFRIGERATION	19
2.4.1. Types of Solar Electric Refrigerators	21
2.4.1.1. Commercial Solar Refrigerators (Without Inverter)	22
2.4.1.2. Conventional Refrigerators Powered by Solar Energy via an Inverter	24
2.4.1.3. Conventional AC Refrigerator Converted to Serve as a DC Refrigerator	25
2.4.2. Future of Solar Powered Refrigerators.....	26
2.4.3. Summary of Modes of Powering VCRS with Solar Energy	27
2.5. PERFORMANCE ANALYSIS OF VAPOUR COMPRESSION SYSTEMS	28
2.5.1. Refrigerator Test Standards	28
2.5.2. Performance Analysis of Compressors	30
2.5.3. Theoretical Analysis of Vapour Compression Systems	31
2.6. SOLAR ENERGY POTENTIAL OF GHANA	34
2.7. COMPONENTS OF OFF-GRID PV SYSTEM WITH BATTERY BACKUP ...	38
2.7.1. Solar Modules and Types	39
2.7.2. Charge Control Unit/ Charge Regulator.....	40
2.7.3. Solar Batteries	41
2.7.4. Types of Solar Batteries	44
2.7.4.1. Flooded Lead Acid (FLA)	44
2.7.4.2. Gelled Electrolyte Sealed Lead Acid (GEL)	45
2.7.4.3. Sealed Absorbed Glass Mat (AGM)	45
Chapter 3 MATERIALS AND METHODS	47
3.0. INTRODUCTION	47
3.1. CONVERTING AN AC REFRIGERATOR TO DC REFRIGERATOR.....	48

3.1.1. Assessment of the Selected AC Refrigerator to be Converted	48
3.1.2. Selecting a Variable Speed Direct Current Compressor	49
3.1.3. Description of VSDC Compressor (BD 35F) and Electronic Control Unit ...	51
3.1.4. Conversion of a 92 L AC Refrigerator to DC Refrigerator.....	52
3.2. DESIGNING A STAND-ALONE SOLAR PV SYSTEM FOR THE CONVERTED SOLAR POWERED DC REFRIGERATOR	53
3.2.1. Solar Resource Assessment of Selected Site (KNUST-Kumasi)	54
3.2.2. Solar PV System Component Selection	55
3.2.2.1. Sizing Battery Bank (AH)	56
3.2.2.2. Sizing Solar PV Panel	58
3.2.2.3. Sizing Charge Controller	58
3.2.3. Parametric Study	59
3.2.4. Preliminary Results of Parametric Study	60
3.3. EXPERIMENTAL AND THEORETICAL FORMULATION	61
3.3.1. Formulation of Experimental Set-up	62
3.3.1.1. AC Refrigerator	62
3.3.1.2. Solar Powered DC Refrigerator	62
3.3.1.3. Power Supply (Solar PV System and the Grid)	65
3.3.1.4. Measuring Instruments	66
3.3.1.5. System Evacuation	70
3.3.1.6. System Charging.....	70
3.3.1.7. Leakage Testing	71
3.3.1.8. Data Acquisition System	71
3.3.2. Experiments Performed and Test Procedure	73
3.3.2.1. Effect of Refrigerant Charge on Performance of the DC Refrigerator	74
3.3.2.2. Performance Characteristics of the Solar Powered DC Refrigerator Operating at Varying Compressor Speed	80
3.3.2.3. Comparing the Performance of the Solar Powered DC Refrigerator to an Identical AC Refrigerator	82

3.3.3.	Economic Assessment of the Developed DC Refrigerator and AC Refrigerator Running on Inverter all Powered by Solar PV	86
--------	--	----

Chapter 4 RESULTS AND DISCUSSIONS 87

4.0.	INTRODUCTION	87
4.1	EFFECT OF REFRIGERANT CHARGE ON THE PERFORMANCE OF THE SOLAR POWERED DC REFRIGERATOR	88
4.1.1.	Effect of Refrigerant Charge on Pull-down Time of the Solar Powered DC Refrigerator	88
4.1.2.	Effect of Refrigerant Charge on Cooling Capacity (Q_{ref}), Power Consumption (P_{in}), and COP of the Solar Powered DC Refrigerator	90
4.2	PERFORMANCE CHARACTERISTICS OF THE SOLAR POWERED DC REFRIGERATOR AT VARYING COMPRESSOR SPEEDS	95
4.2.1.	Evaporator Temperature Profile of the Solar Powered DC Refrigerator Operating at Low Temperature Settings (“cut out” Temperature of -20 °C)	96
4.2.2.	Power Consumption of the Solar Powered DC Refrigerator Operating at Low Temperature Settings (“cut-out” Temperature of -20 °C)	98
4.2.3.	Evaporator Temperature Profile of the Solar Powered DC Refrigerator Operating at High Temperature Settings (“cut out” temperature of -5 °C)	101
4.2.4.	Power Consumption of the Solar Powered DC Refrigerator Operating at High Temperature Settings	102
4.2.5.	Energy Analysis of the Solar Powered DC Refrigerator Operating at High Temperature Settings	104
4.2.6.	Maximum Energy Consumption of the Solar Powered DC Refrigerator	108
4.3.	PERFORMANCE COMPARISON OF THE SOLAR POWERED DC REFRIGERATOR AND A CONVENTIONAL AC REFRIGERATOR	110

4.3.1. Evaporator and Cabinet Temperature Characteristics of AC and Solar Powered DC Refrigerators	110
4.3.2. Power Consumption of AC and Solar Powered DC Refrigerators	112
4.3.3. Energy Consumption of AC and Solar Powered DC Refrigerators	114
4.3.4. Comparing the Coefficient of Performance of the Conventional and Solar Powered DC Refrigerator	116
4.3.5. Economic Comparison of on AC Refrigerator and DC Refrigerator all Powered by Solar PV System	116
Chapter 5 CONCLUSIONS AND RECOMMENDATIONS	119
REFERENCES	124
 LIST OF FIGURES	
PAGE Figure 1.1: Electricity Consumption in Ghana	5
Figure 2.1: Schematic view of a refrigerator with various components and their locations	9
Figure 2.2: Schematic of Hermetic Refrigerator Compressor	11
Figure 2.3: Fixed Speed Design Rules	12
Figure 2.4: Relationship between motor power reduction and rated speed	16
Figure 2.5: Comparison of various capacity control techniques at half load	18
Figure 2.6: Operation of Variable and a Single Speed Compressor	19
Figure 2.7: A Schematic Diagram of a Solar Powered DC Refrigerator	22
Figure 2.8: Summary of Reviewed Literature on Powering Vapour Compression Systems with Solar PV Electricity	28
Figure 2.9: T-s and P-h diagram of Vapour compression refrigeration system.....	32
Figure 2.10: Solar Map of Ghana	35
Figure 2.11: Peak Sun Hours	36

Figure 2.12 Types of Solar Modules.....	40
Figure 2.13: Relationship Between Number of Cycles and Daily Depth of Discharge	44
Figure 2.14: A 12 Volts Flooded Lead Acid Battery	45
Figure 2.15: A 12V Absorbed Glass Mat Battery.....	46
Figure 3.1: Schematic of the methodology of converting a conventional AC refrigerator to solar refrigerator.....	47
Figure 3.2: Variable Speed Direct Current Compressor (VSDC).....	51
Figure 3.3: Electronic Control Unit for VSDC Compressor BD 35F	51
Figure 3.4: Schematic of the DC Refrigerator Connected to 12 Volts Solar Battery	53
Figure 3.5: Schematic of the Solar Powered DC Refrigeration System	54
Figure 3.6: Temperature Correction Graph	57
Figure 3.7: Peak Wattage of Solar Panel versus Refrigerator Power Consumption	60
Figure 3.8: Size of Battery Bank versus Refrigerator Power Consumption	60
Figure 3.9: Wiring Diagram of Electronic Control Unit of BD 35F Compressor,	64
Figure 3.10: Resistors connected to the Electronic Control Unit of the VSDC Compressor ..	64
Figure 3.11: Connecting the Solar PV System to the DC Refrigerator	66
Figure 3.12: Connection of AC and DC Power Measurement Instruments	68
Figure 3.13: Schematic Diagram of the Fabricated Cross Fitting for Connecting the Thermocouples and Pressure Gauges to the Refrigeration Line	69
Figure 3.14: Location of Pressure Gauges and Thermocouples	69
Figure 3.15: Evacuation and Charging of the Refrigeration System	71
Figure 3.16: Thermocouples and Pressure Gauges Connected to Data Logger	72
Figure 3.17: Photograph of the Complete Experimental Set-Up	72
Figure 3.18: List of Experiments Performed	73
Figure 3.19: Schematic Diagram of the Experimental Set-up	74

Figure 3.20: Pressure - Specific Entropy Diagram (R134a)	77
Figure 3.21: Experimental set Up for comparing the Performance of the Solar Powered DC refrigerator with a conventional AC refrigerator	82
Figure 3.22: Schematic diagram of experimental set-up formulated to study the performance of AC and solar powered DC refrigerator	84
Figure 4.1: Variation of Pull-down Time with Respect to Amount of Refrigerant Charge	89
Figure 4.2: Overall performance characteristics of the solar powered DC refrigerator with different quantities of refrigerant charge	91
Figure 4.3: Variation of Discharge Temperature with Increasing Levels of Refrigerant Charge	92
Figure 4.4: Variation of Density of Refrigerant Entering the Compressor With Increasing Levels of Refrigerant Charge	92
Figure 4.5: Variation of Refrigerant Mass Flow Rate with the Amount of Refrigerant Charge	94
Figure 4.6: Effects of Refrigerant Charge on Compressor Discharge Pressure	94
Figure 4.7: Evaporator Temperature Profile of the Solar Powered DC Refrigerator Operating at Low Back Pressure.....	97
Figure 4.8: Instantaneous Power Consumption of the Solar Powered DC Refrigerator Operating at Low Temperature Settings	99
Figure 4.9: Formation of Ice by the Solar Powered DC Refrigerator Operating at Low Speeds	100
Figure 4.10: Pull Down and Cycling Characteristics of the Solar Powered DC Refrigerator operating at high temperature settings	101
Figure 4.11: Power consumption of the solar powered DC refrigerator Operating at high	

temperature setting	103
---------------------------	-----

Figure 4.12: Compressor Run Time of the Solar Powered DC Refrigerator Operating at 2000

RPM	104
-----------	-----

Figure 4.13 Compressor Run Time of the Solar Powered DC Refrigerator Operating at

2500RPM	104
---------------	-----

Figure 4.14 Compressor Run Time of the Solar Powered DC Refrigerator Operating at

3000RPM	105
---------------	-----

Figure 4.15 Compressor Run Time of the Solar Powered DC Refrigerator Operating at

3500RPM	105
---------------	-----

Figure 4.16: Compressor Run Time of the Refrigerator Operating at Different Compressor

Speeds	106
--------------	-----

Figure 4.17: Average Power Consumption of the Refrigerator Operating at Different

Compressor Speeds	106
-------------------------	-----

Figure 4.18 Daily Energy Consumption of the Solar Refrigerator Operating at Different

Speeds	107
--------------	-----

Figure 4.19 Annual Energy Consumption of the Refrigerator Operating at Different Speeds

.....	107
-------	-----

Figure 4.20 Energy Consumption and Energy Savings of the Refrigerator Operating at

Different Speeds.....	107
-----------------------	-----

Figure 4.21 Percentage Energy Consumption and Energy Savings of the DC Refrigerator

Operating at Different Speeds	107
Figure 4.22: Temperature Profile of the Refrigerator Operating at 3500 RPM	109
Figure 4.23: Compressor Run time of the refrigerator operating at 3500 RPM	109
Figure 4.24: Pull Down and Cycling Characteristics of AC and Solar Powered DC Refrigerators (Both Operating at 3000 RPM)	111
Figure 4.25: Comparing Power Consumption of the AC Refrigerator with the Solar Powered DC Refrigerator all Operating at 3000 RPM	112
Figure 4.26: Compressor Run Time of AC Refrigerator	114
Figure 4.27 Compressor Run Time of the Solar Powered DC Refrigerator Operating at 3000 RPM	114
Figure 4.28: Daily Energy Requirement of the Refrigerator and Size of Solar Panel Required	117
Figure 4.29: Daily Energy Requirement of Refrigerator versus Battery Capacity	117

LIST OF TABLES

PAGE Table 2.1: Summary of Test Conditions	30
Table 2.2: Summary of Refrigerator Test Conditions	31
Table 2.3: 10 - Year Monthly Averages of Peak Sun Hours (hours/day) at 19 Synoptic Stations	37
Table 2.4: Peak Sun Hours (Hours/Day) Data for KNUST	38
Table 2.5: Recommended Days of Autonomy for Storage	42
Table 2.6: Battery Design Temperature Correction Factor	43
Table 3.1: Technical specifications of Selected AC Refrigerators.	49

Table 3.2: Cooling capacities of Danfoss BD50F compressor	50
Table 3.3: Cooling Capacities of Danfoss BD35F Compressor	50
Table 3.4: Performance data of BD 35F VSDC compressor at STCs	52
Table 3.6: Design parameters and equation for parametric study	59
Table 3.7: Technical Specification of Variable Speed DC Compressor	63
Table 3.8: Sizes of Resistors used for Controlling the Speed of the VSDC Compressor.....	63
Table 3.9: Panel specifications (photovoltaic module catalogue)	66
Table 3.10: Specifications of the Installed PV Model	66
Table 3.11: Characteristics of the Instrumentation used	67
Table 4.1: COP Values of the selected compressor,	95
Table 4.2: Sizes of the Solar Photovoltaic System	110
Table 4.3: Energy Analysis of AC and Solar Powered Refrigerators.....	115
Table 4.4: Economic Analysis of Direct Solar Refrigerator and Operating AC Refrigerator on Solar via an Inverter	118

CHAPTER 1 INTRODUCTION

1.1 BACKGROUND

The overall goal of this work is to develop an energy efficient stand-alone solar photovoltaic DC refrigerator for off-grid communities. This concept seeks to change the over-dependence of currently available domestic refrigerators on the national grid. This will provide opportunity for off-grid refrigeration or locations where refrigeration is critical, but grid electricity is non-reliable.

The present study focuses on the design considerations of converting a domestic/conventional AC refrigerator to serve as a solar powered DC refrigerator. A domestic refrigerator with single speed AC compressor was converted to solar powered DC refrigerator. This was done by replacing the single speed AC compressor of the domestic refrigerator with a variable speed direct current (VSDC) compressor and then powered with a stand-alone solar PV system without an inverter.

Variable speed direct current compressors are strong candidates to be employed in energyefficient refrigeration systems, especially for renewable energy powered units. These VSDC compressors do not require power inverters that an alternating current compressor would need. This ensures a significant decrease in the initial cost and inefficiencies of the solar PV system. Secondly, VSDC compressors are capable of matching the compressor work to the cooling requirement in the cooling compartment thereby reducing wastage of energy. This control strategy would not only ensure better temperature management in the refrigerator cabinet, but decrease in refrigerator power consumption due to a reduction in the average speed of the compressor and fewer stops during part-loading.

The success of this research would go a long way to reduce current challenges in the energy sector, thus; reduction in demand on the national grid, decrease in energy related environmental challenges,

enhanced refrigeration in remote communities and a solution to individuals/institutions requiring reliable refrigeration (hospitals, clinics, cold stores and small businesses).

1.2 PROBLEM STATEMENT

The electricity sector of Ghana is characterised by significant challenges ranging from low energy access rates, erratic power supply to insufficient generation capacity to meet rapidly rising demand. Therefore, the supply of reliable electricity for refrigeration of temperature sensitive items such as vaccines and perishable products has always remained a challenge. Hospitals, clinics, cold store operators, as well as individuals relying on the national grid for meeting their refrigeration needs have to seek alternate sources of energy or risk losing their products in the event of a power outage.

For off-grid communities in Ghana and other Sub-Saharan African countries where energy access is a challenge, but renewable energy resources are in abundance, generation of power from these renewable energy resources has been identified as an option. (Brew-Hammond, Edjekumhene, & Amadu, 2001), (Miller et al. 2011), (Alanne & Saari, 2006), (Suberu, Mustafa, & Bashir, 2013).

According to Ghana Energy Commission, household refrigerators account for 54.4% of residential energy consumption in Ghana. In addition, many of the isolated remote/rural communities do not have access to the national grid.

Currently, many individuals and small businesses who seek alternate solutions for their refrigeration needs (with the on-going energy challenges) power their refrigerators with solar energy via inverters. This approach poses three main challenges; (i) high cost of power inverters, (ii) DC-to-AC conversion losses, and (iii) poor capacity control of the single speed AC compressor which translates into high power consumption.

Therefore, the specific problems are high initial cost when running the refrigerator with solar PV via an inverter and high operation cost due to high system power consumption (refrigerator power consumption plus inverter power requirement).

1.3 THE SPECIFIC OBJECTIVES

The overall goal of this work is to develop an energy efficient stand-alone solar photovoltaic DC refrigerator for off-grid communities. The specific objectives developed for this study are:

- To develop the design considerations of converting a conventional AC refrigerator to a stand-alone solar powered DC refrigerator.

This involves the technical procedure of assessing an AC refrigerator to be converted to DC refrigerator, VSDC compressor selection, conversion procedure and the design of a standalone solar PV system for harnessing energy from the sun for powering the refrigerator.

- To determine the optimum amount of refrigerant charge required by the solar powered DC refrigerator after the conversion.

This involves conducting a parametric study to determine the optimum amount of refrigerant level required by the converted solar powered DC refrigerator. The optimum amount of refrigerant charge would be determined experimentally by charging the refrigerator with different amount of refrigerant and evaluating the performance of the entire system using the coefficient of performance, cooling capacity of a refrigerator and the corresponding compressor work. Based on these performance parameters the optimum amount of refrigerant would be selected.

- To compare the performance of the solar powered DC refrigerator to an identical AC refrigerator running on the national grid.

The performance of the solar powered DC refrigerator would be compared with an identical AC refrigerator in terms of pull-down time, evaporator and cabinet temperature profile, power consumption and the percentage compressor run time. These parameters represent a simple approach to determining how the DC refrigerator performs compared to an identical AC refrigerator.

- To investigate the performance of the solar powered DC refrigerator at selected speeds of the variable speed DC compressor.

The consumption, evaporator and cabinet temperatures of the refrigerator would be determined at various compressor speeds. Other performance parameters such as pull-down time, percentage compressor run time, average power consumption and evaporator temperature profiles of the refrigerator would also be determined.

- To perform an economic analysis of the DC refrigerator (without an inverter) and an AC refrigerator (with an inverter) both powered by a solar PV system.

The total investment cost of the solar powered DC refrigeration system includes the cost of the AC refrigerator, cost of solar PV system, cost of VSDC compressor and accessories and conversion cost. On the other hand, the cost of an AC refrigeration system would include the cost of the solar PV system, cost of inverter and cost of AC refrigerator.

1.4 JUSTIFICATION

In recent times, refrigeration has become indispensable in human life, but the high power consumption of refrigerators has always remained a big challenge to various nations. In Ghana, domestic refrigerators stand as the highest energy consuming appliance in the residential sector. According to the Energy Commission, household refrigerators account for more than 54.4% (as shown in Figure 1.1) of residential power consumption (AhiatakuTogobo, 2014). This

means that improvement (reduction) in the power consumption of these refrigerators or providing alternative means of powering them will have the potential of reducing the burden on the national grid.

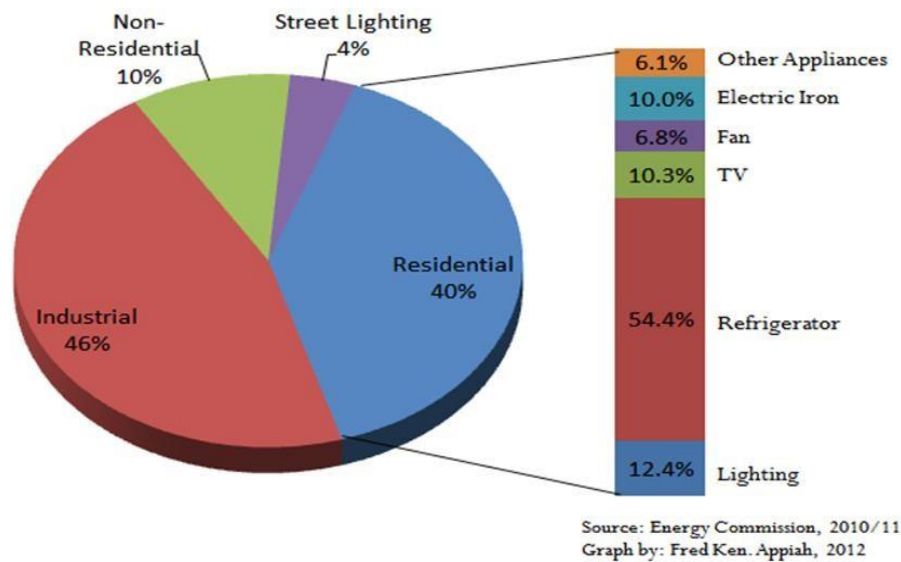


Figure 1.1: Electricity Consumption in Ghana

Source: (Ahiataku-Togobo, 2014)

Ghana over the past decade has been hit with serious energy challenges. Individuals and small business have therefore been seeking alternative energy to power their appliances/equipment. Currently, many individuals and small businesses who seek alternate solutions for their refrigeration needs (with the on-going energy challenges), in particular, power their refrigerators with solar energy via inverters. This approach poses three main challenges; (i) high cost of power inverters, (ii) DC-to-AC conversion losses, and (iii) poor capacity control of the single speed AC compressor which translates into high power consumption.

There is therefore the need to design an appropriate refrigerator that will be independent of the national grid in terms of power requirement. In addition, the designed refrigerator that uses a VSDC compressor (low power consumption and better capacity control) powered by a solar PV system without an inverter has huge potential for energy savings.

1.5 SCOPE OF THESIS

The scope of this MSc thesis is to develop the methodology of converting a domestic (AC) refrigerator to a stand-alone solar powered (DC) refrigerator with a battery backup without an inverter. The major considerations involve the selection of an appropriate VSDC compressor as a replacement for the AC compressor on a selected domestic refrigerator. The study also involves the design of a stand-alone solar PV system for powering the converted refrigerator. As a case study, the design considerations developed were used to convert a 92 L AC refrigerator to serve as a solar powered DC refrigerator. This research work was conducted at the solar energy application laboratory at the Department of Mechanical Engineering, KNUST.

1.6 THESIS ORGANIZATION

The thesis is organised into five chapters. The first chapter introduces the project topic. The chapter includes background of the study, the objectives, justification of the work and scope of the thesis.

Chapter 2 presents the literature review of this research work. The chapter is made up of three main sections; the first section covers a review of the fundamentals of the vapour compression refrigeration system (VCRS). The technology of powering VCRS with DC compressor with direct current from the solar energy was also reviewed. Review of refrigeration capacity control methods and variable speed DC compressor selection was also conducted. The second section looks at refrigerator performance analysis tests, required test standards, refrigerator test rig formation and a review of similar works by other authors on the research objectives. The final section reviews the solar energy potential of Ghana, a review of the design of a stand-alone solar PV system and components selection.

Chapter three presents the proposed methodology of converting AC refrigerator to serve as a solar powered DC refrigerator. The design of a stand-alone solar PV system to power the DC

refrigerator is also presented in this chapter. The chapter also includes description of experimental setup for this research work.

Results obtained from the experimental study are analysed and discussed in chapter four. The various findings of both refrigerators were discussed and compared to similar studies in the open literature. The thesis ends with the conclusion and recommendation which are presented in chapter five.



CHAPTER 2 LITERATURE REVIEW

2.0.INTRODUCTION

This section presents the literature on the technology of combining the vapour compression refrigeration system with a solar photovoltaic system for the purpose of providing domestic refrigeration. The chapter begins with a general review of the fundamentals of the vapour compression refrigeration system (VCRS) in relation to domestic refrigeration. Measures of reducing refrigerator power consumption were also reviewed, especially by employing variable speed compressors as opposed to single speed compressors. The review focuses much on the use of a VSDC compressor as a means of reducing energy consumption of VCRSs especially when powered by direct current from solar PV source. The final section of the chapter reviews the literature on solar energy potential and the design considerations of sizing a stand-alone solar photovoltaic system (SPVS) for powering refrigerators.

2.1 REFRIGERATION

Refrigeration is the process of removing heat from the space to be cooled and transferring it to the immediate surrounding. The primary purpose of all refrigeration systems is producing and maintaining a temperature which is lower than that of the surroundings. A schematic of a typical refrigeration system is shown in Figure 2.1.

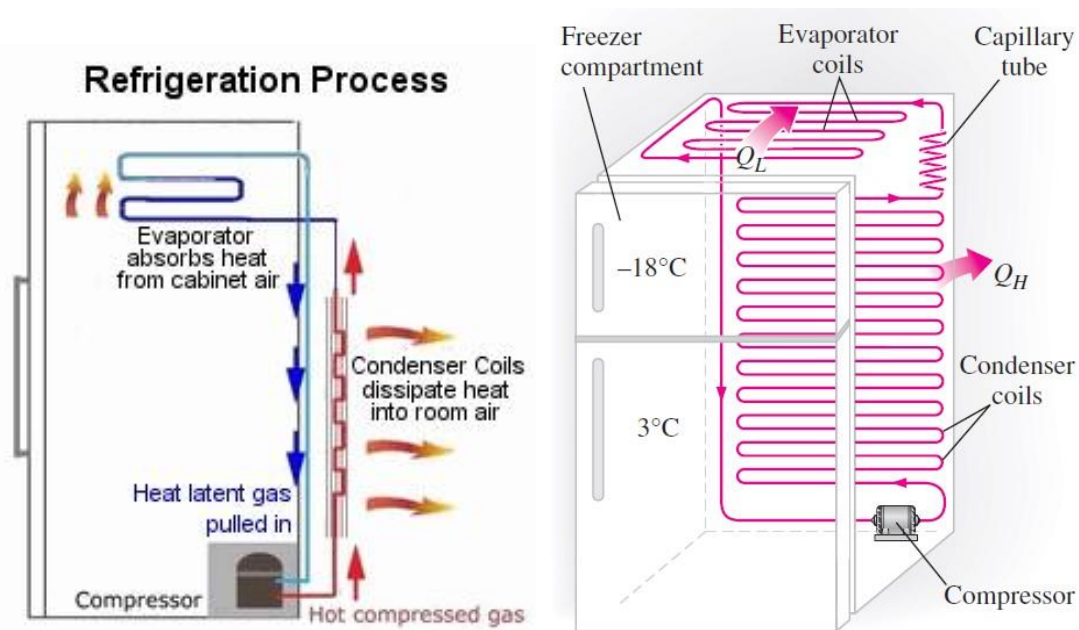


Figure 2.1: Schematic view of a refrigerator with various components and their locations Source: (Cengel & Boles, 2006)

2.2 TYPES OF REFRIGERATION CYCLES

Generally, refrigeration systems are classified into three main types, thus: vapour compression refrigeration system, vapour absorption refrigeration system, and gas cycle refrigeration system. These are briefly discussed in the following sections.

Absorption Systems

In an absorption system, the refrigeration effect is produced by means of thermal energy input. After liquid refrigerant produces refrigeration during evaporation at a low pressure, the vapour is absorbed by an aqueous absorbent. The solution is heated by a direct fired gas furnace or waste heat, and the refrigerant is again vaporized and then condensed into liquid form. The liquid refrigerant is throttled to a very low pressure and is ready to produce the refrigeration effect again. These systems are normally with a coefficient of performance of (COP) of about 0.4.

Gas Expansion Systems

In an air or other gas expansion system, air or gas is compressed to a high pressure by compressors. It is then cooled by surface water or atmospheric air and expanded to a low pressure. Because the temperature of air or gas decreases during expansion, a refrigeration effect is produced.

Vapour Compression Systems

In these systems, a compressor compresses the refrigerant to a higher pressure and temperature from an evaporated vapour at low pressure and temperature. The compressed refrigerant condenses into liquid form by releasing the latent heat of condensation to the condenser water. Liquid refrigerant is then throttled to a low-pressure, low-temperature vapour, producing the refrigeration effect during evaporation. Vapour compression is often called mechanical refrigeration, that is, refrigeration by mechanical compression. Most domestic refrigerators operating on the vapour compression system are designed to maintain the freezer section at -18°C and the refrigerator section at 3°C . Vapour compression refrigeration is one of the oldest technologies and still the most widely used in meeting domestic refrigeration needs mainly because of their simplicity, reliability, practically maintenance free and high COPs as compared to other refrigeration cycles. The system has an average COP of about 1.3 (Cengel & Boles, 2006).

2.3 FUNDAMENTALS OF VAPOUR COMPRESSION REFRIGERATION SYSTEM

The vapour compression cycle is essentially a reversed Rankine vapour cycle that uses a refrigerant as the working fluid to absorb and reject heat energy. The cycle can be fundamentally described by the action of four components, thus: compressor, condenser, expansion device, and evaporator. However, this review is mainly focused on the compressor of the refrigeration system since it is the component that is to be replaced.

2.3.1 Refrigerator Compressors

A refrigerator compressor is a combination of mechanical compression part and an electrical motor. The electrical motor converts electrical energy to mechanical energy in a refrigeration compressor. The mechanical energy developed by the motor is used by the piston to compress and circulate the refrigerant in the refrigeration cycle. In vapour compression refrigerators, compressors are the main prime movers responsible for providing the motive force for circulating refrigerant throughout the system and for creating a sufficiently high refrigerant pressure differential that allows the transport of heat from spaces or products to the outside environment. A schematic view of a hermetic refrigerator compressor is shown in Figure 2.2.

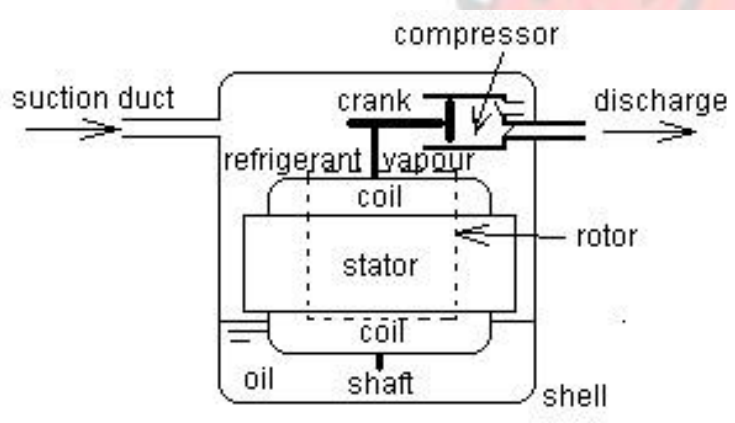


Figure 2.2: Schematic of Hermetic Refrigerator Source: (Ekren et al., 2013) **Compressor**

2.3.2 AC and DC Refrigerator Compressors

An AC current compressor is powered by alternating current sources such as 120 or 220 V and 50 Hz. The electric motor of the AC compressor is an AC induction type. On the other hand, DC compressor requires low voltage and direct current supply such as 12V or 24 V. Even though, DC compressors have similar mechanical compression part with AC

compressor, it has a brushless electrical motor. Green energy technologies (direct current) can be used to power a DC compressor directly while an AC compressor requires a power inverter.

Energy usage reduction through improved efficiency and use of renewable energy employing DC compressors is an advantage of such systems (Ekren et al., 2013).

2.3.3. Capacity Control of Refrigerator Compressors

Normally refrigerant compressors are designed to take care of the most severe operating conditions such as shown in Figure 2.3. However, when the operating conditions are not so severe, then the compressor designed for maximum load turns out to be oversized during long stretches (most refrigeration systems spend most of their operating hours at reduced capacity, it has been estimated that on average systems runs partially loaded more than 65% of the time) (Embraco, Marcos, & Schwarz, 2001). Therefore, there is the need for capacity control mechanisms to match the capacity of the compressor to the ever-changing load of the system. This is a solution for both food preservation and energy performance issues relies on alternative control strategies.

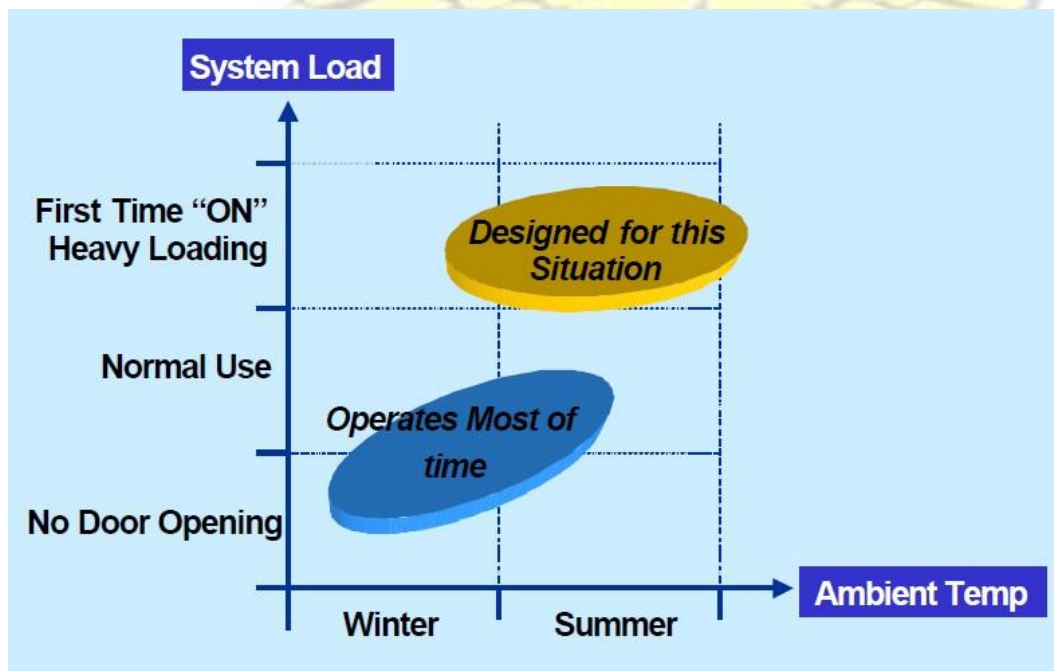


Figure 2.3: Fixed Speed Design Rules

Source: (Embraco, Marcos, & Schwarz, 2001)

2.3.4. Capacity Control Methods

Capacity modulation methods have been studied in the open literature with different benefits of using each, however, there is a general consensus that compressors with capacity modulation systems have high energy management and higher overall system efficiency compared to fixed capacity compressors (Ekren et al., 2013), (Bessler & W. Hwang, 1980) (Chatuverdi & Abazeri, 1987) (Kuang, Sumathy, & Wang, 2003).

According to (Qureshi & Tassou, 1996), the commonly used capacity control methods in refrigeration are: on/off control, hot gas bypass, evaporator temperature control, clearance volume control, multiple compressor control, cylinder unloading and variable speed control. However, this review is limited to ON and OF and variable speed control methods only due to the scope of the study, however the advantages and disadvantages of various capacity control methods have been discussed in greater detail in (Sheldrake, 1991).

2.3.4.1. ON and OFF Capacity Control (Constant Speed AC Compressors)

In most conventional hermetic refrigeration compressors, the electrical motor and crankshaft rotate around a speed of 2900 RPM (50 Hz), which locks the compressor into a single fixed capacity. These compressors rely solely on the ON/OFF capacity control system. This is the most common capacity control method in domestic refrigerators and freezers. With this method, the single speed compressor starts when a pre-set temperature in the refrigerated space is exceeded (“cut-in” temperature) and shuts down as a low temperature (“cut-out” temperature) is reached. This generates a cyclic behaviour of the refrigerant flow, and thereby also of the cooling capacity (Danfoss, 2003).

A typical course of events at compressor start and stop is as follows: At the moment before the compressor starts, the evaporator is at its highest temperature. Most refrigerant, by mass, is located

in the evaporator and compressor whereas the condenser and the capillary tube contain only superheated gas. As the compressor starts, the initial compressor mass flow is high (high evaporation pressure) whereas the capillary tube mass flow is low (superheated gas). The result is that the refrigerant is displaced towards the condenser, which may starve the evaporator with refrigerant liquid. As a result the evaporator pressure decreases, thereby lowering the compressor mass flow. A liquid pool is formed at the condenser outlet which increases the mass flow through the capillary tube. Now the evaporator “refilling” begins. This means that the dry-out point (position in the evaporator where superheat starts) moves downstream gradually ‘activating’ the evaporator as the wetted area, active for evaporation, increases. It is important that this process is short in comparison to the compressor on-period since the system during this time period operates inefficiently due to the superheat and lowered the evaporation temperature.

When the “cut-out” temperature is reached the compressor stops and the pressure equalizes within the system as refrigerant continues to flow through the capillary tube. The condenser pressure decreases and slowly approaches the saturation pressure in the evaporator while refrigerant is forced into the evaporator. During this migration process it is important that the refrigerant liquid is freely drained towards the condenser outlet. If pockets of liquid remain in the condenser as the capillary tube inlet liquid seal is broken a reversed heat transfer follows, where liquid in the condenser evaporates and condensation occurs in the evaporator.

Though it is the simplest and inexpensive method of capacity control, however, the cycling causes refrigerant displacements within the cooling system that affects the overall performance. According to (Bjork & Palm, 2006), there are two types of losses caused by the on/off cycling: Firstly, during the on-period (time period in the on/off cycle when the compressor is on) the thermal load of the heat exchangers is higher than it would before a continuously controlled system (variable speed compressor). This lowers the thermodynamic efficiency through increased temperature lift. Secondly, there are losses due to refrigerant displacements

following a compressor start and stop. Moreover, the losses may be quantified in terms of capacity or efficiency. In total, efficiency losses of 5–37% are reported. On/off control also results in increased wear and tear on compressor components and shortens service life. These compressors require large starting current, sometimes 6 times more than the running current. Lubrication problems under light load conditions; this could lead to short cycling and could reduce the life of the compressor (Qureshi & Tassou, 1995).

2.3.4.2. Variable Speed Control (VSDC Compressors)

The capacity of a compressor can also be controlled by varying the rotational speed of the compressor motor. This is accomplished by using a device called an adjustable frequency drive (AFD) or variable-speed drive. On a reciprocating compressor, the AFD varies the speed at which the crankshaft rotates, thus controlling the rate at which the piston travels back and forth in the cylinder. On a scroll compressor, the speed at which the driven scroll rotates is varied. In applying to a helical-rotary compressor, this would vary the speed at which the rotors rotate. On a centrifugal compressor, the speed at which the impeller rotates is varied. Controlling the capacity of the compressor by regulating its speed is one of the most efficient methods as the required power input reduces almost in the same proportion with cooling load. This is illustrated by Saidur, Rahim, and Hasanuzzaman (2009) in Figure 2.4 below.

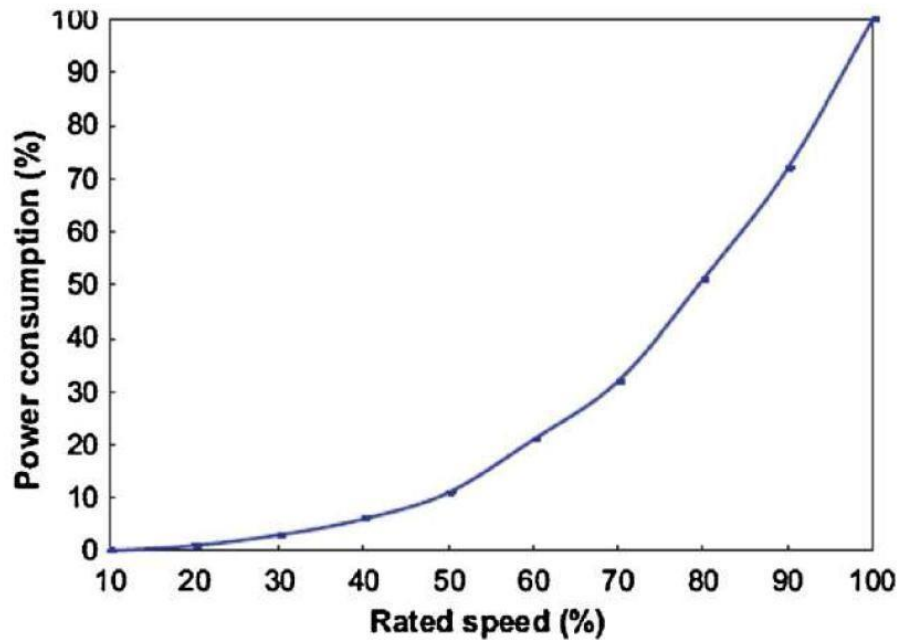


Figure 2.4: Relationship between motor power reduction and rated speed Source: (Saidur, Rahim, & Hasanuzzaman, 2009)

In most variable-speed compressors, the motor's rotational speed may be varied from 1800 to 5400 RPM. Hence the capacity of the compressor is controlled directly at the source, thereby eliminating any temperature overshoot. There are always a lot of energy savings generated from doing away with the need to design compressors that meet extreme conditions encountered just a few days a year. Due to their numerous advantages many compressor manufacturers have started to develop and sell hermetic compressors with variable speed drive. One disadvantage of this solution is the electronics, which supply the variable frequency current also consumes electric power, which may be in the order of magnitude of 2 to 5 % of the motor power (Binneberg, Kraus, & Quack, 2002).

Advantages of VSDC Compressors over Fixed Speed AC Compressors

VSDC compressors have a series of advantages over single (fixed) speed compressors as found on conventional AC refrigerators in terms of energy sustainability. Firstly, a theoretical comparison of various capacity control methods at full and part-load by (Qureshi & Tassou,

1995) revealed that the most efficient method of capacity control is variable speed capacity modulation. Embraco et al. (2001) observed energy savings up to 40% by comparing variable capacity compressor to conventional fixed speed compressors. In general, an energy saving ranging from 5 to 40 have been documented by different authors in the open literature (Aprea, Mastrullo, & Renno, 2009), (Aprea, Mastrullo, & Renno, 2006), (Wong & James, 1988), (Embraco et al. 2001) (Qureshi & Tassou, 1996). Therefore, the combined advantages of DC compressors and the variable speed modulation method makes VSDC compressors a suitable replacement for AC compressors in the 21st century, when renewable energies and energy efficiency have been identified to be the best means of ensuring sustainable energy supply. Variable speed DC compressors will help in the reduction of refrigerator power consumption as well as making it possible to power such systems with direct current from renewable energy sources such as solar.

Ekren et al. (2011) simplified the analysis by noting that variable speed direct current compressors are the best candidates to be employed in energy-efficient refrigeration systems, especially for renewable energy powered units since they do not require power inverters that an alternating current compressor would require. He further emphasised that VSDC compressors are capable of matching the compressor work to the cooling requirement in the cooling compartment thereby reducing wastage of energy.

According to Embraco et al. (2001), up to 40% reduction in overall energy consumption reduction were obtained by applying variable capacity compressors as compared to conventional fixed speed compressors. They also noted that improvements up to 40% are possible by applying Variable Capacity Compressor to existing systems, and much more value can be added to new designs using this new technology. Experiments conducted by (Aprea, Mastrullo, & Renno, 2009) (Qureshi & Tassou, 1996) showed that cooling capacity control by means of varying the compressor speed is a suitable solution to improve partial load efficiency

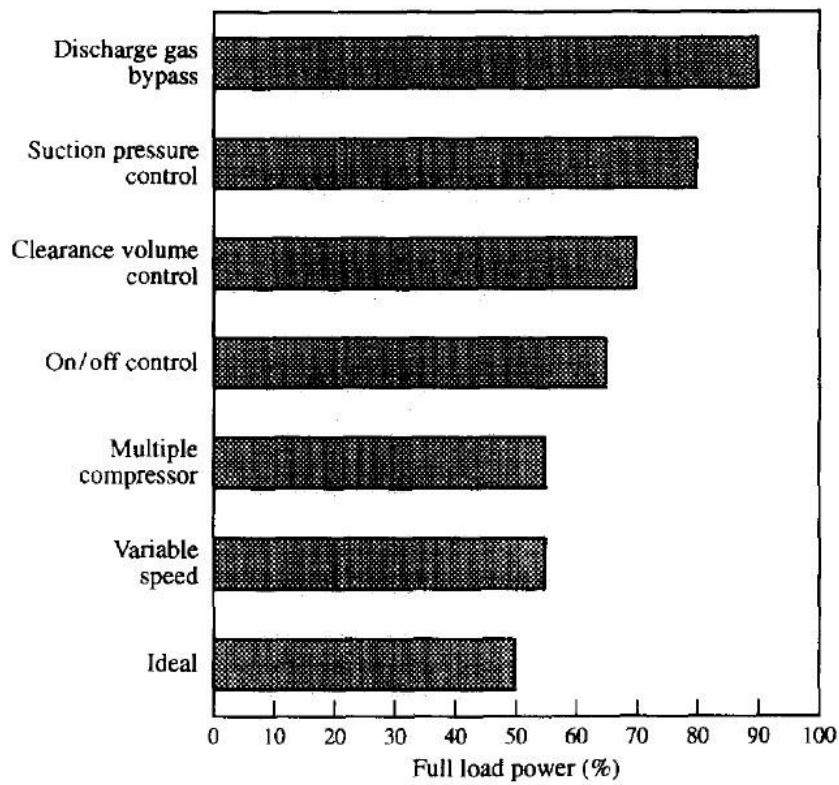
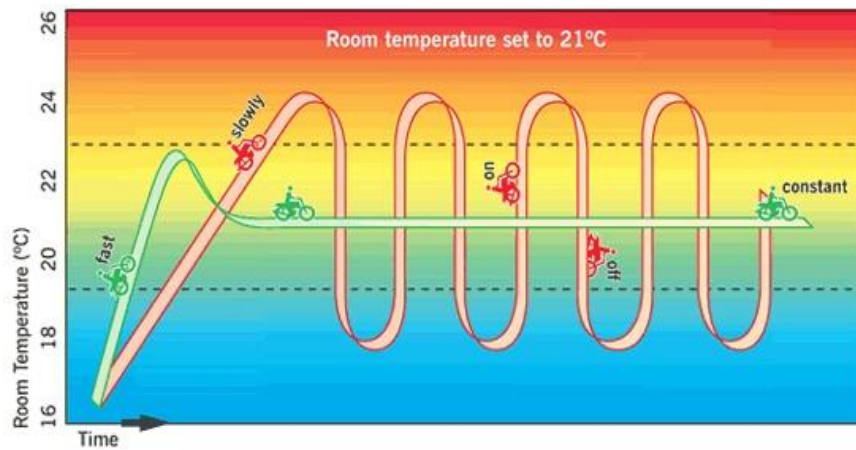


Figure 2.5: Comparison of various capacity control techniques at half load Source (Qureshi & Tassou, 1996)

Since a refrigerator with variable speed compressor could use the capacity modulation technique, it will consume less energy compared to the conventional refrigerators operating in on-off mode by using the smaller capacity compressor, reducing the refrigerant circulation rate, enhancing the heat exchangers' performance and the significant improvement in the operating conditions. It has been advocated in the open literature (Kim & Lee, 2000) that refrigeration systems employing a variable-speed compressor is more energy efficient compared to the conventional single speed counterpart due to their ability to match refrigeration capacity and the cooling load. Figure 2.6 shows the evaporator temperature of compressor operating on the on and off and variable speed control modes as used in an air condition system.



Source: Mitsubishi, 2009

Figure 2.6: Operation of Variable and a Single Speed Compressor

2.4. SOLAR ELECTRIC REFRIGERATION

Solar refrigeration technology involves a system where solar power is used for refrigeration purposes. According to Kim and Ferreira (2008), solar cooling can be achieved through four basic methods: solar PV cooling, solar thermo-electrical cooling, solar thermo-mechanical cooling and solar thermal cooling. The first is a PV-based solar energy system, where solar energy is converted into electrical energy and used to run the conventional vapour compression cycle. The second one produce cool by thermo-electric processes. The third one converts the thermal energy to mechanical energy, which is utilized to produce the refrigeration effect. The fourth method utilizes a solar thermal refrigeration system, where a solar collector directly heats the refrigerant through collector tubes instead of using solar electric power. There have been many papers in the open literature enumerating the various advantages of each of the above methods as a feasible approach of refrigeration, however, in the present study; only solar electric refrigeration using the vapour compression system has been the main focus. Solar PV vapour compression refrigeration has gained much popularity because of their simplicity and high COPs. The energy supply in the system is provided by an array of solar cells which convert the incident solar radiation to electricity. The latter is used to drive the compressor and the excess charges a battery system for use at periods of low or no insulation.

Kim and Ferreira (2008) simplified the mechanism by documenting that a solar electric refrigeration system consists mainly of photovoltaic panels (PV) and an electrical refrigeration device. According to Kim and Ferreira (2008), the biggest advantage of using solar panels for refrigeration is the simplicity in construction and high overall efficiency when combined with a conventional vapour compression system. The overall efficiency of the refrigerator is equal to the product of the efficiency of the PV system and the vapour compression refrigerator.

Efficiency (η) = Efficiency of the PV x Efficiency of the refrigerator

$$\text{Efficiency of the PV system} = \frac{E}{I \times A}$$

efficiency of the refrigerator defined as $\frac{Q_{\text{ref}}}{E}$

$$\text{Efficiency } (\eta) = \frac{E}{I \times A} \times \frac{Q_{\text{ref}}}{E} = \frac{Q_{\text{ref}}}{I \times A}$$

Where work, Q_{ref} = refrigeration effect. ref

W = energy generated by the solar panel = energy consumed by the mechanical compressor.

A = surface area of the solar panel (m^2) and

I = the direct irradiation of solar beams (kW/m^2).

2.4.1. Types of Solar Electric Refrigerators

Powering a refrigerator with solar electric depends on the type of compressor used by the refrigerator, direct current (DC) can be supplied to refrigerators using DC compressors (DC refrigerators). On the other hand, an inverter is required to convert the DC provided by the solar PV to alternating current (AC) before supplying it to the refrigerator using an AC compressor (conventional refrigerators). Though there are few places where direct solar refrigerators are

used for preservation of vaccines and other biological components, refrigeration with AC compressor is usually the case in most locations in Ghana and SubSaharan Africa as a whole. Therefore, a complete off grid solar PV cooling system typically consists of four basic components: photovoltaic modules, a battery, an inverter circuit and a vapour compression refrigerator (Ekren et al. (2013), Kim and Ferreira (2008)).

Contrary to the above approaches, the present study is aimed at developing the design steps of replacing the AC compressor on a conventional domestic refrigerator with a variable speed direct current compressor to serve as a DC refrigerator for off grid refrigeration. This will eliminate the use of power inverters and as well as reduce power consumption because of the better capacity control method used by variable speed compressors. Variable speed compressors are noted to be the best option in terms of energy savings because of their ability to match cooling requirement with power consumption thereby reducing energy wastage. The following sections take a critical look at the major approaches of providing refrigeration needs by using a DC energy source (Solar). The review covers solar refrigeration system without inverters (DC refrigerator), conventional refrigerators running on solar PV via inverters (AC refrigerator), and conventional refrigerators modified to serve as DC refrigerators.

2.4.1.1. Commercial Solar Refrigerators (Without Inverter)

Commercial DC refrigerators can be powered by a direct current from a solar PV system without an inverter. These systems do not require a power inverter. The schematic diagram of these of kinds refrigerators is depicted in Figure 2.7 below.

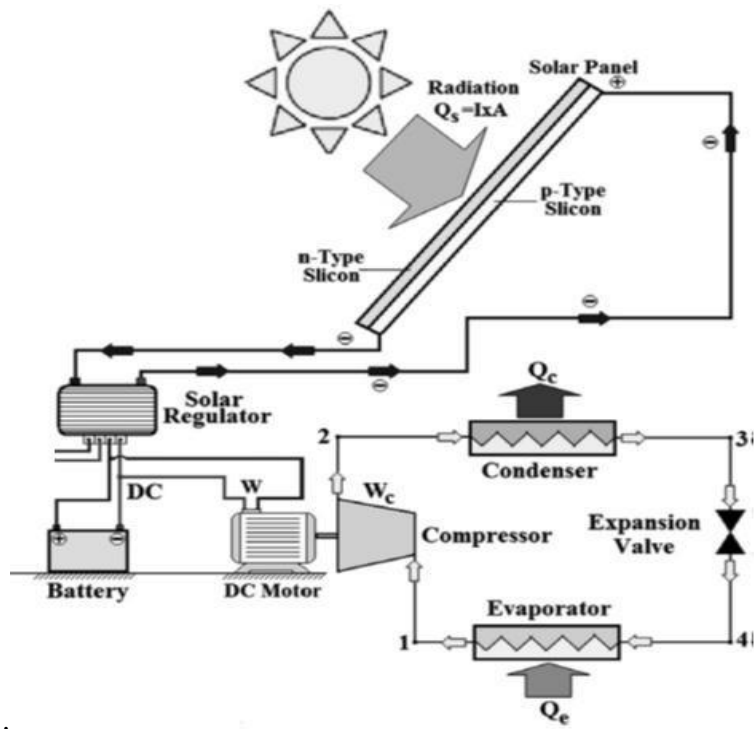


Figure 2.7: A Schematic Diagram of a Solar Powered DC Source (Kim & Ferreira, Refrigerator 2008)

Solar PV refrigeration is becoming more practical for household refrigeration needs as prices of solar PV systems have reduced drastically over the past five years. This development coupled with growing demand for alternative source of energy due to the numerous environmental issues and global energy insecurity. Research in solar electric refrigeration has therefore increased and it is targeted towards enhanced design, application and optimization of such systems. There is a widespread consensus that, PV refrigeration systems are economical and reliable solution for remote, or urban areas where the supply of electricity is non-reliable such as found in many developing countries (Yesilata & Isiker, 2006). The area most researched into in the field of solar electric refrigeration using the conventional vapour compression system is the operation of DC household refrigerators with direct current generated by solar PV. Aktacir (2011) established and investigated experimentally the daily and seasonal operating performance of a multi-purpose stand-alone PV powered refrigeration system. An evaporator temperature of $-10.6\text{ }^{\circ}\text{C}$ was observed over a 28 day period when the system was under test. It was concluded that such small-scale stand-alone systems are suitable

for rural regions where electricity is unreliable or non-existent but refrigeration is continually critical.

Other researches including (Ekren et al., 2013, Ekren et al., 2011, McCarneya et al., 2013, (Otanicar, Robert, & Phelan, 2012), (Sarbu & Sebarchievici, 2013), (Bacon, 1997) and (Kim & Ferreira, 2008)) have also presented different designs, system optimisation measures and performance analysis of direct current solar refrigerators. Though these kinds of refrigerators are commercially available, their high initial cost limits their use in developing countries such as Ghana.

According to McCarneya et al. (2013) and Essandoh-Yeddu (1994), about 80 solar refrigerators were installed in Ghana in the late 1980s, but they experienced a high failure rate (about 50%) soon after installation. Several of the problems were attributed to inadequate installation quality, including faulty controllers, fire-damaged components (possibly not using high-quality components rated to the expected electric loads), deteriorated solar support structures, faulty wiring, heat-damaged solar panels (due to poor positioning of panels on roof), and shaded solar panels.

According Obeng and Hans-Dieter (2009), the presence of solar PV-powered icemakers in rural communities can assist micro enterprises in fishing, sale of ice cubes and cold stores, especially small rural stores especially in the tropical and sub-tropical countries such as Ghana to expand their inventory by adding items that can be preserved using solar-powered refrigerators.

2.4.1.2. Conventional Refrigerators Powered by Solar Energy via an Inverter

In Ghana and most part of the Sub-Saharan Africa, to provide refrigeration needs using solar energy, individuals run their refrigerators via inverters. This mode of application refrigeration

possesses two main challenges; (i) inverter's initial cost and conversion losses, (ii) AC compressors running ON the OF and off mode as the only means of capacity control is associated with many inefficiencies compared to variable speed DC compressors found on commercial solar electric refrigerators. Notwithstanding these challenges, there has been a series of researches on powering refrigerators with solar PV via inverters in the open literature.

Modi et al. (2009) described the fabrication, experimentation and simulation stages of converting a 165 L domestic electric refrigerator to a solar powered one. The conventional domestic refrigerator used in their experiment was redesigned by adding battery bank, inverter and a charge controller, and powered by solar photovoltaic panels. The coefficient of performance (COP) of the system was observed to decrease with time from morning to afternoon and a maximum COP of 2.102 was observed at 7 AM. Economic analysis of the system with RETScreen 4 indicated that the system can only be viable with carbon trading option taken into account, and an initial subsidy or a reduction in the component costs – mainly solar panels and battery bank.

Bilgili (2011) proposed and investigated the performance of a solar electric-vapor compression refrigeration system under different evaporating temperatures and months in Adana city located in the southern region of Turkey. Conventional refrigerator was operated by solar PV system via a battery, it was found that the proposed system driven by solar PV can be successfully operated in the chosen province in Turkey and it may be more applicable and encouraged when the cost of solar panel system decreases. Moreover, it was observed that the photovoltaic panel area of the solar electric vapour compression refrigeration system increases as the evaporating temperature decreases. In a typical day, a photovoltaic panel surface area of 18.691 m² was required for evaporating temperature of 10 °C, but it increased to 38.65 m² for evaporator temperature of -10 °C.

Thomachan and Kattakayam (2000) also presented the cool-down, warm-up and steady state performance of a 100 W AC operated domestic refrigerator powered by a field of photovoltaic panels, a battery bank and an inverter. The authors noted that there was no degradation in the performance when a non-sinusoidal waveform AC source is used to operate the refrigerator, although it may involve only a slight additional heating of the hermetic compressor. After analysis the performance of the system with RETScreen the authors realized that the system is not financially viable without discount and carbon trading.

2.4.1.3. Conventional AC Refrigerator Converted to Serve as a DC Refrigerator

Due to the shortfalls in powering conventional refrigerators via inverters, the question is, isn't it possible to convert conventional refrigerator to serve as solar powered one by replacing the fixed speed AC compressor with a VSDC compressor? The author's search identified two results in the open literature (McCormick, 1986) and (Kaplanis & Papanastasiou, 2006), these are reviewed as follows:

In 1986, McCormick converted a 110 volt old refrigerator to solar. The converted unit was found to maintain an internal temperature of -18°C with compressor running time of 30 to 40 minutes per hour at an ambient temperature of 21°C . The compressor was found to drawing 4.1 Amps from a battery bank. To reduce the energy consumption of the system the author added more insulation to the system. All four sides and top of the refrigerator cabinet were insulated with a 5.1 cm thick Styrofoam board. After completing the super-insulation of the box, a no-load test conducted revealed that average running time of approximately 18 was cut from 30-40 minutes per hour to 15-20 minutes. Further reduction in the compressor run time was observed after filling the cabinet and the items were frozen (McCormick, 1986). The author noted that the closer to full capacity the freezer is, the less its running time. He also reported converting and selling several refrigerators and freezers ranging from 141 L up to 340 L. It was

also observed that the power consumption of the system can be reduced further by increasing the amount of insulation. On the cost of the system, it was noted that a converted refrigerator was about 1/3 to 1/2 the cost of ready-made solar refrigerators (McCormick, 1986).

In a similar work, Kaplanis and Papanastasiou (2006) studied the performance of a modified conventional refrigerator to serve as a PV powered one. They observed that increasing the polyurethane insulation thickness by 25 mm reduced the useful volume capacity by 30 %. However, the extra insulation reduced the cooling load requirement, thereby resulting in power consumption savings of 1.53 kWh/day.

2.4.2. Future of Solar Powered Refrigerators

According to Aprea et al. (2009), PV systems are the most appropriate system for small capacity refrigeration plants used for food or medical applications in areas far from conventional energy sources, where a high level of solar radiation is present. Similarly, both Kim and Ferreira (2008) and Bilgili (2011) documented that solar refrigeration is a logical solution of meeting cooling demands since high cooling requirements are usually in phase with high solar radiation.

On the other hand, Kim and Ferreira (2008) noted that there are two major challenges for a broader commercialization of solar electric refrigerators; Firstly, the systems need to be equipped with some means to cope with the varying electricity production rate with time, e.g. electric battery, mixed use of solar- and grid-electricity or a variable-capacity compressor. Secondly, the price of a solar photovoltaic panel should decrease further to enable solar PV system to be able to compete with conventional systems.

2.4.3. Summary of Modes of Powering VCRS with Solar Energy

Literature review on vapor compression, solar electric refrigeration can be classified into three main categories; commercial solar refrigerators, conventional refrigerators powered via inverter, modifying conventional refrigerators to serve as DC solar refrigerator. From the above literature review it can be observed that, for the same size of a refrigerator, the power requirement of the system can be depicted with the size of solar PV as shown on Figure 2.8. Commercial solar refrigerators have better insulation systems (thus; materials with low thermal conductivity) and at the same time use a variable speed direct current compressor such as discussed in the previous sections. On the other hand the modified refrigerator incorporates a variable speed DC compressor into a conventional AC refrigerator. All these two systems require no inverter to run on solar PV systems. Secondly, they have better capacity control due to the presence of the variable speed compressors. The conventional refrigerator, which runs on single speed AC compressor requires a power inverter to run on a solar PV system and at the same time operates with lower capacity control. All these translate into higher power consumption than those operating on variable speed direct current compressors.

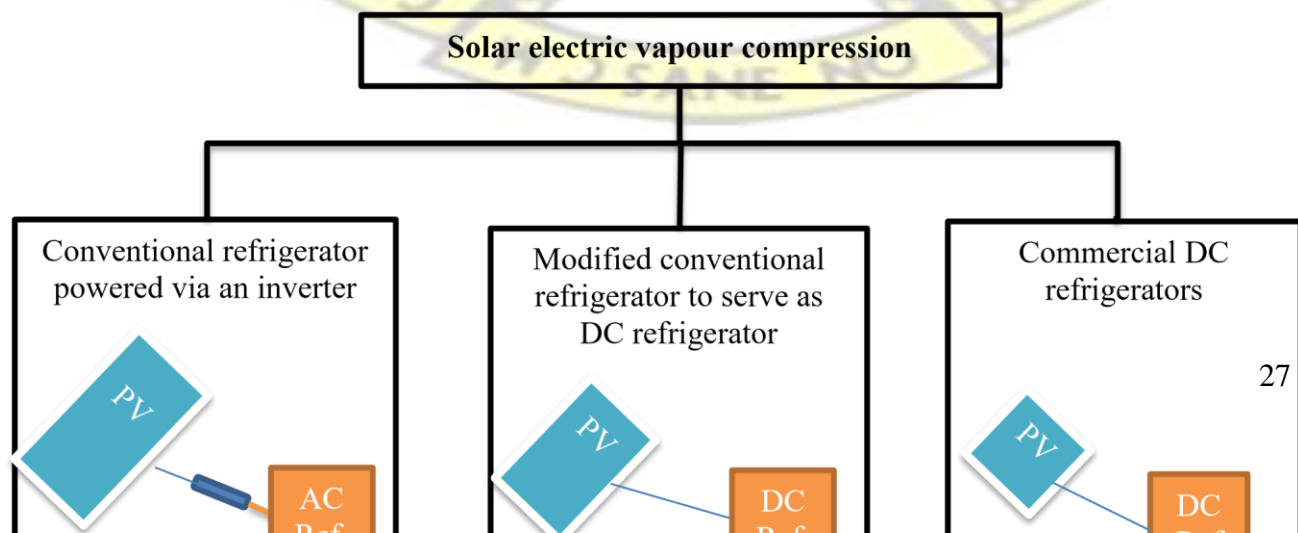


Figure 2.8: Summary of Reviewed Literature on Powering Vapour Compression Systems with Solar PV Electricity

2.5. PERFORMANCE ANALYSIS OF VAPOUR COMPRSSION SYSTEMS

Performance studies of refrigerators have been reported by many researchers. Previously, air temperature distribution inside domestic refrigerators have been measured and analyzed worldwide as an indicator for performance of the refrigerators. Besides the temperature measurement, the refrigerator performance is measured by determining the coefficient of performance (COP) of the entire refrigeration system. In this study both approaches would be used in assessing the performance of the solar powered refrigerator to be developed. However, this section looks at the procedure and test standards of determining the COP of refrigeration system after determining the enthalpy values at the various states of the refrigeration cycle.

2.5.1. Refrigerator Test Standards

Experimental performance analysis involves the investigation of the general performance of household refrigerators and freezers at standard test conditions using generalized procedures.

The following four test standards were found in the open literature:

The North American standard AHAM HRF-1 (2004)

According to the AHAM HRF-1 (2004) standard, the refrigerator must be tested with the surrounding environment at 32.2°C and 75±5 % relative humidity. The average fresh-food compartment temperature must be kept at 7.2°C and the frozen-food (freezer) average temperature at -9.4 °C or -15 °C, depending on the product classification. The test must last at least 3 hours and not exceed 24 hours. During the test period, the compressor must complete two or more on-off cycles. Door-openings are not required.

The Australasian standard (AS/NZS 4474.1, 2007)

The AS/NZS 4474.1, (2007) standard requires the refrigerator to be tested following a cycling pattern under ambient conditions of 32 °C and 75±5 % relative humidity. No door openings are needed. The fresh-food compartment must be kept at 3 °C and the freezer at -9 °C or -15 °C, also depending on the product classification. The energy consumption must be monitored and recorded until it reaches 1 kWh or the test time exceeds 16 hours.

The Japanese standard (JIS C 9801, 2006)

The Japanese standard (JIS C 9801, 2006) requires two test runs to be performed, one at 15°C and another at 30°C ambient temperature, both with a relative humidity of 75±5%. This standard adopts three classification grades depending on the freezer compartment temperature (-6 °C, -12 °C or -18 °C), whereas the fresh-food temperature must be kept at 3°C, independent of the product classification. Different from the other standards, this one requires door openings with the door fully opened for at least 5 s. The test must last 24 hours.

The International Standards

ISO 8561 (1995) used to be the international standard for testing frost-free refrigerators until 2005, when it was replaced by ISO 15502, which in turn was replaced by IEC 62552 (2007). In general, all of these standards follow a similar test procedure. Firstly, the refrigerator is tested according to its climate classification: for subtropical regions (N-class) the test is carried out at an ambient temperature of 25.0±0.5°C; and for tropical regions (T-class) the ambient temperature is 32.0±0.5°C. A summary of the various test standards is presented in **Table 2.1**

Table 2.1: Summary of Test Conditions

Test standard	Domain	Ambient (°C)	Fresh-food (°C)	Freezer (°C)
---------------	--------	--------------	-----------------	--------------

AHAM HRF	North America	32.2	7.2	-9.4 or -14.0
AS/NZS 4474.1	Australasia	32.0	3.0	-9.0 or -15.0
JIS C 9607	Japan	15.0 or 30	3.0	-6.0, -12.0 or -18.0
ISO 8561	International	25.0 or 32	5.0	-6.0, -12.0 or -18.0
ISO 15502				
IEC 62552				

2.5.2. Performance Analysis of Compressors

This is done to investigate the performance of a particular compressor on a refrigerator under standard test conditions. The standard test conditions make it possible to compare two or more compressors. This is based on the fact that cooling capacities of two compressors can only be compared only if they are both measured at the same test conditions. The ambient, condensing, suction and sub-cooling temperatures must be maintained as presented in Table 2.2.

The two standard test conditions in literature are;

1. The EN12900/CECOMAF
2. The ASHRAE

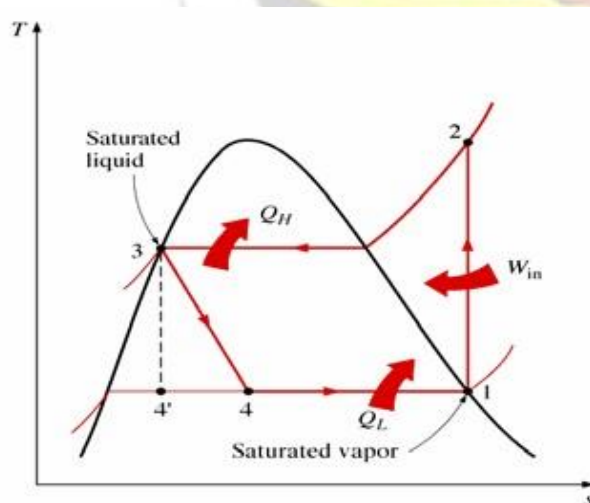
Table 2.2: Summary of Refrigerator Test Conditions

Test condition	ASHRAE (°C)	CECOMAF (°C)
Condensing temperature	55	54.4
Ambient temperature	32	32
Suction gas temperature	32	32
Sub-cooling	No sub-cooling	32

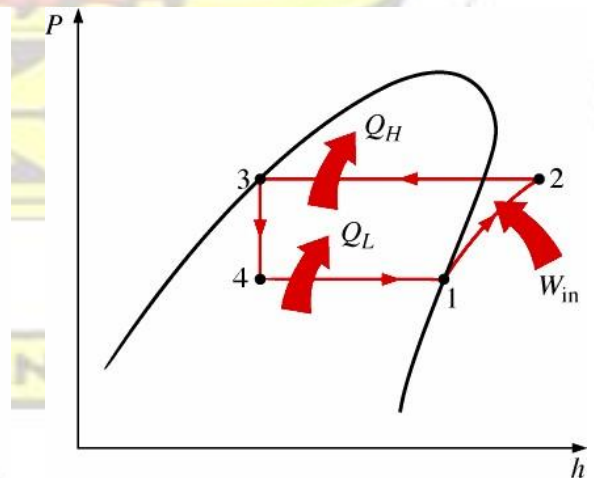
Evaporator Temperature (Cooling capacity varies with evap. Temp. Cooling capacities at these temperatures are normally used for sizing compressors) eg. a compressor rated 151W means the cooling capacity of the compressor at evaporator temperature of -23.3 or -25 depending on the standard used.	-23.3	-25
---	-------	-----

2.5.3. Theoretical Analysis of Vapour Compression Systems

The refrigerant undergoes four main changes during the cycle: evaporation (4-1), compression (1-2), condensation (2-3) and expansion (3-4). To identify the thermodynamic changes of the refrigerant during a cycle, the properties; temperature (T), pressure (p), enthalpy (h) and entropy (s) are used. These four processes alter the properties of the refrigerant in different ways. To conduct an energy analysis on a typical vapour compression system, the enthalpy values at all four state points are required. Enthalpy values are conveniently read from the appropriate refrigerant tables by using the pressure and temperature values obtained from the refrigerator.



a. Temperature- entropy diagram



b. Pressure – Enthalpy diagram

Figure 2.9: T-s and P-h diagram of Vapour Source: (Cengel & Boles, 2006) compression refrigeration system

Compressor Power Requirement

The power required by the compressor, W_{comp} can be determined as the product of the refrigerant mass flow rate (\dot{m}), and the change in specific enthalpy of the refrigerant as it passes through the compressor, this is given in equation 2.1

$$W_{comp} = \dot{m}(h_2 - h_1) \quad \text{Equation 2.1}$$

The Mass flow rate of the refrigeration system can be measured experimentally with a mass flow meter or estimated theoretically using equation 2.3. Compressor power consumption can also be determined by equation 2.3

$$\dot{m} = \frac{\dot{V} \times N}{v_1} \quad \text{Equation 2.2}$$

Therefore,

$$W_{comp} = \frac{\dot{m}(h_2 - h_1)}{\eta_{is}} = \frac{\dot{V} \times N \times (h_2 - h_1)}{\eta_{is} v_1} \quad \text{Equation 2.3}$$

Heat Rejection in Condenser

Heat rejected by the refrigerant to the ambient while flowing through the condenser is given by the equation 2.4.

$$\dot{Q}_c = \dot{m}(h_2 - h_3)$$

$$Q_{\text{cond}} = m(h_2 - h_3)$$

Equation 2.4

Isentropic Expansion

There is no change in enthalpy in the expansion device, thus $h_2 = h_3$

$h_2 = h_3$

$h_2 = h_3$

Heat Absorbed in Evaporator

The heat gained by the refrigerant or the refrigerating capacity is given by equation 2.4

$Q_{\text{ref}} = m(h_1 - h_3)$

$$Q_{\text{ref}} = m(h_1 - h_3)$$

Equation 2.5

Coefficient of Performance of the Refrigerator

The coefficient of performance (COP) is a dimensionless index used to indicate the performance of a thermodynamic cycle or thermal system. In order to compare different refrigeration systems, a Coefficient of Performance (COP) was defined by Sadi Carnot in 1824. The magnitude of COP can be greater than 1. The COP is defined as shown in equation 2.5.

$$\text{COP} = \frac{Q_{\text{ref}}}{W_{\text{comp}}}$$

Equation 2.6

Total system energy balance

$Q_{\text{cond}} = Q_{\text{ref}} + W_{\text{comp}}$

$$Q_{\text{cond}} = Q_{\text{ref}} + W_{\text{comp}}$$

2.6. SOLAR ENERGY POTENTIAL OF GHANA

The size of components as well as the overall viability of solar systems depend largely on the solar irradiance reaching ground level at the area where its application is required, hence the solar resources potential (based on peak sun hours) of different locations in Ghana has been thoroughly reviewed.

Ghana has an abundant amount of solar energy with an annual theoretical amount of 400,000 GWH. It has appreciable amounts of both direct and diffuse solar irradiance (thirty (30) percent diffused and seventy (70) percent (direct) which are both good for solar PV applications (Dadzie, 2008).

According to SWERA (2003) average duration of sunshine in Ghana varies from a minimum of 5.3 hours per day in the cloudy forest region to about 7.7 hours per day in the dry savannah region. However, the peak sun hours varies from 4.02 to 6.07 for August and April respectively, with an average of 5.05 peak sun hours as against approximately 5 peak sun hours for worldwide daily average for optimally oriented surfaces. Most European countries such as the United Kingdom have approximately 4 to 5 peak sun hours in summer, reducing to 1 peak sun hour in winter. This comparison indicates that Ghana has a high solar energy potential. Figure 2.10 and Table 2.3 give the average monthly irradiance of various locations in Ghana.



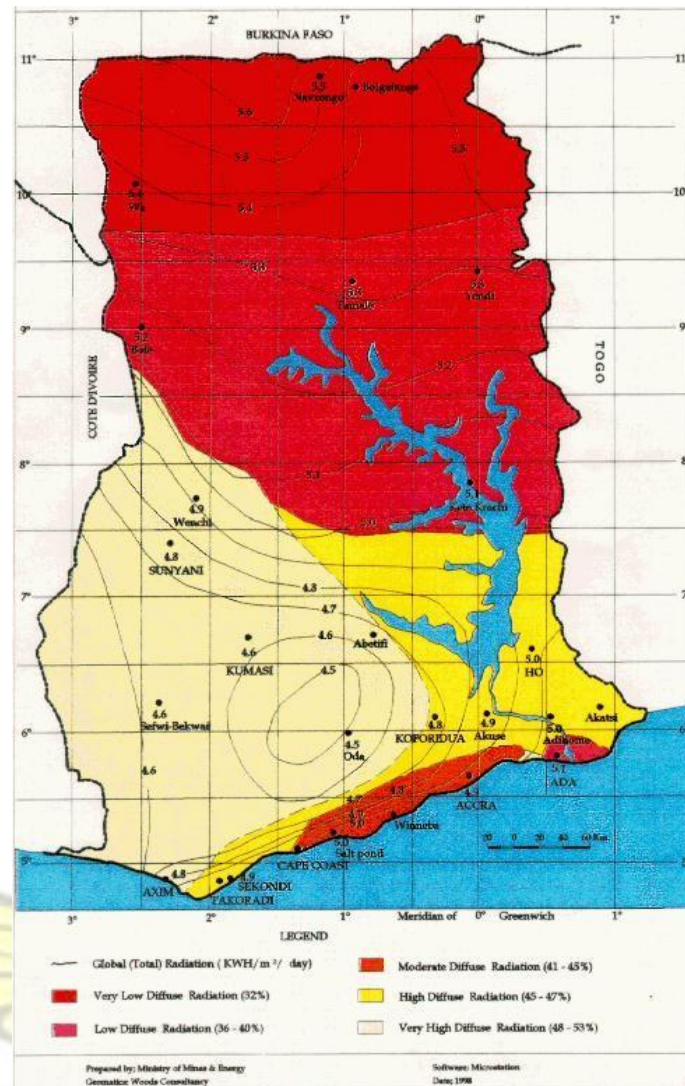


Figure 2.10: Solar Map of Ghana

Source (MoME, 1998)

Peak Sun Hours

Peak sun hours are the number of hours required for a day's total solar irradiation to accumulate at peak sun condition. It indicates the amount of incident solar power on a unit

surface, commonly expressed in units of $\text{KWH/m}^2/\text{day}$. It is the time of the day that solar

panels are expected to produce their rated power. Solar Panels are rated in peak watts,

indicating the maximum electricity that the panel can produce at standard test conditions that

is when the sun's intensity is $1000 \frac{W}{m^2}$. The peak sun hour of an area is the major

parameter that affects the performance of the solar panel.

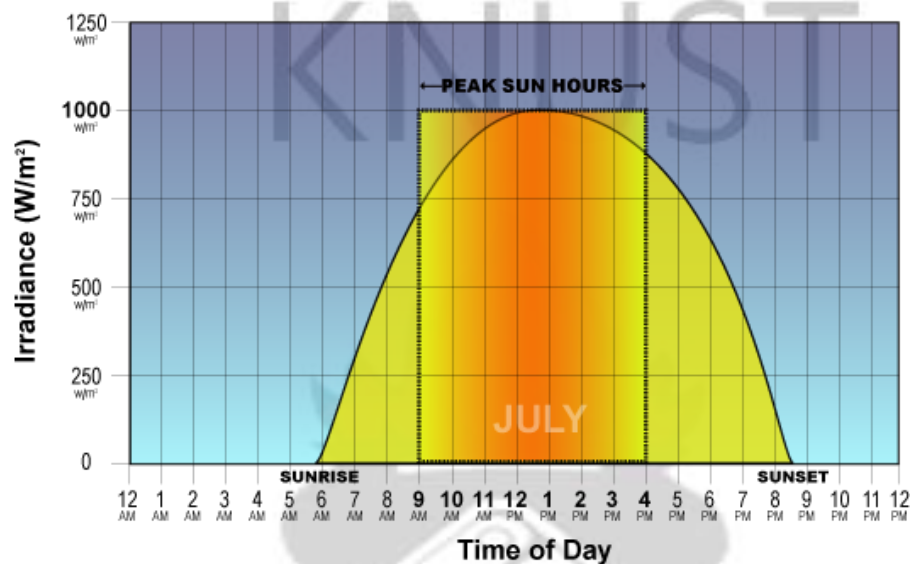


Figure 2.11: Peak Sun Hours

Source: (Solar Choice, 2000)

Solar PV systems are normally designed/sized for the month with the lowest irradiation that is lowest peak sun hours (PSH). However, in typical detailed designs the variation of both the solar irradiation and the load energy requirement are considered and matched accordingly for optimization purposes. In the current design it was assumed that the variation in daily power requirement of the refrigerator is negligible. Hence the month with the lowest number of peak sun hours, which occurs in August would be considered in sizing the solar panel. Peak sun hours is interchangeable with solar irradiance ($kWh / m^2 / day$) since they have equal values,

this is only through based on the globally accepted fact that peak sun equal to $1000 \frac{W}{m^2}$.

Detail peak sun hours for different months at 19 Synoptic Stations in Ghana is given in Table 2.3. It can be observed that August has the least number of peak sun hours with the maximum sun hours for most locations occurring in April. To ensure that the panels produce enough

energy all year round, it is always advisable to use the least peak sun hours of the area instead of using the average.

Table 2.3: 10 - Year Monthly Averages of Peak Sun Hours (hours/day) at 19 Synoptic Stations

MONTH	KUMASI	ACCRA	AXIM	NAVRO NGO	SALTPO ND	ADA	KOFOR IDUA	WENC HI	TAMALE
JAN	4.818	4.660	4.882	5.391	4.899	4.995	4.711	5.193	5.124
FEB	5.313	5.206	5.399	5.400	5.555	5.381	5.139	5.495	5.479
MAR	5.305	5.256	5.569	5.783	5.486	5.649	5.260	5.483	5.613
APR	5.356	5.665	5.605	5.958	5.684	5.937	5.434	5.711	5.890
MAY	4.709	5.416	5.051	5.934	5.354	5.570	5.287	5.507	5.869
JUN	4.029	4.613	3.936	5.719	4.44	4.978	4.641	4.972	5.510
JUL	4.036	4.189	4.242	5.339	4.67	5.064	4.074	4.356	4.954
AUG	3.783	4.527	4.230	5.098	4.482	5.065	3.842	4.120	4.841
SEP	3.992	5.107	4.382	5.324	4.997	5.510	4.437	4.405	5.004
OCT	4.707	5.623	5.178	5.677	5.678	5.872	5.174	4.927	5.472
NOV	5.000	5.510	5.466	5.616	5.692	5.480	5.241	5.127	5.695
DEC	4.552	4.930	4.986	4.824	5.153	5.359	4.857	4.905	5.213
AVERAGE	4.633	5.059	4.911	5.505	5.174	5.409	4.841	5.017	5.389

MONTH	WA	HO	BEKW AI	AKIM ODA	KRACH I	YENDI	TAKOR ADI	BOLE	ABETI FI	AKUSE
JAN	5.464	4.872	4.695	4.505	5.107	5.156	4.79	5.422	5.032	4.634
FEB	5.809	5.224	5.084	4.771	5.414	5.462	5.376	5.821	5.525	5.056
MAR	5.798	5.509	5.265	4.884	5.679	5.558	5.463	5.762	5.558	5.247
APR	5.859	5.716	5.495	5.176	5.968	5.862	5.663	5.797	5.58	4.951
MAY	5.873	5.576	5.311	4.896	5.859	5.919	5.227	5.71	5.406	5.281
JUN	5.611	4.916	4.559	4.303	5.188	5.415	4.361	5.091	4.824	4.591
JUL	5.135	4.601	4.114	4.015	4.684	5.044	4.384	4.645	4.752	4.304
AUG	4.937	4.187	3.753	3.802	4.531	4.629	4.227	4.494	4.602	4.108
SEP	5.125	4.663	4.069	4.24	4.771	4.957	4.589	4.827	4.682	4.727
OCT	5.641	5.500	4.954	4.783	5.347	5.623	5.518	5.54	5.243	5.297
NOV	5.649	5.624	5.007	4.931	5.65	5.674	5.553	5.52	5.559	4.766
DEC	5.381	5.074	4.446	4.501	5.121	5.165	4.975	5.251	5.072	4.81

AVERAGE	5.524	5.122	4.729	4.567	5.277	5.372	5.011	5.323	5.153	4.814
----------------	--------------	--------------	--------------	--------------	--------------	--------------	--------------	--------------	--------------	--------------

Source: (SWERA, 2003)

Table 2.4: Peak Sun Hours (Hours/Day) Data for KNUST

Months	1995	1995	1997	1998	1999	2000	2001	2002	8-YEAR AVERAGE
JAN	3.534	7.132	6.876	7.335	7.335	3.775	3.790	3.906	5.460
FEB	4.727	7.031	4.631	-	4.727	4.923	4.520	3.905	4.923
MAR	4.151	-	9.501	5.335	4.151	5.028	5.197	5.114	5.497
APR	3.445	4.940	10.211	3.445	4.826	5.406	5.360	5.198	5.354
MAY	5.335	-	4.897	5.335	5.333	5.151	5.335	5.169	5.222
JUN	4.943	8.086	8.711	4.950	4.940	4.178	5.361	4.401	5.696
JUL	3.905	7.852	6.866	7.892	3.905	3.590	3.759	3.610	5.172
AUG	3.635	6.464	3.635	6.464	3.637	3.243	2.773	3.047	4.112
SEP	3.445	6.716	6.942	4.926	3.444	3.294	3.358	3.633	4.470
OCT	5.287	8.423	5.287	4.022	4.151	4.196	4.615	4.856	5.105
NOV	4.563	9.880	-	4.824	4.826	4.581	4.654	4.832	5.451
DEC	5.287	6.570	6.57	4.030	4.027	3.436	3.640	3.969	4.691
Annual Average	4.355	7.309	6.739	5.323	4.609	4.233	4.364	4.303	5.096

Source: (Akuffo F. O., Forson, Agbeko, Edwin, Sunnu, & Brew-Hammond, 2004)

2.7. COMPONENTS OF OFF-GRID PV SYSTEM WITH BATTERY BACKUP

Providing solar energy for off-grid refrigeration normally requires four major components namely, solar PV generator (module), battery backup, inverter, charge controller if not included

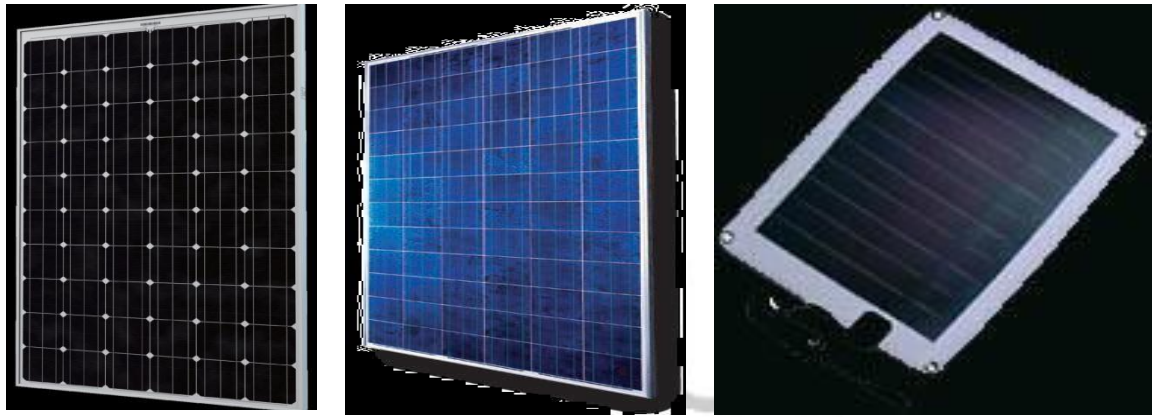
in the inverter). In the current study, the use of inverter was eliminated because the load (refrigerator) requires the supply of direct current from the PV generator. Therefore, this review did not cover power inverters.

2.7.1. Solar Modules and Types

For almost all applications, the one-half volt produced by a single cell is too little. Therefore, cells are connected together in series to increase the voltage. Several of these series strings of cells may be connected together in parallel to increase the current as well. These interconnected cells and their electrical connections are then sandwiched between a top layer of glass or clear plastic and a lower level of plastic or metal to form a solar panel (Shankar, Nawaz, & Ankur, 2012) (Polar Power, 2001).

Solar modules are rated in Peak Wattage which represents the power that the panel can produce at standard test conditions of 1000 W/m^2 of sunlight ('peak sun'); 25°C ; and air mass of 1.5. Generally, the output of solar panels varies depending upon: the amount of solar radiation; the temperature of the module (output decreases as temperature rises); the voltage at which the load (or battery) is drawing power from the module, shading etc. due to the above fact, solar panels seldom produce their rated capacities, hence to ensure that the required amount of energy is produced by the panels to run the refrigerator as well as charge the batteries, the peak sun hours of the location is a critical factor that determines the size of solar panel.

There are three main types of solar cells used in solar system today. They are monocrystalline, polycrystalline and amorphous cells. Pictures of the various types of solar PV systems are presented in Figure 2.12.



Mono-crystalline panel Poly crystalline panel Amorphous panel **Figure 2.12**

Types of Solar Modules

According to Tatsuo (2010), standard poly-crystalline industrial cells offer efficiencies between 15–17%, while mono-crystalline PV cells remain in the range of 16–18% and amorphous solar cells 5%. The efficiency of a solar cell is the ratio of the power produced by the cell to the power impinging on the cell. Reasons for the loss of efficiency include grid coverage, reflection loss and spurious absorption (some of the electrons ejected from their shell are absorbed by impure atoms in the crystal). Amorphous solar cells are the cheapest of all the solar cells, but the challenges of stability and its degradation of performance over time have not made it very popular.

2.7.2. Charge Control Unit/ Charge Regulator

The CCU is the component that regulates the flow of electricity from the solar panel into the load or storage system. In photovoltaic systems the charge controller is used between solar module and battery bank. The main work of a charge controller is to protect the battery from deep discharging and overcharging (Abhishek & Karale, 2013). The common types of charge controllers are the Pulse Width Modulated (PWM) and the Maximum Power Point Tracking (MPPT). PWM is the traditional style types of charge controllers, they are less expensive and very robust, however, they are less efficient in terms of charging the battery bank. On the other

hand MPPT provides the most efficient technology of charging the battery bank. The MPPT is capable of detecting the optimum operating voltage and amperage of the solar panel array and match that with the battery bank. In effect the MPPT is capable of adding 15-30% more power out of the solar array. However, they are more expensive compared with the PWM hence they are best used for solar systems with over 200Wp.

2.7.3. Solar Batteries

Batteries are recognized as the heart of an off-grid photovoltaic system with battery backup. The SPV system does not include any other auxiliary energy sources, such as diesel generators or wind generators. The battery in the system only stores energy when the solar power is higher than load demand; excess power is used to charge the battery. When the solar power is lower than the load demand during cloudy or rainy days or at nights, the battery provides the deficient part of power or full power to the load. In sizing the battery bank the following design parameters are paramount

Designed Number of Days of Autonomy of Solar PV System

This represents the number of days that the battery must support the refrigerator without relying on the solar PV. The sun does not shine with equal intensity every day, at night and during inclement weather. Cloud cover, rain, etc., diminishes the daily insolation. To ensure consistent power supply to the refrigerator during such periods a storage factor must be employed to allow the photovoltaic battery system operate reliably throughout these periods.

The number of days is established by evaluating the peak hours per day (h/day) for the lowest insolation month of the year; the minimum number of days that should be considered is 5 days of storage for even the sunniest locations on earth. In these high sun locations, there will be days when the sun is obscured and the desired battery's average daily depth of discharge is

limited to 20%. Therefore, the recommended days of autonomy storage are presented in Table 2.5.

Table 2.5: Recommended Days of Autonomy for Storage

Peak sun hours	Days of Autonomy
4.5+	5
3.5 to 4.5	6
2.7 to 3.5	7
2.0 to 2.7	8
<2.0	Up to 14

Source: (Concorde, 2006)

According to the solar refrigerator performance specification published by the World Health Organization (WHO, 1988), all solar direct drive refrigerators must pre-qualify with at least a minimum autonomy of three (3) days at the specified solar radiation reference period and temperature.

Temperature correction factor

The temperature of the battery can be a major factor in sizing the system. Lead acid battery capacity is reduced in cold temperatures similarly its life is shortened in high temperatures. The temperature of the battery and ambient temperature can be vastly different. While ambient temperatures can change very quickly, battery temperature change is much slower. This is due to the mass of the battery. It takes time for the battery to absorb temperature and it takes time for the battery to relinquish temperature. In many cases it can be difficult or impossible to heat or cool the battery hence it is necessary to take temperature into consideration. A battery that is required to operate continuously at 0° F (-18 °C) will provide about 60 % of its capacity. This same battery operated continuously in a 95° F (35 °C) environment can lose half its expected life. Temperature affects performance, life, and recommended charging voltages

The operating temperature helps in selecting the appropriate design or temperature correction factor for the battery bank, the design factor depends on the battery's average temperature during the coldest time of the year. The capacity of battery cells are typically quoted for a standard operating temperature of 25°C therefore where this differs with the installation temperature, a correction factor must be applied. Based on the expected lowest ambient temperature of the place where a battery bank would be stored a design factor must be selected from Table 2.6.

Table 2.6: Battery Design Temperature Correction Factor

Battery Temperature	Multiplier
80°F/26.7°C	1.00
70°F/21.2°C	1.04
60°F/15.6°C	1.11
50°F/10.0°C	1.19
40°F/4.4°C	1.30
30°F/-1.1°C	1.40
20°F/-6.7°C	1.59

Maximum Depth of Discharge

The maximum depth of discharge of the battery represents the percentage of the battery's capacity that can be discharged without causing harm to the life of the battery. For instance, a depth of discharge (DoD) of 70% will mean that the battery can be discharged to 70% of its full capacity without any worries. Once it reaches this level, the battery has to be recharged again so that it can still function to provide power to the load. It's recommended that a deepcycle battery should not be discharged below 50% of its capacity; however, many battery manufacturers recommend even shallower DoDs. For off-grid applications, a 25% DoD will extend battery life significantly. On the other hand, if the batteries are to be used occasionally, as a backup system, then a DoD of 50% or perhaps more can be used. There is always a trade-off between the depth of discharge and battery life. Figure 2.13 shows the relationship between

depth of discharge and number of cycles a battery can give for the entire life. As a design requirement, batteries are not supposed to be discharged completely. The recommended limit of depth of discharge is 80% or less.

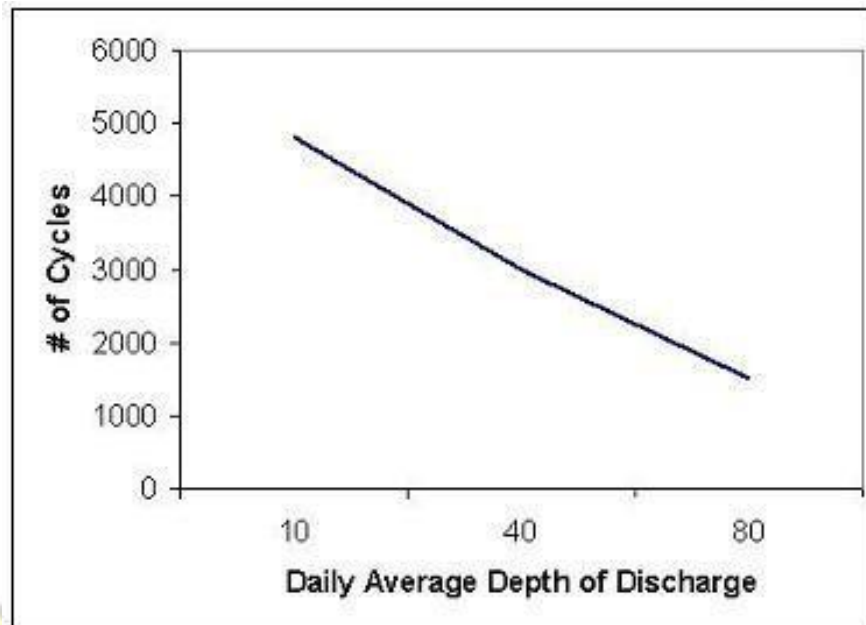


Figure 2.13: Relationship Between Number of Cycles Source: (Btek Renewable Energy, and Daily Depth of Discharge 2000)

2.7.4. Types of Solar Batteries

There are two main types of batteries commonly used in solar PV systems, namely flooded lead acid (FLA) battery and valve regulated lead acid (VRLA) /sealed battery. Valve regulated lead acid batteries can further be classified into Gelled Electrolyte (GEL) and Absorbed Glass Mat (AGM). These are discussed in the following sections.

2.7.4.1. Flooded Lead Acid (FLA)

Flooded lead acid batteries are the most commonly used batteries in stand-alone and grid connect photovoltaic systems because they have longer life and least cost per amp-hour of any of the choices. The

downside, however, is that they require regular (every 3 months) maintenance in the form of watering, equalizing charges and keeping the terminals clean.



Figure 2.14: A 12 Volts Flooded Lead Acid Battery

2.7.4.2. Gelled Electrolyte Sealed Lead Acid (GEL)

Gel sealed batteries use silica to stiffen or “gel” the electrolyte solution, greatly reducing the gasses, and volatility of the cell. Since all matter expands and contracts with heat, batteries are not truly sealed, but are "valve regulated". This means that a tiny valve maintains slight positive pressure. AGM batteries are slowly phasing out gel technology, but there still are many applications for the gel cells. The recharge voltage for charging Gel cells are usually lower than the other styles of lead acid batteries, and should be charged at a slower rate. When they are charged too fast, gas pockets will form on the plates and force the gelled electrolyte away from the plate, decreasing the capacity until the gas finds its way to the top of the battery and recombines with the electrolyte.

2.7.4.3. Sealed Absorbed Glass Mat (AGM)

Absorbed Glass Mat (AGM) is a class of valve-regulated lead acid battery (VLRA) in which the electrolyte is held in glass mats as opposed to freely flooding the plates. Absorbed glass

mat sealed lead acid batteries are completely sealed and cannot be spilled therefore they do not require periodic topping of water level and emit no corrosive fumes; they can hold roughly 1.5 times the amp hour capacity of a similar size flooded battery due to their higher power density. Their advantages include that their electrolyte does not satisfy and no equalization charging is required. The main disadvantage of this battery is the cost per amphour.



Figure 2.15: A 12V Absorbed Glass Mat Battery

Based on the knowledge and information obtained from the literature, the specific objectives for this research work were developed. The specific objectives and tasks as presented in Chapter 1 have been addressed by developing the necessary methods and materials to meet the overall goal of this research work. The methods and materials which were developed to achieve the specific objectives are presented in Chapter 3 below.

CHAPTER 3 MATERIALS AND METHODS

3.0. INTRODUCTION

The methodology used in this study for converting a conventional AC refrigerator to a standalone solar powered DC refrigerator has been grouped under three major sections.

The first section discusses the design considerations and procedure of converting a conventional AC refrigerator to serve as a solar powered one; the second section captures the design of a solar PV system for powering the converted refrigerator. The last section, however,

comprises of the experimental setup and theoretical formulation used to study the performance of the DC refrigerator compared to a base system (AC refrigerator). Figure 3.1 shows a schematic diagram of the methodology used in this research work.

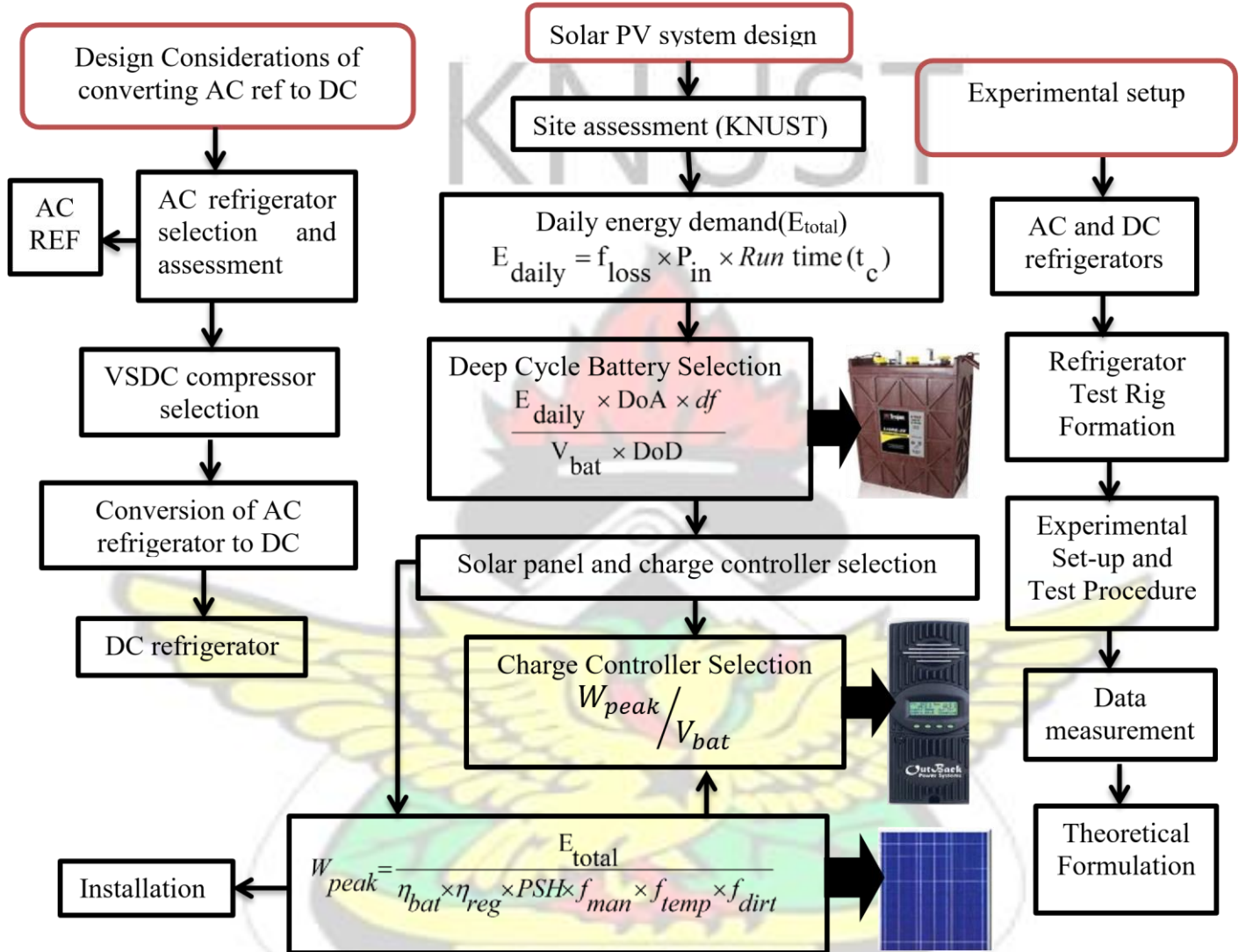


Figure 3.1: Schematic of the methodology of converting a conventional AC refrigerator to solar refrigerator

3.1. CONVERTING AN AC REFRIGERATOR TO DC REFRIGERATOR

This section presents the design considerations and procedures for converting a conventional AC refrigerator to serve as a stand-alone solar powered DC refrigerator. These steps were developed based on knowledge obtained from the open literature and interaction with heating, ventilation and air-condition (HVAC) companies such as Danfoss and Aspera. Theoretically, the domestic refrigerator comprises of a thermally insulated cabinet and a vapour-compression refrigeration loop. In conventional refrigerators, the refrigerant is circulated by an AC

compressor relying on AC power source. To convert such a system to a stand-alone DC power dependent, the AC compressor of the cooling unit is replaced with an equivalent DC compressor. This makes it possible to power the system with direct current from a stand-alone solar PV system without an inverter. Therefore the major work of the conversion process is based on the selection of appropriate DC compressor to replace the existing AC compressor. Apart from the bulb inside the refrigerator cabinet, all other components such as the evaporator, condenser, capillary tube and thermostat do not require replacement. In this study it was desired to use variable speed direct current (VSDC) compressor instead of a single speed compressor due to their numerous advantages discussed in section 2.3.4.2. To ensure appropriate VSDC compressor design selection, adequate knowledge of the characteristics of the AC refrigerator and its corresponding compressor to be converted is paramount. The next section looks at the procedure used to assess the AC refrigerator to be converted.

3.1.1. Assessment of the Selected AC Refrigerator to be Converted

The starting point of the conversion process is the selection of an AC refrigerator to be converted. In this study, two identical (same performance characteristics) domestic AC refrigerators of 92 L volume were obtained from the open market (one of the common refrigerator sizes in Ghanaian homes). One is converted to DC while the other serves as a control system. The refrigerator to be converted was assessed to enable the selection of appropriate VSDC compressor for this work. Presented in Table 3.1 are the technical specifications of the AC refrigerator.

Table 3.1: Technical specifications of Selected AC Refrigerators.

REFRIGERATORS	
Type	Brand-new/Domestic / Refrigerator only/Table top / Single door
Brand	Nakai
Climate Class	sub-tropical

Power rating	60 Watt
Rated current	0.5 A
Energy efficiency rating	Three star / 135kWh/year
Foaming (insulation material)	Cyclopentane
Weight	21kg
Volume	92 litre
Refrigerant	R-600a (18g)
Condenser	External natural convection air cooled wire- on-tube arranged in a serpentine manner in a vertical plane
Evaporator	Flat plate
Type of expansion device	Capillary Tube
Compressor model	VY33R45A
Cooling Capacity at ASHARE test conditions	50 W
Compressor type	Hermetic Reciprocating
Refrigerant	R600a
Application	LBB
Evaporating temperature range	-25°C to +5°C
Energy source	220-240V AC, 50 hertz
Speed (RPM)	Single Speed 3000 RPM

3.1.2. Selecting a Variable Speed Direct Current Compressor

Based on the above system characteristics of the AC refrigerator, two VSDC Compressors namely BD 35 F and BD 50 F were identified as the best replacement for the AC compressor.

Both compressors are designed for low, medium and high back pressure applications (thus evaporator temperature range of -30°C to +10°C). They are of the same size externally, but the BD 50 F has 30% greater capacity with a -12 °C evaporator temperature than the BD 35

F. Presented in Table 3.2 and Table 3.3 are the cooling capacities of the two compressors by ASHRAE standards.

Table 3.2: Cooling capacities of Danfoss BD50F compressor

Capacity (ASHRAE)										watt
rpm \ °C	-30	-25	-23.3	-20	-15	-10	-5	0	5	10
2,000	24.7	38.3	43.1	52.9	69.5	89.3	113	143	178*	221*
2,500	33.3	48.1	53.6	65.0	85.1	110	140	178*	224*	
3,000	38.2	56.0	62.5	75.9	100	129	166*	212*		
3,500	47.0	65.7	72.9	88.7	117	153*	196*			

Table 3.3: Cooling Capacities of Danfoss BD35F Compressor

Capacity (ASHRAE)										watt
rpm \ °C	-30	-25	-23.3	-20	-15	-10	-5	0	5	10
2,000	19.5	29.4	33.1	40.7	54.0	69.8	88.6	111	137	169
2,500	24.9	36.8	41.3	50.7	67.3	87.1	111	139	172	
3,000	27.7	39.9	44.9	55.9	76.1	101	130	164		
3,500	32.2	44.2	49.7	62.2	86.0	115	150			

Source: (Danfoss, 2007)

Though the compressors have different capacities at different evaporator temperatures, the standard adopted by ASHRAE is to rate low back pressure (LBP) application compressors at evaporator temperature of -23.3 °C. Therefore, from Table 3.2 and Table 3.3 the rated capacities of the BD 35 F and BD 50 F compressors at maximum speed are approximately 50 W and 73 W respectively.

Though, both compressors (BD 35F and BD 50F) can be a good replacement for the existing AC compressor, the BD 35F was selected over the BD 50F for this experimental study due to its availability in the Ghanaian market. The next section gives detailed description of the selected compressor.

3.1.3. Description of VSDC Compressor (BD 35F) and Electronic Control Unit

The compressor is designed for connection to 12V or 24V DC power supply and for refrigerant R134a (CF₃-CH₂F). The compressor is suitable for use in mobile applications such as cooling boxes, boats, caravans, trucks, vans and buses. In additions, it can be used in stationary applications powered by photovoltaic solar panels such as used in this thesis due to their low energy consumption and the option for a wide supply voltage range. This is the same type of

compressor used on commercially available solar refrigerators such as Sun Frost units. It can be used in refrigerators and freezers designed for capillary tube and thermostatic expansion valve (TEV) as the throttling device (Danfoss, 2007). Figure 3.2 shows the selected BD 35 F compressor.

Source:



(Danfoss, 2007)

Figure 3.2: Variable Speed Direct Current Compressor (VSDC)

The BD 35F VSDC compressor concept includes an electronic unit which features overload and battery protection. The compressor has four different speeds of 2000 RPM, 2500 RPM, 3000 RPM, and 3500 RPM. The electronic control unit (shown in Figure 3.3) has internal voltage recording and calibration to the applied voltage.



Source: (Danfoss, 2007)

Figure 3.3: Electronic Control Unit for VSDC Compressor BD 35F

One advantage of this compressor is the ability to connect it directly to a PV or other source of DC energy supply without an inverter. In addition to being quiet in operation, the compressor has a good COP values. Though most household refrigerators operate at -8°C (Cengel & Boles, 2006), this compressor is capable of reaching storage temperatures down to -30°C . The various performance parameters of ASHRAE standard of the compressor at different speeds are presented in Table 3.4.

Table 3.4: Performance data of BD 35F VSDC compressor at STCs

Capacity (ASHRAE)										watt
rpm \ °C	-30	-25	-23.3	-20	-15	-10	-5	0	5	10
2,000	19.5	29.4	33.1	40.7	54.0	69.8	88.6	111	137	169
2,500	24.9	36.8	41.3	50.7	67.3	87.1	111	139	172	
3,000	27.7	39.9	44.9	55.9	76.1	101	130	164		
3,500	32.2	44.2	49.7	62.2	86.0	115	150			

Power consumption										watt
rpm \ °C	-30	-25	-23.3	-20	-15	-10	-5	0	5	10
2,000	17.6	23.4	25.3	28.7	33.6	38.3	43.0	48.0	53.4	59.5
2,500	23.3	30.9	33.3	37.8	44.1	50.2	56.2	62.3	68.7	
3,000	29.9	36.0	38.3	43.0	50.7	58.7	66.8	74.8		
3,500	36.0	42.8	45.4	50.8	59.5	68.9	78.5			

COP (ASHRAE)										W/W
rpm \ °C	-30	-25	-23.3	-20	-15	-10	-5	0	5	10
2,000	1.10	1.25	1.31	1.42	1.61	1.82	2.06	2.31	2.57	2.84
2,500	1.07	1.19	1.24	1.34	1.53	1.74	1.97	2.23	2.50	
3,000	0.93	1.11	1.17	1.30	1.50	1.72	1.95	2.20		
3,500	0.89	1.03	1.09	1.23	1.44	1.68	1.91			

Source: (Danfoss, 2007)

3.1.4. Conversion of a 92 L AC Refrigerator to DC Refrigerator

To convert the AC refrigerator to DC, the AC compressor on the conventional refrigerator was removed. The system was then evacuated (of the refrigerant R600a, air and moisture). The dryer of the system was also replaced. The selected VSDC compressor (Danfoss BD 35F) was then mounted on the compressor seat; both the discharge and suction copper tubes of the compressor were brazed to the condenser and evaporator respectively. The electronic control unit of the compressor was also installed. The system was then charged with the required mass of R134a. The system was then connected to a DC source as shown in Figure

3.4.

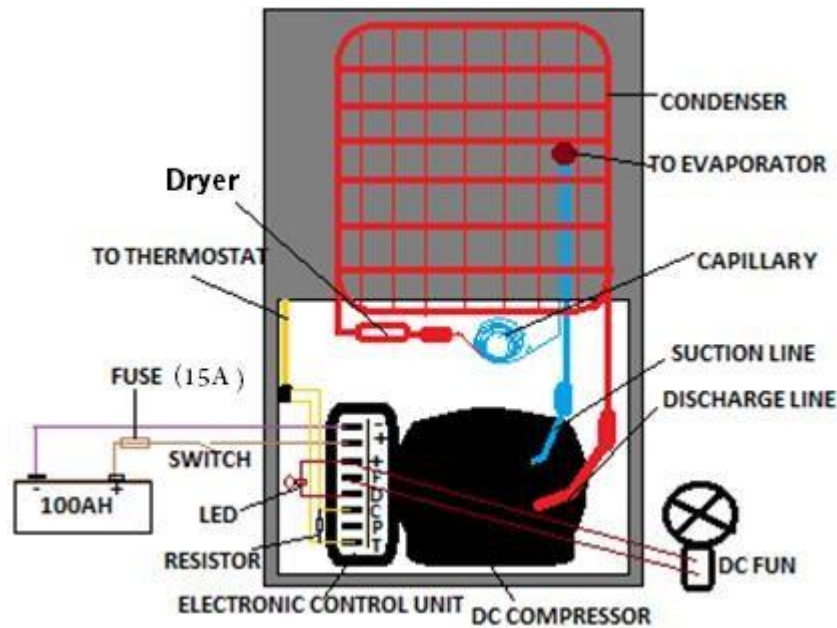


Figure 3.4: Schematic of the DC Refrigerator Connected to 12 Volts Solar Battery

3.2. DESIGNING A STAND-ALONE SOLAR PV SYSTEM FOR THE CONVERTED SOLAR POWERED DC REFRIGERATOR

Solar energy is geographically distributed and highly dependent on location, changing weather and climate conditions. This makes their direct control extremely challenging and requires proper sizing and system optimization to ensure maximum power generation. This section discusses the approach used in sizing the various components of the system (solar PV Panel, Charge controller and battery Bank). Column 2 of Figure 3.1 shown above is a summary of the steps used to design the solar PV system. The schematic of the solar PVrefrigeration system is shown in Figure 3.5. It is composed of four major parts; i) the refrigeration unit (refrigerator), ii) the energy production unit (PV panels), iii) the energy control unit, and iv) the energy storage unit (the battery bank).

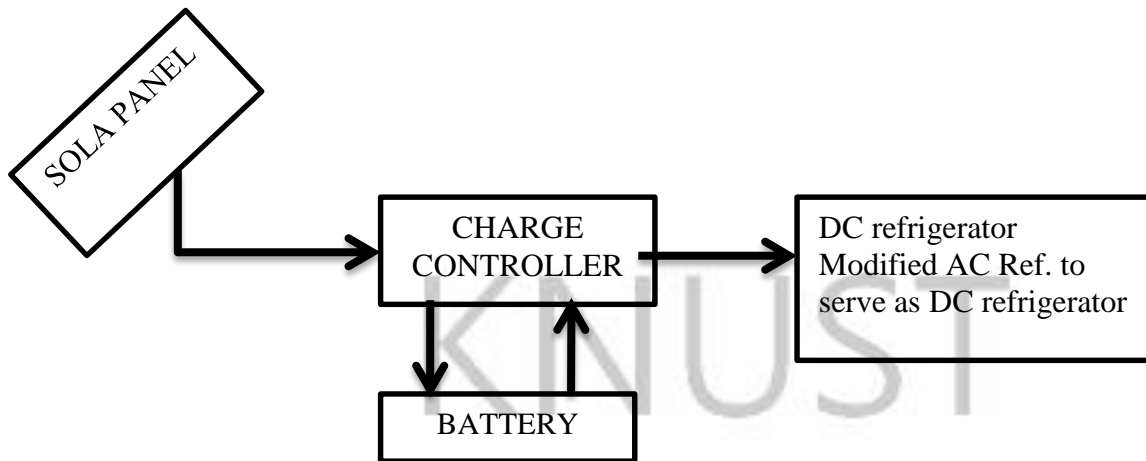


Figure 3.5: Schematic of the Solar Powered DC Refrigeration System

3.2.1. Solar Resource Assessment of Selected Site (KNUST-Kumasi)

According to NABCEP (2009) and Nyarko-Kumi (2012), the planning of a solar PV system involves a number of assessments such as site and solar energy potential. These include; assessment of roof properties such as the roof type, area, pitch/slope, the strength of the roof, location of the array, shaded during critical hours (thus 9 a.m. to 3 p.m.). In the current study, premium was placed on the solar resource assessment of the selected site (KNUST-Kumasi). An earlier research by Akuffo et al. (2004), at the same laboratory where this experiment is conducted found the average monthly solar irradiation for KNUST-Kumasi as presented in Table 3.5.

Error! Reference source not found.: **Monthly Mean Solar Irradiation Data for KNUST kWh/m² - day)**

Months	8-YEAR AVERAGE (1995-2002)
JAN	5.460
FEB	4.923
MAR	5.497
APR	5.354
MAY	5.222
JUN	5.696
JUL	5.172
AUG	4.112
SEP	4.470
OCT	5.105

NOV	5.451
DEC	4.691
Annual Average	5.096

Source: (Akuffo *et al.*, 2004)

For the purpose of the solar PV system design, the minimum monthly solar irradiation is used in determining the peak sunshine hours. This approach is usually required for the design of solar PV systems (designing for worst conditions).

3.2.1. Peak Sun Hours of KNUST- Kumasi

Performance of a stand-alone solar PV system depends largely on the peak sun hours of the location of application. The peak sun hour(s) of an area is determined from the available solar irradiance of the location. The peak sun hours and total irradiation are related by Equation 3.1.

$$\text{PSH} = \frac{\text{Irradiation } \text{Wh m}^{-2} \text{ day}^{-1}}{1000 \text{ Wh m}^{-2} \text{ day}^{-1}}$$

Equation 3.1

Peak Sun m²

By definition Peak Sun is equivalent to 1000 $\text{Wh m}^{-2} \text{ day}^{-1}$ or $1 \text{ kWh m}^{-2} \text{ day}^{-1}$ therefore the number

of peak sun hours can be obtained by equation 3.2 using irradiation data from Table 3.5.

$$\text{Irradiation } \text{Wh m}^{-2} \text{ day}^{-1} \div 1000 \text{ Wh m}^{-2} \text{ day}^{-1} = \text{Peak Sun hours}$$

$$PSH = \frac{\text{m - day} \times 1000 \times W_2}{m}$$

Equation 3.2 The PSH

is determined and presented in chapter four (4) in the results and discussions.

3.2.2. Solar PV System Component Selection

The major components of the solar PV system as shown in Figure 3.5 are: a deep cycle battery, solar panel and a charge controller. The size of each component depends on the required energy input of the refrigerator and a specified number of days of autonomy. The following sections document the various design considerations and sizes of components required.

3.2.2.1. Sizing Battery Bank (AH)

The sun does not shine with equal intensity every day, at night and during inclement weather, hence the use of batteries is inevitable in the design of a stand-alone solar PV system where consistent supply of power, such as refrigeration, is critical. Sizing of the battery bank is a very critical task in the design of standalone systems. For oversized battery bank, there is a high risk of not being able to keep it fully charged. On the other hand, if the battery bank is sized too small, it won't be able to run the intended load. It is also worth noting that for system optimization purposes; it is recommended to use 12 Volt batteries for panel with peak wattage less than 300W, 24 volt battery for panels with 300 W to 1000 peak wattage. Panel wattages higher than 1000W up to 4000W must use 48 volts. In this study the batteries were sized based on the following design parameters:

1. Watt Hours of electricity used per day by the refrigerator
2. Number of Days of Autonomy
3. Ambient temperature of battery bank
4. Depth of Discharge (limitation of the battery discharge)

The required capacity of the battery bank was determined by equation 3.3.

$$C_{bat} = \frac{E_{total}}{V_{bat} \cdot DoD_{max}} \quad \text{Equation 3.3}$$

Where:

$$E_{total} = (f_{losses} + 1) \cdot P \cdot t_c$$

E_{total} represents the total daily energy demand of the refrigerator in Wh
 f_{losses} is system wiring losses taken as 5% of daily energy demand.
 P is the compressor power consumption; t_c is the compressor run time

f_{losses} is system wiring losses taken as 5% of daily energy demand.

DoD_{max} is the depth of discharge; DoA (days of autonomy) representing the number of days the battery must support the refrigerator without relying on the solar panel. V_{bat} is the specified voltage of the battery bank, typically 12 V for small systems (< 1 kWh).

For the purpose of temperature correction in sizing the battery equation 3.3 is redefined with a correction factor (df) as given in equation 3.4.

$$C_{bat} = \frac{E_{total}}{V_{bat} \cdot DoD_{max} \cdot df} \quad \text{Equation 3.4}$$

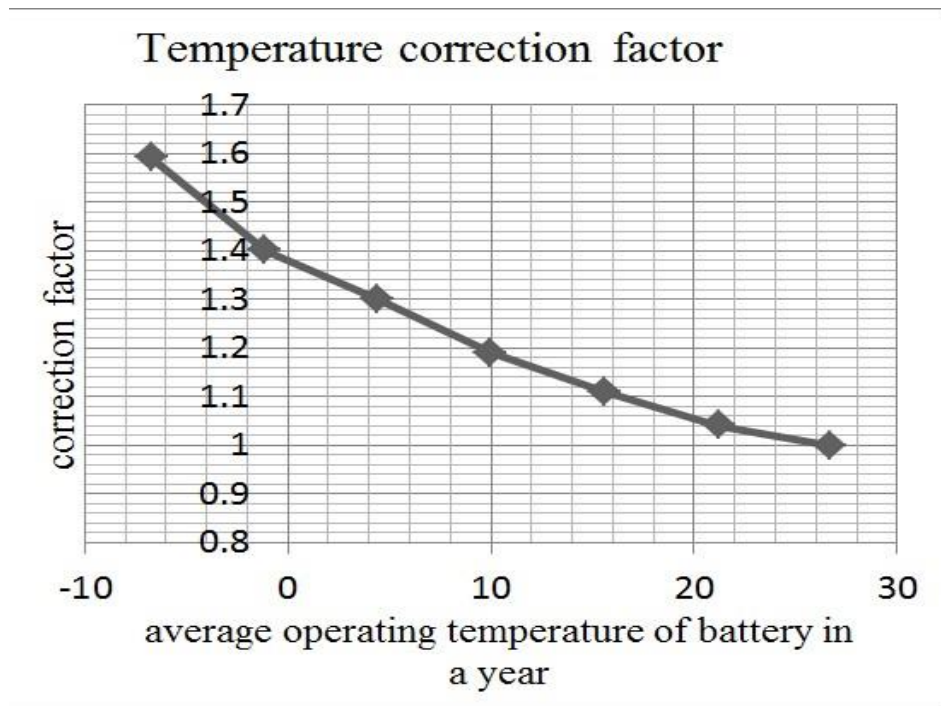


Figure 3.6: Temperature Correction Graph Source: (Solar Energy International, 2004)

For Ghana, particularly Kumasi where KNUST is situated, the average ambient temperature is about 25 degree Celsius; therefore a temperature correction factor of 1 is used.

3.2.2.2. Sizing Solar PV Panel

The required wattage of the solar panel depends on the amount of energy needed to replace energy drawn from the battery by the refrigerator per day. The energy demand from the solar panel depends on: the power consumption of the refrigerator, compressor running time of the refrigerator per day, inefficiencies in the solar PV system and the peak sun hours of the location. These parameters are related mathematically by Equation 3.5.

$$W_{\text{panel}} = \frac{E_{\text{total}}}{\eta_{\text{bat}} \eta_{\text{reg}} \text{PSH}}$$

Equation 3.5

Where:

PSH is the peak sun hours of the location where the system would be installed, η_{bat} and η_{reg} are the efficiencies of battery and charge controller.

To determine the Peak Wattage of the solar PV panel at standard test conditions, Equation 3.5 is modified as presented by Equation 3.6.

$$W_{peak@stc} = \frac{W_p}{\eta_{man} \eta_{temp} \eta_{dirt}} \quad \text{Equation 3.6}$$

Where: η_{man} is the manufacture's tolerance for the solar panel

$\eta_{temp} = 1 - \gamma (T_{temp} - 25)$
 η_{temp} is the temperature correction factor given as γ is a temperature co-efficient (which depends on the type of solar PV module) η_{dirt} is derating factor for dirt.

3.2.2.3. Sizing Charge Controller

The size of charge controller in amps is determined by equation 3.7 as follows:

$$C_c = \frac{W_{panel}}{V_{bat}} \quad \text{Equation 3.7}$$

3.2.3. Parametric Study

The above equations for determining the sizes of the components of the solar PV system were programed in MATLAB® using design factors and parameters presented in Table 3.5.

Table 3.5: Design parameters and equation for parametric study

PARAMETER	SYMBOL	VALUE	UNIT
Day of Autonomy	DoA	1 to 5 [1, 2, 3]	days
Battery Efficiency	η_{bat}	85	%

Charge Regulator Efficiency	η_{reg}	85	%
Voltage of Battery Used	V_{bat}	12	Volts
Depth of Discharge	DoD	70	%
Peak Sun Hours - thus for kumasi	PSH	5.1	hrs/day
Solar PV Panel Manufacture's Tolerance (obtained from the selected Solar panel's catalogue)	f_{man}	90	%
Effect of Dirt/Shading on Panel Performance (obtained from the selected Solar panel's catalogue)	f_{dirt}	97	%
Compressor Power Consumption	P	50 to 160W	W
Compressor Run Time Per Day	H	8 to 20 [8, 10, 15, 20]	Hours
Calculated parameter		Determined by	
Wiring Losses	f_{losses}	5% of [P_{xh}]	W
Battery Capacity	C_{max}	Equ 3.4	AH
Daily Energy Demand	W_{panel}	Equ.3.5	W_{panel}
Panel Size at STCs	$W_{peak@stc}$	Equ.3.6	W_p
Battery Temperature Correction Factor	D_f	Fig. 3.6	-
Charge Controller Size	C_c	Equ. 3.7	Amps
Solar PV Temperature Correction Factor	γ	0.45	%

3.2.4. Preliminary Results of Parametric Study

The results of the parametric study are presented in Figure 3.7 and Figure 3.8.

Required Solar Panel Size at Different Compressor Run Times

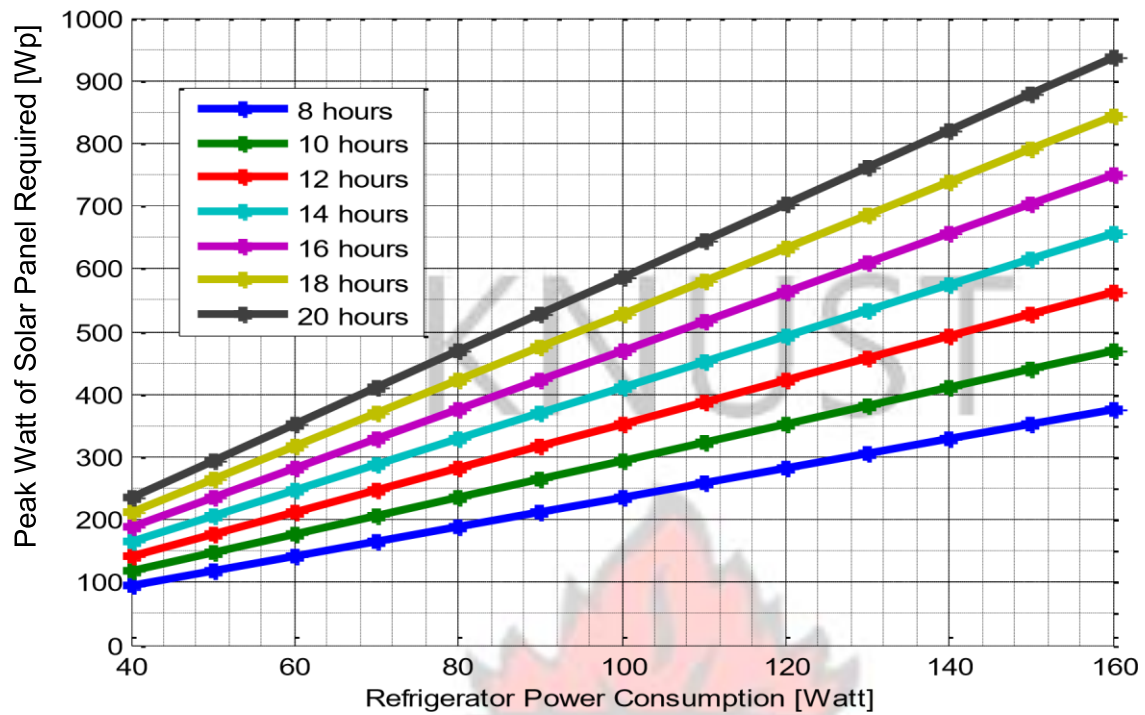


Figure 3.7: Peak Wattage of Solar Panel versus Refrigerator Power Consumption

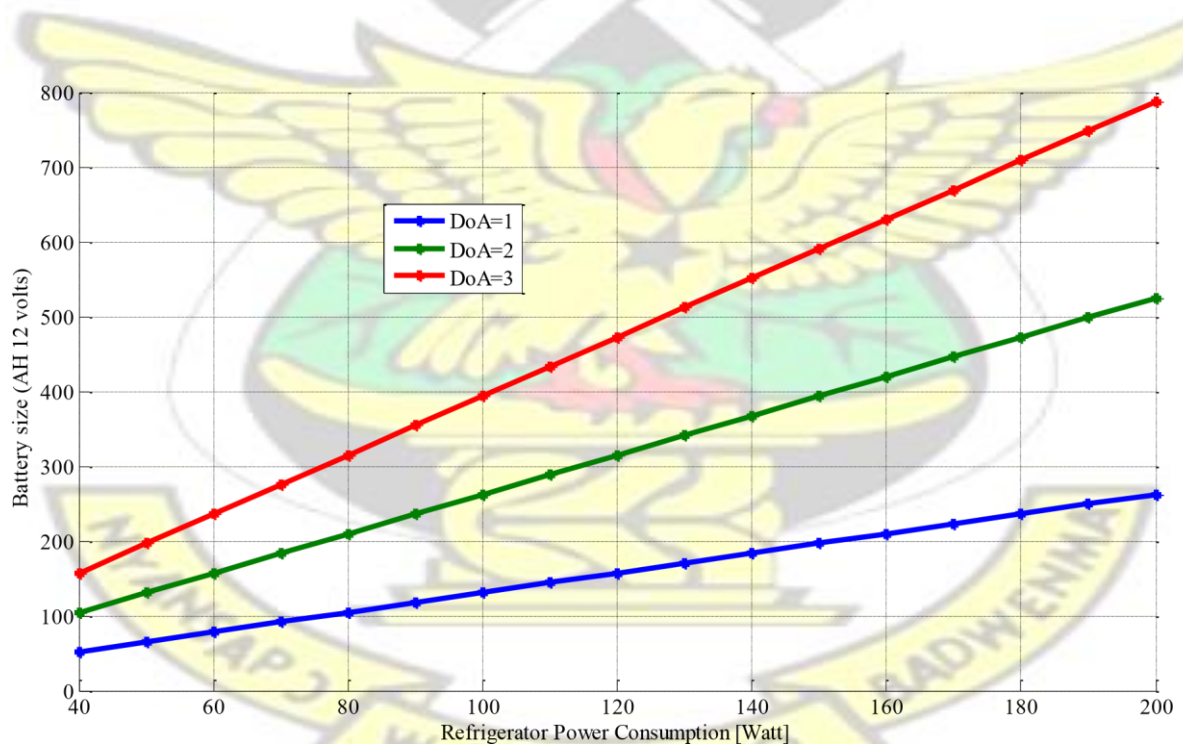


Figure 3.8: Size of Battery Bank versus Refrigerator Power Consumption

From the preliminary results in Figure 3.7 and Figure 3.8, for the required power consumption of 80 W of the refrigerator, 170 W solar panel, a 12 Volts-100 AH deep cycle battery and a 20 A charge controller are determined. These components are installed for the experiment works.

3.3. EXPERIMENTAL AND THEORETICAL FORMULATION

This section presents the methodology used to formulate the refrigerator test rigs, the experiments performed and the theoretical formulations used to determine the performance parameters of the refrigerators in this study.

To achieve this, two identical domestic AC refrigerators were obtained from the open market. These refrigerators have the same technical specifications/characteristics (refer to section 3.1.1.). Prior to the conversion of one of them to a solar one, the performance of both refrigerators was studied. Both AC refrigerators were connected to the national grid (220V to 240V). The evaporators and cabinet of the refrigerators were instrumented with a thermocouple each. A similar thermocouple was also set to measure ambient temperature of the test room. All five thermocouples were connected to a data acquisition system (TC 32K) with dedicated switch box (CSW-5A), a product of Tokyo Sokki Kenkyujo Co., Ltd. This instrument has the capability of automatically logging temperature readings onto an SD card at a pre-set time interval.

Power consumption of each refrigerator was measured with a digital energy meter. All experiments were conducted at room temperature. The power consumption and evaporator temperature profile of both refrigerators were recorded every minute for four hours. It was observed that both refrigerators give the same performance characteristics, in terms of power consumption and thermal characteristics of the refrigerator cabinet and evaporator.

After confirming that both refrigerators give the same results under the same test conditions, the design considerations discussed in section 3.1 were used to convert one of the refrigerators to DC solar powered refrigerator, hereinafter referred to as solar powered DC refrigerator/ solar refrigerator. The designed considerations proposed in section 3.2 were used to size and install a solar PV system for powering the solar refrigerator.

3.3.1. Formulation of Experimental Set-up

Based on the objectives of this thesis, two separate experimental setups were developed. The first set-up was used to conduct an optimisation and performance study of the solar powered DC refrigerator. The second set-up on the other hand, was used to undertake a comparative study of the solar powered DC refrigerator and the AC refrigerator under the same test conditions. The following sections discuss the various components of the experimental setup.

3.3.1.1. AC Refrigerator

The test facility used in this experimental study is a 92 L domestic refrigerator (with AC compressor). It is one of the most commonly used types of refrigerators in Ghana. Details of the AC refrigerator are presented in Table 3.1 above.

3.3.1.2. Solar Powered DC Refrigerator

The solar powered DC refrigerator was developed from an identical AC refrigerator with technical specifications presented in Table 3.1. The refrigerator operates on direct current supplied by the solar PV system. This was possible due to the replacement of the AC compressor with a VSDC compressor. No other components were modified; the DC refrigerator, therefore has the same components as before the conversion, though the system now operates on R134a. The energy requirement and optimum amount of refrigerant required by the system are yet to be determined. Details of the installed compressor are presented in Table 3.6.

Table 3.6: Technical Specification of Variable Speed DC Compressor

TECHNICAL SPECIFICATION				VSDC COMPRESSOR
Manufacturer/ model				Danfoss(Escope) / BD35F
Cooling Capacity at	ASHARE	conditions	test	33.1 W at 2000 RPM 50 W at 3500 RPM

Compressor type	hermetic reciprocating
Refrigerant	R134a (max 300g)
Application	LBP/ MBP/HBP
Evaporating temperature range	-30°C to +10°C
Energy source	12/24V DC
Speed (RPM)	Variable speed 2000 RPM - 3500 RPM

Source: (Danfoss, 2007)

It must be noted that the installed compressor operates at four speeds, thus; 2000 RPM, 2500 RPM, 3000 RPM, and 3500 RPM. To regulate the speed of the compressor, different sizes of resistors were connected to the electronic control unit. Connecting specified sizes of resistance (Table 3.7) to the compressor yields different running speeds. The resistors control the current supplied to the motor which regulates the rotational speed of the compressor (Danfoss, 2007).

Table 3.7: Sizes of Resistors used for Controlling the Speed of the VSDC Compressor

Resistance	Compressor speed	Control Circuit Current mA
0	2000 RPM	5
277Ω	2500 RPM	4
692 Ω	3000 RPM	3
1523 Ω	3500 RPM	2

Source: (Danfoss, 2007)

In the present study, a resistance box is fabricated by connecting 270 Ω and 7 Ω in series to give 177 Ω, similarly 680 Ω is connected in series with 12 Ω to give 192 Ω and finally, 1523 Ω is obtained by connecting 1.5k Ω and 23 Ω in series. In addition, a 220K Ω was also added to the resistance box, and by connecting this to the P and C ports allows the compressor to operate directly from the solar panel without a battery bank.

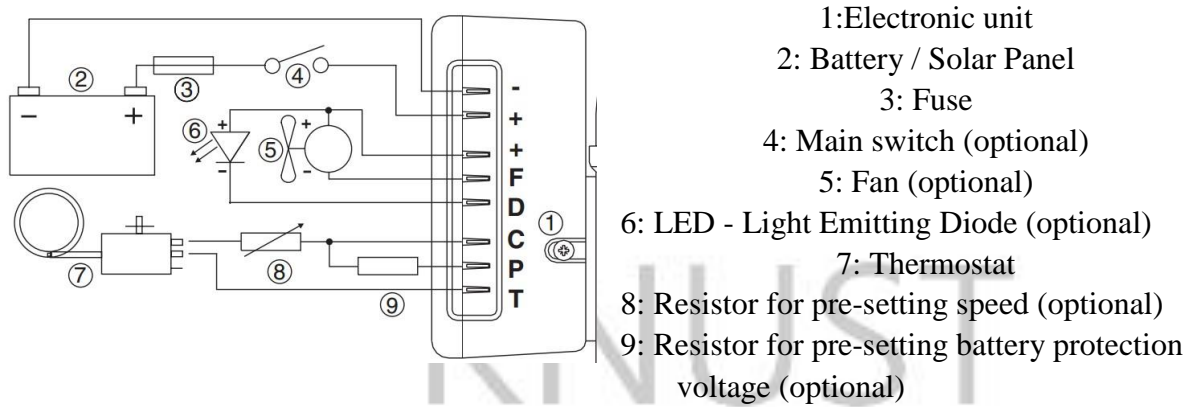


Figure 3.9: Wiring Diagram of Electronic Control Unit of BD 35F Source: (Danfoss, Compressor, 2007)

Figure 3.10 shows the VSDC compressor and a resistance board connected between the P and C terminals of the electronic control unit. With the resistance box in place, the speed of the compressor can be changed based on the selected resistance. In the present study, the current running through the electronic control circuit was verified with the help of a digital multimeter any time the speed of the compressor was changed. This was done to confirm that the compressor is running at the desired output speed.



Figure 3.10: Resistors connected to the Electronic Control Unit of the VSDC Compressor

3.3.1.3. Power Supply (Solar PV System and the Grid)

During the experimental study, the AC refrigerator is connected to the national grid (220/240V) while the DC refrigerator is run by an installed solar PV system. The solar PV system comprises of three main components, thus the solar panel, battery bank and a charge controller. These components are interconnected with 5 mm electrical cables. For the preliminary study, two 85 Wp Suntech photovoltaic panels were installed to provide the needed energy for running the solar powered DC refrigerator. The panels were arranged in series to produce 170 Wp, 12 volt system. The purpose of this arrangement is to have sufficient potential difference across the 12 V battery bank to enhance adequate charging. The solar panels were then connected to a 100 Amp-hour 12V battery via a 20 Amps charge controller. A charge controller is used to step down the high voltage from the PV generator for charging the battery bank as well as prevent the battery from over-charging and fully discharging. The charge controller has six terminals, one–positive–negative terminal pair for connection to the solar panels, one for battery bank and one for load. The solar panel, battery bank and the solar refrigerator were connected to the charge controller as shown in Figure 3.11 below. This kind of arrangement was possible because the charge controller was sized above the maximum current drawn during the compressor start-up. Table 3.10 presents the specifications of the solar panel.



2 X 85 Suntech photovoltaic panels

Connection of DC refrigerator and battery to the charge controller

Table Figure 3.83: Panel specifications (photovoltaic module catalogue11: Connecting the Solar PV System to the DC Refrigerator)

Table 3.9: Specifications of the Installed PV Model

Model	Suntech STP085S-12/Bb
Open - Circuit Voltage (Voc)	22.2V
Optimum Operating Voltage (Vmp)	17.8V
Short - Circuit Current (Isc)	5.15A
Optimum Operating Current (Imp)	4.80A
Maximum Power at STC (Pmax)	85Wp
Operating Temperature	-40°C to +85°C
Maximum System Voltage	715V DC
Total efficiency	13.1%
Maximum Series Fuse Rating	15%
Power Tolerance	±5 %
STC: Irradiance 1000W/m2, Module temperature 25°C, AM=1.5	

Source: (Suntech, 2007)

3.3.1.4. Measuring Instruments

The measuring instruments used in this experimental study are: five thermocouples, three high side and two low side R134a pressure gauges, a DC ammeter, voltmeter, digital AC energy meter and a digital (DC/AC) multi-meter. K - Type thermocouples (Product of Omega Company Ltd) with 0.3 mm diameter designed for a temperature range between -50°C to 250°C is used. Before connecting the thermocouples to the refrigeration system, all five thermocouples obtained from SEAL were calibrated with boiling and ice water. The accuracies of the thermocouples were found to be about $\pm 0.1^\circ\text{C}$. A voltmeter and ammeter were obtained from the Electrical Engineering Department of KNUST. These instruments were calibrated with the help of the digital DC/AC multi-meter. The accuracy of the voltmeter and ammeter were found to be $\pm 0.02\text{ V}$ and $\pm 0.023\text{ A}$ respectively. All 5 pressure gauges (products of Giant Tree Com. Ltd.) and digital energy meter

were obtained from the open market. Table 3.10 presents a summary of the various instruments used and their respective properties.

Table 3.10: Characteristics of the Instrumentation used

PARAMETER	DEVICE/INSTRUMENT	RANGE
Temperature	K-type thermocouple	-50 °C to 250 °C
Pressure	High Pressure Gauge	0 bar to 500 bar
	Low pressure gauge	-30 bar to 300 bar
Power	DC Watt-Meter	0 W to 200 W
	Digital AC Energy-Meter	-
DC current	DC ammeter	0 to 30 A
DC voltage	DC voltmeter	0 to 50 V
Data logger	TC 32K and Switch Box (CSW-5A)	(five channel for temperature measurement)

To determine the energy consumption of the two systems, the digital energy meter is connected between the AC energy source (national grid) and the AC refrigerator. Secondly, the DC voltmeter and ammeter (shown in Figure 3.12) are connected between the DC refrigerator and the solar PV system as shown in Figure 3.11 above.



Digital AC energy meter



DC Voltmeter ammeter, watt meter and digital DC Wattmeter

Figure 3.12: Connection of AC and DC Power Measurement Instruments

During the first set of experiments, the solar powered DC refrigerator loop was instrumented with three K-type (copper–constantan) thermocouples and three R134a pressure gauges for measuring refrigerant temperature and pressure at compressor's discharge, suction and condenser exit temperatures.

The technique used to measure the temperature is the same as the one used by (Philipp, Kraus, & Meyer, 1996), where the thermocouple wire was put inside the refrigerant tube so that the measurement made is exactly the temperature of the refrigerant. Figure 3.13 shows the approach used to connect the temperature and pressure measurement instruments to the refrigerant tube. By using this method, three pressure gauges and four thermocouple wires were connected to the refrigeration system, the low and high side pressure gauges were both connected at a distance of about 300 mm from the compressor. To do this, the discharge, suction, and condenser exit copper tubes were cut with a copper tube cutter and the ends flared with the help of a screw type flaring tool. Prior to the flaring process, a quarter inch nut was connected to each of the connecting lines. Three pieces of a quarter copper tubes were also cut and flared for connecting the thermocouples to the cross fittings. The flared copper pieces were used to hold the thermocouple wires; this was done by inserting the thermocouple into the copper tube and effectively sealed with Araldite, as shown in Figure

3.13. With the help of an adjustable spanner, the flared copper tubes holding the thermocouples were mechanically connected to the cross fitting by tightening all the connecting nuts. The temperature of the refrigerant which now flows through each cross fitting is measured by the thermocouple junction or head.

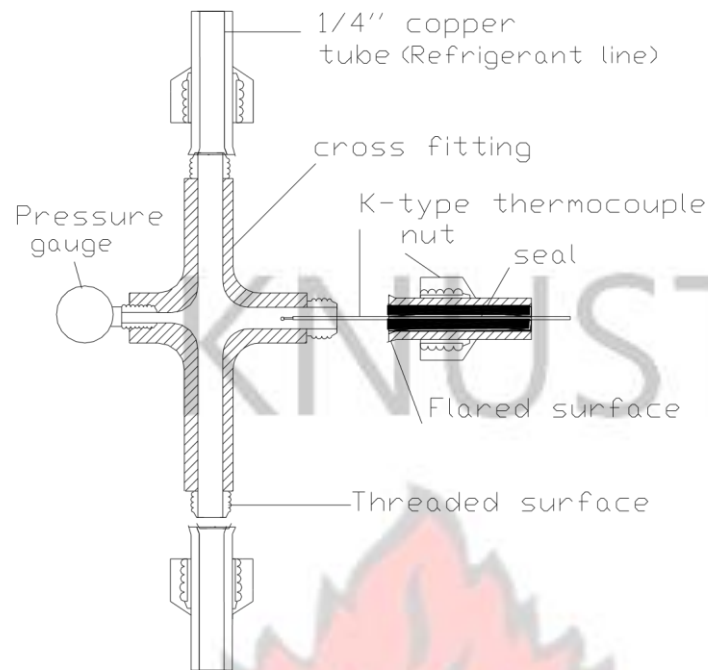


Figure 3.13: Schematic Diagram of the Fabricated Cross Fitting for Connecting the Thermocouples and Pressure Gauges to the Refrigeration Line



Figure 3.14: Location of Pressure Gauges and Thermocouples

3.3.1.5. System Evacuation

After mounting all the measuring instruments, the vapour compression system was initially cleaned by nitriding the entire system, this was later followed by the evacuation process. This was done to get rid of all traces of refrigerant R600a, air, moisture and other foreign materials

inside the system, which could affect the accuracy of the experimental results. The evacuation process was carried out by a Robin A/C smart cart vacuum pump shown in

Figure 3.15.

3.3.1.6. System Charging

Charging of the refrigeration system with a specific amount of refrigerant was achieved with the help of an electronic balance and an R134a two-way valve, double headed (low and high side) pressure gauge with a hand wheel. Charging was done by placing the refrigerant can on the electronic scale. The can was then connected to the pressure gauge with charging hose (yellow). The low side of the pressure gauge was connected to the service port of the compressor using the low side charging hose (blue). The hose was filled with refrigerant and the air inside it was expelled by slightly loosening and re-tightening the connection to the charging valve (yellow). It was ensured that the hose did not move during charging. The weight of the can and refrigerant was read and recorded. Then the charging valve of the pressure gauge was opened gradually. This pushes part of the refrigerant into the refrigeration system. In order to drive a complete charge into the system, the refrigerator compressor was switched on. When sufficient charge (as specified in the experimental procedure) had entered the system, the weight of the refrigerant can and refrigerant was read from the electronic scale. The charging hose was removed and the service port closed with a valve cover. It must be noted that the high side valve was not touched at all during the charging process. Figure 3.15 b shows the set-up for charging the refrigerator with the refrigerant.



a. Vacuum Pump



b. System Charging

Figure 3.15: Evacuation and Charging of the Refrigeration System

3.3.1.7. Leakage Testing

Leakage test was performed over the entire refrigeration circuit and around the connected instruments by using soap solution. Minor leaks were found around areas where the flared copper tubes were connected to the cross fittings. With the help of an adjustable spanner, all leaks were plugged by further tightening the nuts holding the flared tubes to the cross fittings. All leakages were completely sealed with araldite before the actual experiments.

3.3.1.8. Data Acquisition System

During the optimization process, the refrigeration loop is instrumented with three thermocouples as discussed in section 3.3.1.4. Secondly, two similar thermocouples were set to measure the ambient and refrigerator cabinet temperatures. All five thermocouples were then connected to a data acquisition system (TC-32K data logger) via a dedicated switch box (CSW-5A) as shown in Figure 3.16. The data logger is programmed to log temperature values onto an SD card at a minute interval.



Pressure gauges together with the thermocouples Logging of data onto the SD card connected to the data logger

Figure 3.16: Thermocouples and Pressure Gauges Connected to Data Logger

Refrigerant pressure, voltage and current drawn by the refrigerator were manually recorded. Manual data collection was done simultaneously with logging of temperature readings by the data logger with the help of a stop watch. Figure 3.17 shows the complete experimental set up for this study.



Figure 3.17: Photograph of the Complete Experimental Set-Up

3.3.2. Experiments Performed and Test Procedure

To achieve the specific objectives of this study, series of experiments were conducted. These can be grouped under three major sections. The first section comprises of experiments performed to determine the optimum amount of refrigerant required by the solar powered DC refrigerator. The second section covers the experiments conducted to study the general performance of the solar powered DC refrigerator under varying compressor speeds. The last section captures experiments conducted to compare the performance of the DC and AC refrigerators. Details of these experiments are shown in Figure 3.18.

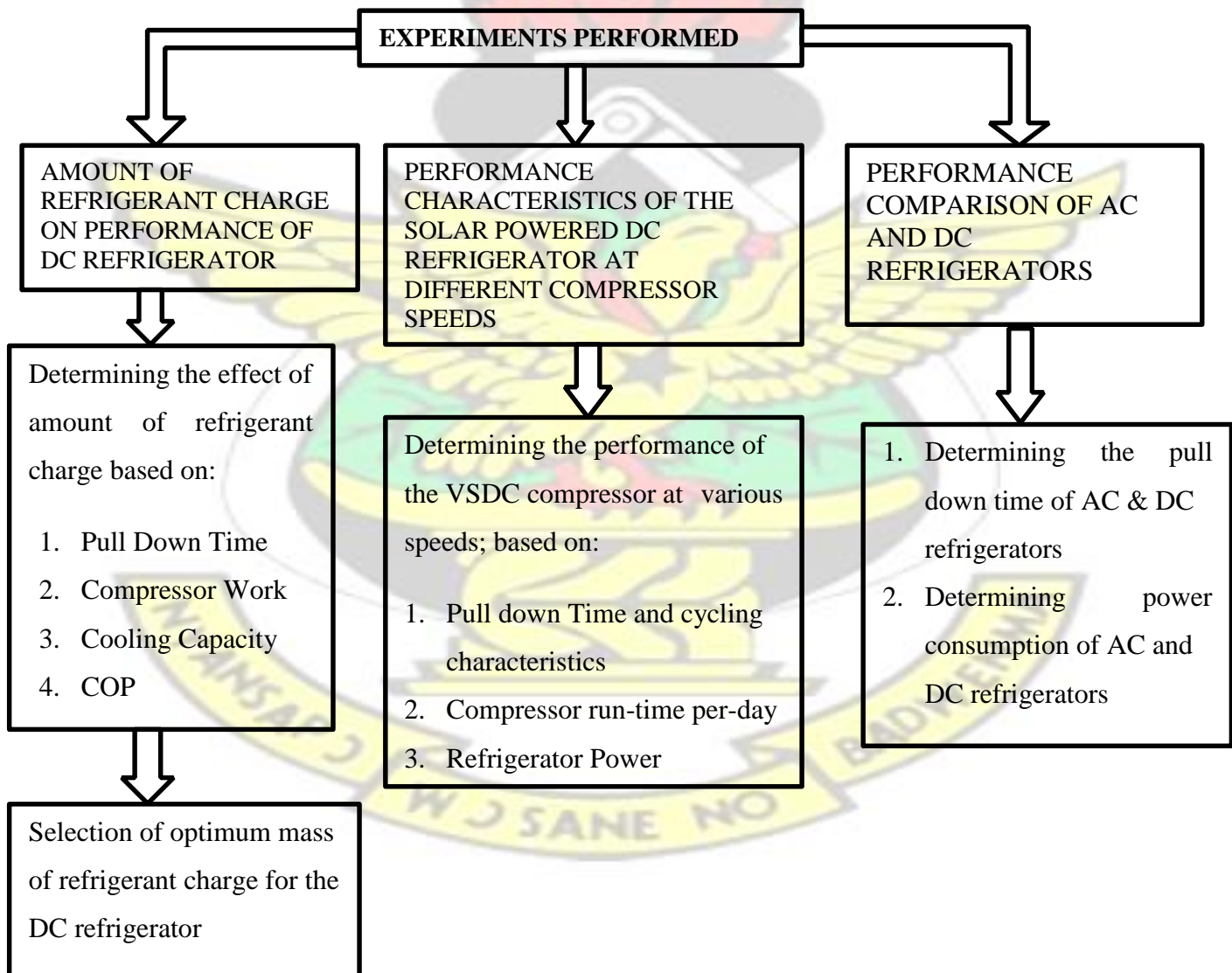


Figure 3.18: List of Experiments Performed

3.3.2.1. Effect of Refrigerant Charge on Performance of the DC Refrigerator

The aim of this section is to determine the optimum amount of refrigerant required by the solar powered DC refrigerator as stated in Chapter 1. The performance parameters used are: refrigerator pull down time, compressor work (kJ/kg), power consumption (W), cooling capacity (W), coefficient of performance (W/W) of the refrigerator. The effect of amount of refrigerant charge on each of the above performance indicators has been studied.

To determine the above parameters, the experimental set-up formulated in section 3.3.1 was used. The schematic diagram of the set-up is shown in Figure 3.19 below.

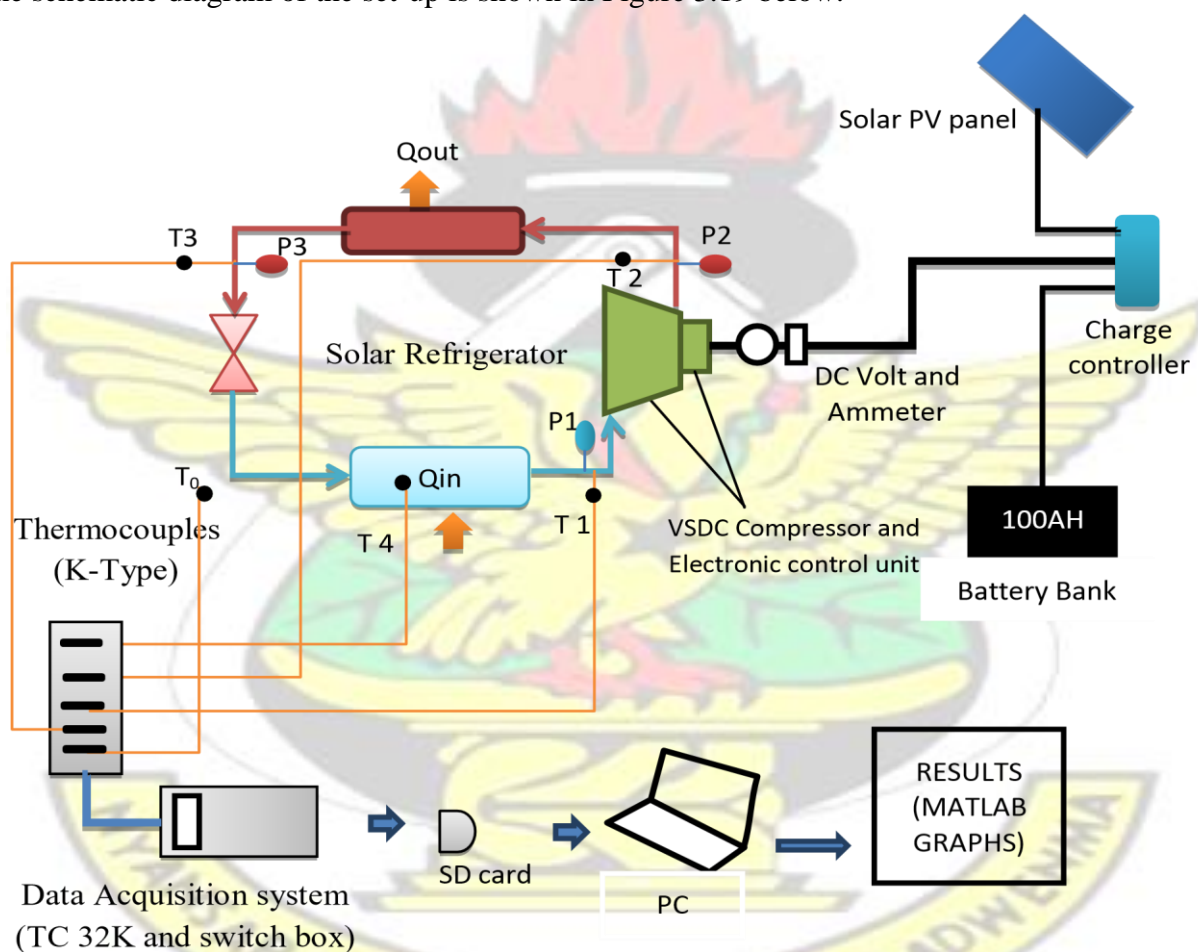


Figure 3.19: Schematic Diagram of the Experimental Set-up

The schematic diagram is made up of the DC refrigerator, the solar PV system, measuring instruments and the data acquisition system. The DC refrigerator was instrumented with a thermocouple and pressure gauge mounted at the exit and the inlet of the compressor and exit

of the condenser. Two additional thermocouples are set to measure the evaporator and ambient temperatures. All five thermocouples are connected to the data logger as discussed in section 3.3.1.4 above. A voltmeter and ammeter were also set to measure the voltage and current drawn by the refrigerator.

Experimental/Test Conditions

All tests were conducted at the Solar Energy and Applications Laboratory (SEAL) under prevailing atmospheric conditions. Average ambient temperature measured during the testing period was 26 ± 2 °C. Prior to this study, (Dmitriyev & Pisarenko, 1984) and (Kuijpers, Janssen, & Verboven, 1988) documented that ambient temperature has no significant effect on the optimum amount of refrigerant charge into the refrigerator.

The following conditions were maintained during the experimental study:

1. All experiments were performed under no load conditions.
2. Before each test begins, the door of the refrigerator is kept open for more than 24 h to allow the temperature inside the refrigerator cabinet to reach thermal equilibrium with the ambient temperature.
3. No heaters were used in the cabinet to produce artificial loads as is sometimes done in refrigerator testing to prevent cycling (Srichai & Bullard, 1997)
4. The refrigerator door was kept closed throughout the testing period.
5. The thermostat knob was set to the maximum point (thus number 8). The thermostat knob set to point 8 maintains a cut in and cut out temperatures of -5 °C and -20 °C respectively.
6. The VSDC compressor was set to operate at maximum speed of 3500 RPM.

Test Procedure

To determine the optimum amount of refrigerant charge, the DC refrigerator was initially charged with 18g of R134a for conducting the baseline test (charging process has been discussed in section 3.3.1.6

above). With all pressure gauges, thermocouples, volt and ammeters in place and all experimental conditions established, the refrigerator was switched on. The effect of the amount of refrigerant charge on two major parameters (pull down time and COP) was determined as follows:

Determining the Effects of Refrigerant Charge on Pull-down Time of the DC Refrigerator

Pull-down time is the time (in minutes) required by a refrigeration system to change the cabinet temperature from ambient temperature to the desired final temperature (Bolaji, Akintaro, Alamu, & Olayanju, 2012). According to (ISO, 1991), small domestic refrigerators such as the one used in this experimental study are tested at $-12\text{ }^{\circ}\text{C}$ (Table 2.1).

In the present study, the evaporator and ambient temperatures of the refrigerator were monitored while the system pull-down from room temperature ($26\text{ }^{\circ}\text{C}$) to $-12\text{ }^{\circ}\text{C}$. Evaporator and ambient temperature readings were measured by thermocouples T_4 and T_o respectively. The refrigerator was allowed to operate continuously for over one hour. Temperature readings were automatically logged onto an SD card every minute by the data acquisition system. The pull down time was then determined from the temperature versus time plot and is presented in chapter four (4).

Determining the effect of refrigerant charge on cooling capacity, compressor work, and COP (actual and cyclic) of the solar powered DC refrigerator

To determine the effect of refrigerant charge on the above performance indicators, the following readings were measured after the refrigerator has operated for 30 minutes.

1. Pressure (P_1) [bar] and Temperature (T_1) [$^{\circ}\text{C}$] at compressor inlet
2. Pressure (P_2) [bar] and Temperature (T_2) [$^{\circ}\text{C}$] at compressor outlet
3. Pressure (P_3) [bar] and temperature (T_3) [$^{\circ}\text{C}$] at condenser outlet
4. Instantaneous current drawn by the refrigerator (I) [Amps]
5. Instantaneous voltage drawn by the refrigerator (V) [Volts]

While the data logger was programmed to automatically log temperature values detected by the installed thermocouples onto an SD card, pressure, current and voltage readings were manually recorded simultaneously with logging of temperature values by the data logger. This method has been used by (Yusof & Yusoff, 2011) in determining the optimum refrigerant charge for a mini bar refrigerator. According to (Yusof & Yusoff, 2011), the pressure in the refrigeration loop becomes stable after this period leading to high accuracy in manual recording of the pressure values.

The various state points of pressure and temperatures are illustrated on the temperature entropy diagram shown in Figure. 3.20.

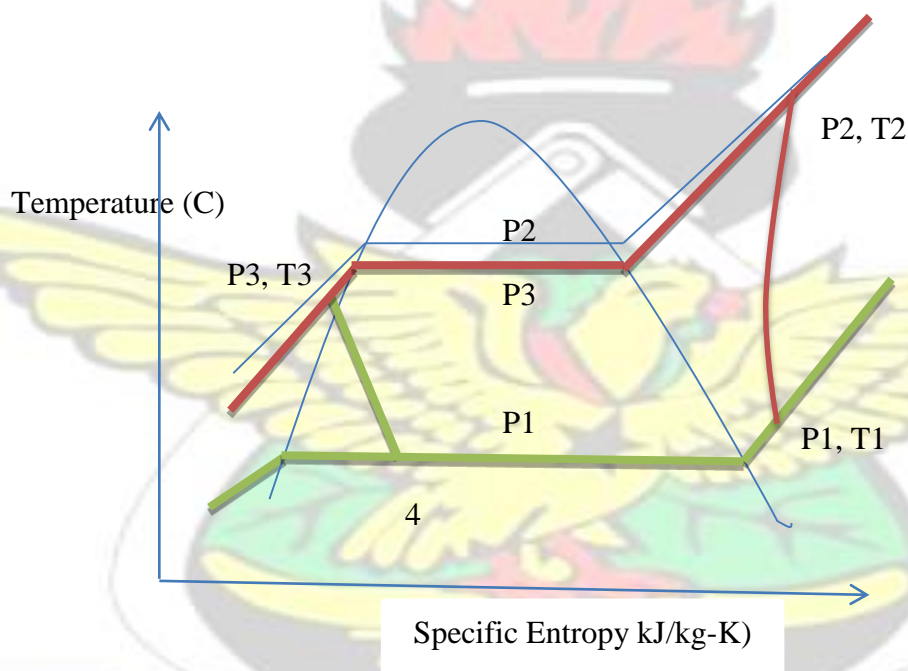


Figure 3.20: Pressure - Specific Entropy Diagram (R134a)

ASSUMPTIONS:

To determine the performance parameters of the refrigerator, the following assumptions were made:

1. The throttling of liquid refrigerant across the capillary tube (state 3 to state 4) is isenthalpic (constant enthalpy)
2. Steady flow system
3. Negligible kinetic and potential energy changes across each component,

4. No heat transfer in connecting pipe lines.
5. The heat and pressure losses are negligible in the lines.

The mass flow rate, refrigeration capacity, compressor work, refrigerator power consumption and coefficient of performance of the refrigerator were determined by the following equations.

(A) The mass flow rate \dot{m} $\frac{\text{kg}}{\text{s}}$ of refrigerant flowing through the refrigeration system is determined mathematically by equation 3.8

$$\dot{m} = \frac{\eta_v \pi d^2 S n}{4 V_1 \times 60} \quad \frac{\text{kg}}{\text{s}} \quad \text{Equation 3.8}$$

Where:

η_v = Volumetric efficiency of the compressor,

V_1 = specific volume of refrigerant at compressor inlet,

d = bore diameter of the compressor,

S = stroke of the compressor,

N = rotational speed of the compressor (3500 RPM),

n = number of cylinders in the compressor

In the current experimental study the volumetric efficiency (η_v) of the compressor is taken to be 80% in all calculations. It is worth noting that the volumetric efficiency (η_v) of reciprocating compressors is usually between 65 % to 85 % (Cengel & Boles, 2006). (B) Refrigeration effect and refrigeration capacity were determined with equations 3.9 and 3.10 respectively.

$$q_{ref} = h_1 - h_4 \quad \frac{\text{kJ}}{\text{kg}} \quad \text{Equation 3.9}$$

$\frac{\text{kg}}{\text{s}}$.

\dot{Q}

□

Equation 3.10

$$Q_{ref} = m \times (h_1 - h_4) \quad \text{W}$$

(C) Specific compressor work (kJ/kg) and compressor work (W) were also determined as follows:

$$\text{Specific Compressor Work (w)} = \frac{h_2 - h_1}{\text{kg}} \quad \text{kJ/kg} \quad \text{Equation 3.11}$$

$$\text{compressor work } W_{comp} = m \times (h_2 - h_1) \quad \text{W} \quad \text{Equation 3.12}$$

□□

(D) The refrigerator power consumption was determined with equation 3.13

Power Consumption = current drawn (Amps) x Voltage (Volts)

$$P_{in} = I \times V \quad \text{Equation 3.13}$$

(E) The actual and cycle coefficient of performance (COP) of the refrigerator can be determined with equation 3.14 and equation 3.15 respectively.

$$\text{Cyclic coefficient of performance } COP_{cycle} = \frac{\text{refrigerator capacity}}{\text{work}}$$

$$COP_{cycle} = \frac{Q_{ref}}{W_{comp}}$$

$$\text{therefore } COP = \frac{h_1 - h_4}{h_2 - h_1}$$

Equation 3.14

$$\text{cycle } \frac{Q_{ref}}{P_{in}}$$

$$COP_{actual} = \frac{Q_{ref}}{P_{in}}$$

Equation 3.15

After conducting the baseline study with 18 g of refrigerant charge, similar performance tests were conducted for 20 g, 25 g, 30 g, 35 g, 40 g and 45 g of refrigerant R134a. Throughout these experiments, the speed of the VSDC compressor was held constant at 3500 RPM (the maximum speed). This approach is justified since (Binneberg, Kraus, & Quack, 2002) have documented previously that the optimum quantity of refrigerant does not vary with the compressor speed.

Based on the measured state properties of the vapour compression system, a computer program was written in Engineering Equation Solver (EES) for solving the various thermodynamic equations discussed above. The code is used to analyse the performance of the refrigerator at the various quantities of refrigerant charge. In this program, thermophysical properties of the refrigerants are used at each step of the calculation, which were obtained from the built-in functions provided by EES (Klein & Alvarado, 2001). This eliminates the need to develop separate property routines for determining the refrigerant properties or read them from refrigerant property tables.

The results of the above experiments as discussed in Chapter 4 demonstrated that the refrigerator gives optimum performance when charged with 30 g of refrigerant (R134a). The performance of the refrigerator at different speeds is then studied by charging the refrigerator with 30 g of R134a. These are discussed in the following sections.

3.3.2.2. Performance Characteristics of the Solar Powered DC Refrigerator Operating at Varying Compressor Speed

After determining the optimum amount of refrigerant required by the solar powered DC refrigerator and the pressure at which it occurs, all pressure gauges and thermocouples were removed from the refrigeration loop. The copper tubes of the VCRS were permanently sealed. The refrigerator was evacuated and recharged with 30 g of R 134aa which resulted in a stable low side pressure of 0.6 bar. The performance of the refrigerator operating at different compressor speeds is evaluated based on the temperature profile of the evaporator and power consumption of the refrigerator. These are discussed in the following sections.

Determining the Effect of Compressor Speed on Refrigerator Pull-Down Time, Cabinet and Evaporator Temperature Characteristics

An experimental matrix has been developed to study the pull-down time and cycling characteristics of the refrigerator cabinet and evaporator. This was done by running the refrigerator at all four individual operating speeds of the VSDC compressor, the compressor was initially set to run at maximum speed of 3500 RPM and later repeated for the rest of the operating speeds (3000 RPM, 2500 RPM and 2000 RPM) of the VSDC compressor. The thermostat knob is initially set to 1 which restricts the operation of the compressor to “cut-in” and “cut-out” temperatures of 5 °C and -5 °C respectively for each speed. Experiments at all four operating speeds were repeated with the thermostat knob set to 8, thus a ‘cut-in’ and ‘cut-out’ temperature of -5 °C and -20 °C respectively. For each test condition, the evaporator temperature of the refrigerator was measured every minute for a period of four (4) hours, thus 240 minutes. Thus evaporator temperature was monitored as the refrigerator pulls down from room temperature (26 °C) to the lowest temperature possible based on the capacity of the compressor at the selected speed. Temperature readings were measured with a thermocouple

(T4) mounted on the evaporator of the refrigerator and automatically logged onto an SD card every minute by the data acquisition system.

Determining the Effect of Compressor Speed on Refrigerator Power Consumption

Similar to temperature measurements, power consumption of the refrigerator at each operating condition as discussed in section 3.3.1.4 was determined from the measured values of the instantaneous current and voltage drawn by the refrigerator. Power consumption is determined by Equation 3.16.

$$\text{Power (P)} = \text{Voltage (V)} \times \text{Current (I)} \quad \text{Equation 3.16}$$

3.3.2.3. Comparing the Performance of the Solar Powered DC Refrigerator to an Identical AC Refrigerator

In this section, a second experimental set is developed to comparatively study the performance of the solar powered DC refrigerator against an identical AC refrigerator. The performance parameters considered include; Pull-down and cycling characteristics, power consumption and coefficient of performance. Experimental data recorded is analyzed in MATLAB and presented in Chapter 4. The complete experimental set is shown in Figure 3.21 below.

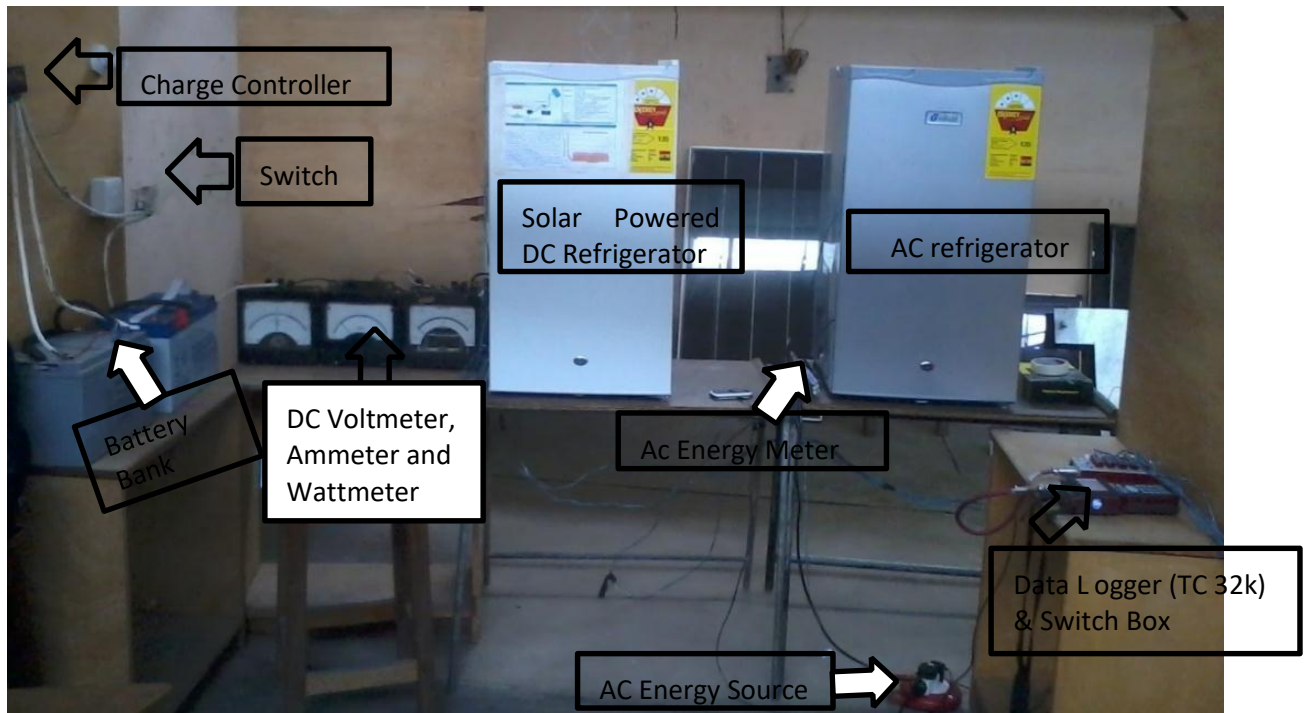


Figure 3.21: Experimental set Up for comparing the Performance of the Solar Powered DC refrigerator with a conventional AC refrigerator

In Figure 3.21, both refrigerators were instrumented with two K-Type (copper–constantan) thermocouples, one for measuring the evaporator and the other for cabinet temperature. A similar thermocouple is set to measure the ambient temperature. All five thermocouples are connected to a five channeled data acquisition system (TC-32K data logger) via a dedicated switch box (CSW-5A). The data logger was programmed to log temperature values onto an SD card every minute for over four hours. The AC refrigerator is connected to the national grid (220-240V) while the DC refrigerator is powered by the installed solar PV system. A digital energy meter with accuracy of $\pm 0.2\%$ is installed between the AC power source and the AC refrigerator to measure the AC refrigerator's power consumption. On the other hand, current and voltage drawn by the solar powered DC refrigerator were measured by a DC voltmeter and an ammeter installed between the battery bank and the electronic control unit of the VSDC compressor. Figure 3.22 shows the schematic diagram of the experimental setup.

KNUST



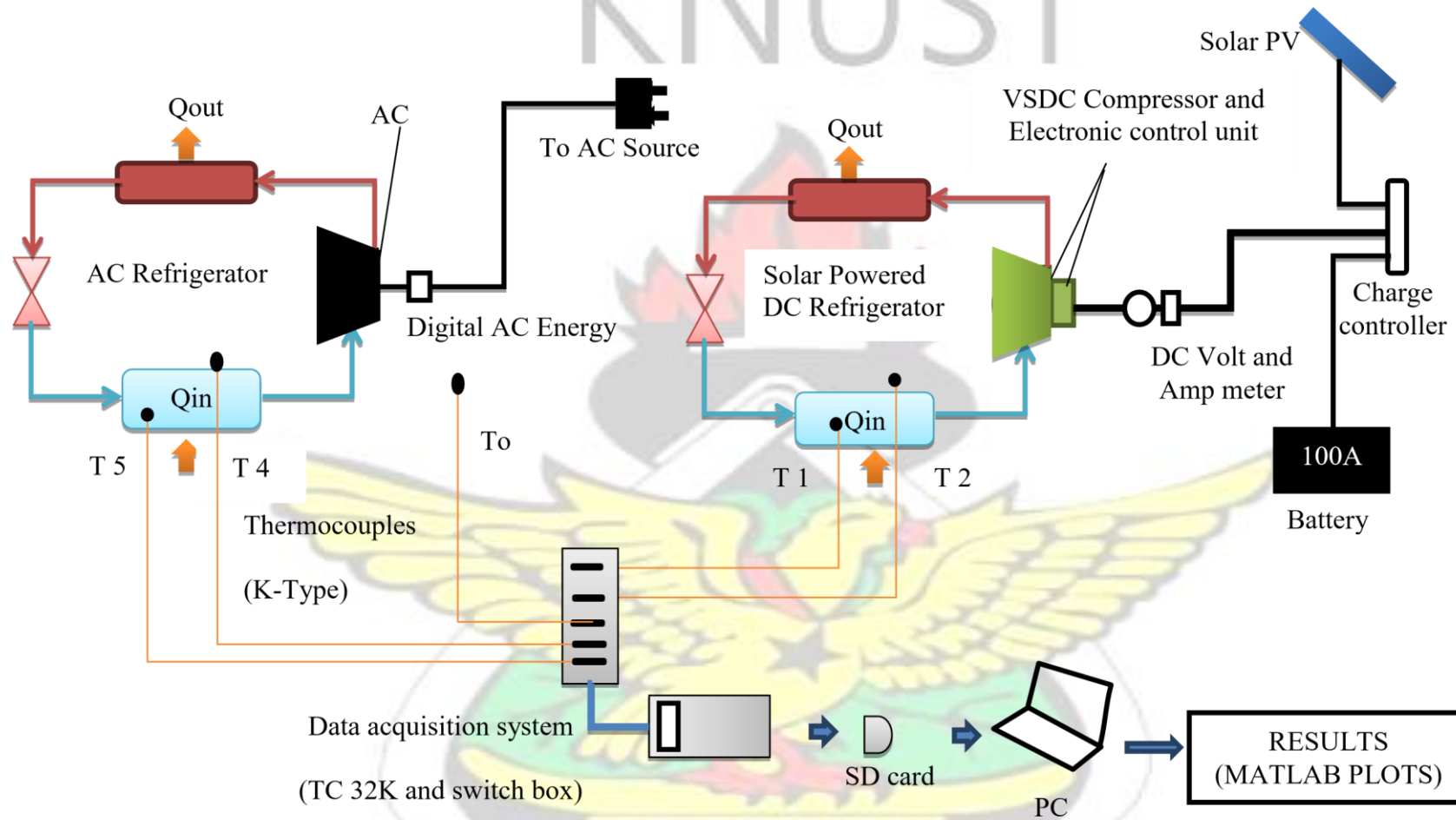


Figure 3.22: Schematic diagram of experimental set-up formulated to study the performance of AC and solar powered DC refrigerator

KNUST

84



Determining the Pull-Down and Cycling Characteristics of both Refrigerators

With all thermocouples and power measuring instruments in place and all test conditions established, both refrigerators were switched on simultaneously. Evaporator, cabinet and ambient temperatures of both refrigerators were measured every minute for over four hours of continuous operation. Temperature readings were logged onto the SD card by the data logger as detected by the thermocouples. Results obtained for continuous running over four hours are presented in Chapter 4.

Determining Power Consumption of AC and DC Refrigerators

Power consumption of the AC refrigerator is measured with a digital AC meter installed between the AC refrigerator and the power source (national grid). Similarly, the voltage and current drawn by the solar powered DC refrigerator were determined with a DC voltmeter and an ammeter installed between the solar powered DC refrigerator and the charge controller. These are illustrated in Figure 3.12. Power consumption of the AC refrigerator, current and voltage drawn by the DC refrigerator are manually recorded simultaneously with the logging of temperature readings as discussed in section 3.3.1.8 above.

From the voltage and current values; the instantaneous power consumption of the solar powered DC refrigerator is determined by Equation 3.16 above

Determining the Energy Consumption of the AC Refrigerator and the Solar Powered DC Refrigerator

From the power consumption and compressor run-time per day, the daily energy consumption of each refrigerator can be determined with Equation 3.17. Similarly, monthly and annual energy is determined by Equation 3.18 and Equation 3.19 respectively.

$$\%t_c = \frac{\text{Summation of On Operations of the Compressor Per Hour}}{60 \text{ minutes}} \times 100$$

where %t Percentage Compressor Run Time Per hour c

$$\%t_c = \frac{\text{Percentage Compressor Run Time Per Hour}}{100} \times \text{hours} \times \text{day} \times t_c$$

where: t_c is Compressor Run Time Per day

$$E_{\text{daily}} = \text{Average Power (Watt)} \times t_c \times \text{hours} \times \text{day} \times t_c$$

Equation 3.17

$$E_{\text{monthly}} = 30 \text{ days} \times E_{\text{daily}} \times \text{Wh} \times 24 \times \text{day}$$

Equation 3.18

$$E_{\text{yearly}} = 365 \text{ days} \times E_{\text{daily}} \times \text{Wh} \times \text{day} \times \text{year}$$

Equation 3.19

3.3.3. Economic Assessment of the Developed DC Refrigerator and AC Refrigerator Running on Inverter all Powered by Solar PV

For the comparative economic analysis, the AC refrigerator and DC refrigerator were both powered by solar PV to ascertain their economic implications in running them on solar energy. The cost of the two modes of solar refrigeration considered in this study has been evaluated based on the following equations:

$$\text{Total Cost of DC Refrigeration System (Without Inverter)} = \text{Cost New AC Refrigerator} + \text{Cost of VSDC Compressor and Accessories} + \text{Cost of Conversion} + \text{Cost of Solar PV System}$$

$$\text{Total Cost of AC Refrigeration System (with Inverter)} = \text{Cost New AC Refrigerator} + \text{Cost of Inverter} + \text{Cost of Solar PV System}$$

These equations have been evaluated based on the measured daily energy consumption of each refrigerator and presented in Table 4.4. The cost of the solar PV system depends on the sizes of solar PV system components required by each refrigerator.

The results obtained from the series of experiments are reported in chapter 4.

CHAPTER 4 RESULTS AND DISCUSSIONS

4.0. INTRODUCTION

In this study, the methodology of developing a stand-alone solar powered DC refrigerator and the approach of sizing a solar PV system for powering the refrigerator has been developed. The design considerations formulated have been used to convert a 92 L AC refrigerator to serve as a stand-alone solar powered DC refrigerator. A solar PV system for powering the refrigerator is designed and installed at the Solar Energy Applications Laboratory. Experiments have been conducted on the system and performance comparison with an identical conventional AC refrigerator has been made.

This chapter presents and discusses the results obtained from this study. The Chapter is grouped under four major sections by making reference to the specific objectives documented in Chapter 1. These are:

1. Effects of refrigerant charge on the performance of the solar powered DC refrigerator.
 2. Performance characteristics of the developed solar powered DC refrigerator at varying compressor speeds.
 3. The performance of the solar powered DC refrigerator compared to a conventional AC refrigerator
 4. Economic analysis of the developed solar powered DC refrigerator
- These are discussed in the following sections:

4.1 EFFECT OF REFRIGERANT CHARGE ON THE PERFORMANCE OF THE SOLAR POWERED DC REFRIGERATOR

To determine the optimum amount of refrigerant required by the solar powered DC refrigerator, the refrigeration system was charged with 18 g, 20 g, 25 g, 30 g, 35 g, 40 g and 45 g of refrigerant 134a as discussed in chapter three. The temperature and pressure values obtained at each quantity of refrigerant charge were used to determine the various enthalpies at all the four thermodynamic state points. The results were analysed with thermodynamic equations as presented in Chapter 3.

This section presents the results of the effect of amount refrigerant charge on the performance of the refrigerator. The performance parameters considered include: pull down time, refrigeration capacity; power consumption, refrigeration effect, COP etc. The following sections present and discuss the how each performance parameter is affected by levels of refrigerant charges.

4.1.1. Effect of Refrigerant Charge on Pull-down Time of the Solar Powered DC Refrigerator

The pull-down time is the time required for changing the refrigerator's air temperature from the ambient condition to the desired final temperature. Figure 4.1 shows a graph of evaporator temperature versus time for 18 g, 20 g, 25 g, 30 g, 35 g, 40 g and 45 g of refrigerant R134a charged into the refrigerator.

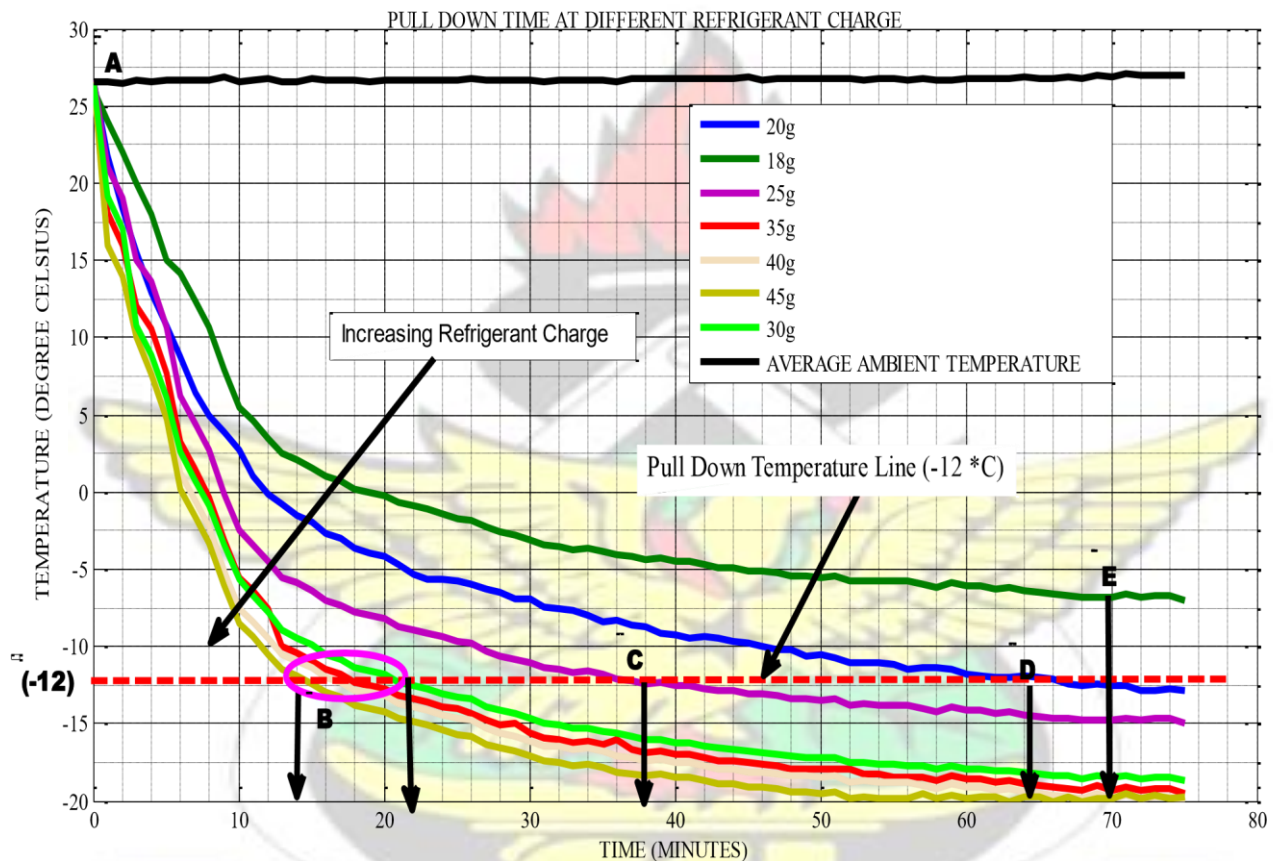


Figure 4.1: Variation of Pull-down Time with Respect to Amount of Refrigerant Charge

According to ISO (1991), small domestic refrigerators such as the one used in this research for tropical countries such as Ghana should have their pull down time determined at evaporator temperature of -12 °C. Figure 4.1 shows a general trend in which the evaporator temperature reduced from room temperature to a certain minimum temperature.

For the levels of refrigerant charges considered, it can be observed that the refrigerator was unable to achieve the desired pull down temperature of $-12\text{ }^{\circ}\text{C}$ when charged with 18 g of refrigerant R134a. Only a minimum temperature of $-7\text{ }^{\circ}\text{C}$ was achieved at a pull-down time of 70 minutes. The pull-down time achieved for 20 g and 25 g are approximately 65 and 38 minutes respectively. However, the refrigerator was able to achieve the $-12\text{ }^{\circ}\text{C}$ evaporator temperatures within a pull down time of 19 minutes, 17 minutes, 16 minutes and 14 minutes when charged with 30 g, 35 g, 40 g and 45 g respectively. The minimum temperatures achieved by charging the system with 30 g, 35 g, 40 g and 45 g of refrigerant are -18°C , -19°C , -19.5°C and -20°C respectively. Therefore, it can be noted that increasing the amount of refrigerant charge has a great impact on the cooling time. However, the results indicate that the effect of increasing the charge beyond 30 g is negligible. As indicated in Figure 4.1 by point B, it is observed that increasing the amount of refrigerant charge beyond 30 g does not cause any significant change in the pull down time of the refrigerator. Therefore refrigerant charge of about 30 g to 40 g R 134a can be used for the 92 L refrigerator.

Theoretically, this pattern of operation of the refrigerator is expected, since increasing the amount of refrigerant increases the mass flow rate, which in turn increases the rate of heat removal (refrigeration capacity) from the refrigerator cabinet. The net effect is lowering the pull down time of the refrigerator. On the other hand, increasing the amount of refrigerant beyond a certain optimum amount of refrigerant resulted in flooding of the evaporator. The end effect is a slower rate of heat removal and a corresponding reduction in rate of pull down time. There is also less superheating at the compressor suction which also results in low refrigeration capacities.

4.1.2. Effect of Refrigerant Charge on Cooling Capacity (Q_{ref}), Power Consumption (P_{in}), and COP of the Solar Powered DC Refrigerator

To determine the optimum quantity of refrigerant required by the developed solar refrigerator, an optimization study was conducted. The performance of the refrigerator was studied at different quantities of refrigerant charge by monitoring its effect on refrigeration capacity (Q_{ref}), power consumption (P_{in}) and coefficient of performance (COP). These performance parameters were calculated at each mass of refrigerant charge by using Equation 3.10 and Equation 3.13, and Equation 3.15, respectively. The results of this study are shown in Figure 4.2.

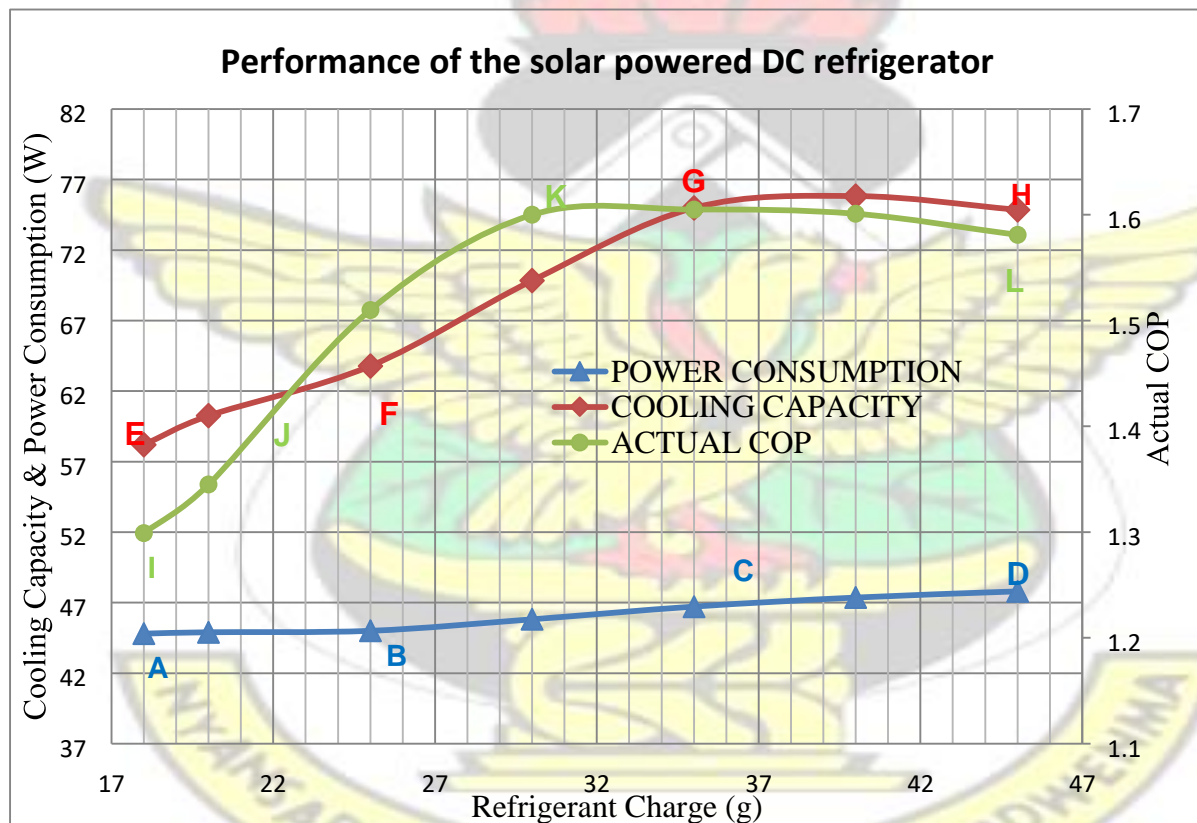


Figure 4.2: Overall performance characteristics of the solar powered DC refrigerator with different quantities of refrigerant charge

Figure 4.2 illustrates the effect of amount of refrigerant charge on the power consumption (P_{in}), cooling capacity (Q_{ref}) and COP of the developed solar powered DC refrigerator. Figure 4.2 shows that amount of refrigerant charge into the refrigerator has a significant effect on all

the three performance indicators (COP , Q_{ref} and P_{in}) considered. It can be observed that as the amount of refrigerant charge is increased from 18 g to 25 g the cooling capacity increased from 58 W to 62 W (thus from point E to point F). Power consumption of the system also saw a marginal increase in capacity from 44.8 W to 45 W (point A to point B), the resulting effect is relatively low COP of the refrigeration system.

This condition is associated with low specific density (shown in Figure 4.4), low mass flow rate (shown in Figure 4.5), high discharge temperatures (shown in Figure 4.3) and increase in discharge pressures (shown in Figure 4.6). The above performance parameters indicate that the refrigerator is operating at undercharged conditions of 18g to 25g of refrigerant charge. Operation of the refrigerator at undercharge conditions is evident in low mass flow rate leading to the starving of the evaporator with refrigerant thereby reducing the rate of heat removal from the refrigerator cabinet (cooling capacity). Under charge conditions also results in the supply of high superheat, low density refrigerant to the compressor. Therefore, apart from the low heat removal (cooling capacity), undercharge condition has the potential of overheating the compressor as well as supplying higher discharge pressures and temperatures to the condenser as encountered in this study. The end effect is increased in compressor power consumption leading to lower system $COPs$ as given earlier.

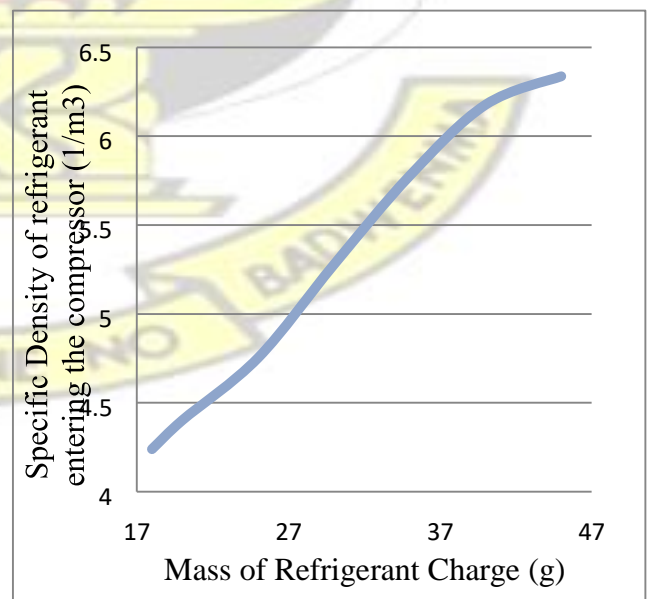
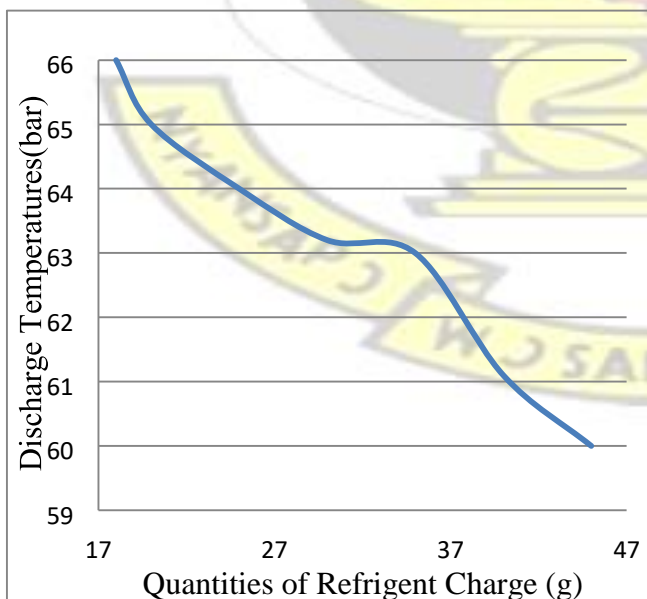


Figure 4.3: Variation of Discharge Temperature **Figure 4.4: Variation of Density of Refrigerant with Increasing Levels of Refrigerant Charge Entering the Compressor With Increasing Levels of Refrigerant Charge**

Continuing from Figure 4.2, it can be observed that from point F to point G, the cooling capacity increases sharply from 59 W to 75 W as the amount of refrigerant charge is increased from 25 g to 37 g. On the other hand, power consumption was noticed to increase mildly from 45.5 W to 47W. This is shown in Figure 4.2 as point B to C. This resulted in a substantial increase in the COP of the refrigerator from 1.4 to a peak value of 1.6. This is indicated in Figure 4.2 as point J to K. At point K (refrigerant charge of 30 g), the COP of the refrigerator was observed to stay fairly constant while the amount of refrigerant is increased. Moreover, this is justified since an increase in cooling capacity was observed to be in the same proportion as an increase in power consumption after the peak COP is reached. However, it can be observed that further addition of refrigerant beyond 10 g after reaching the optimum amount of refrigerant charge results in deterioration of the system performance, which results in a gradual reduction in system COP as illustrate in Figure 4.2 from K to point L. This observed phenomenon indicates the onset of overcharging of the refrigerator with refrigerant. The trend of these results is in agreement with the works of (Datta, Das, & Mukhopadhyay, 2014) and (Grace, Data, & Tassou, 2005).

In general, it can be observed that before the optimum amount of refrigerant is reached, an increase in refrigerant quantity results in higher increases in refrigeration capacity than the refrigerator power consumption which led to increase in system COP. The trend changes after the optimum amount of refrigerant is reached. From Figure 4.2, it be determined that beyond 39 g (overcharge conditions) of refrigerant charge, the rates of increase of compression work is much higher as compared to the rate of cooling capacity. This phenomenon is as a result of the flooding of the evaporator which resulted in higher system pressure and the movement of low degree of superheated refrigerant into the compressor. This is evident in Figure 4.4 in

which the density of the refrigerant entering the compressor was observed to increase with increasing levels of refrigerant charge. Secondly, discharge pressures of the compressor were observed to increase sharply as the amount of refrigerant is increased beyond the optimum (see Figure 4.6). The combined effect of these conditions after the optimum amount of refrigerant is reached is a reduction in COP and overall system instability. Similar trends have been reported by Houcek and Thedford (1984) and Farzard and O'Neal (1994) in a previous study.

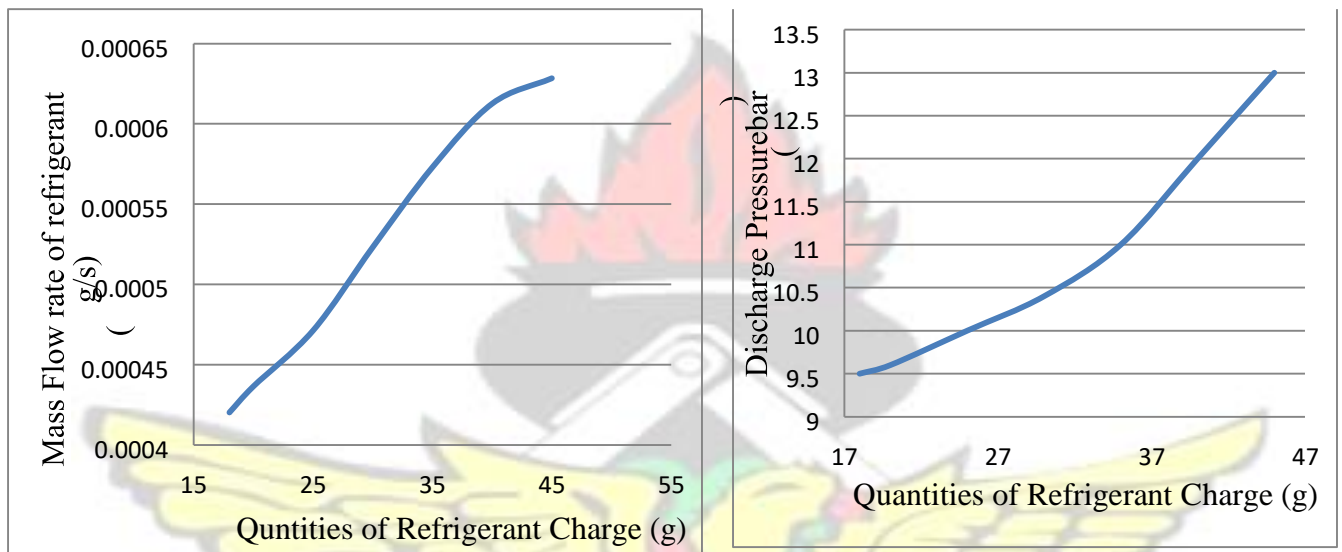


Figure 4.5: Variation of Refrigerant Mass Flow Rate with the Amount of Refrigerant Charge **Figure 4.6: Effects of Refrigerant Charge on Compressor Discharge Pressure**

The two major parameters required to select the optimum amount of refrigerant charge is the pull down time and the COP of the entire refrigerator. It can therefore be concluded that the optimum of refrigerant should give better performance in terms of shorter pull down time and higher COP. From the above analysis, it is obvious that the quantity of refrigerant charge that best satisfies these conditions is 30 g. Any increases in charge resulted in a higher compressor power input than gain in cooling capacity, causing COP to drop. Similarly, as shown in Figure 4.1 increasing the amount of refrigerant charge beyond 30 g does not have any significant effect on the pull down time, however, results in flooding of the evaporator. The opposite is low COP and longer pull down time as shown in Figure 4.1 above.

By comparing the results obtained in this study in terms COP at 30 g of refrigerant charge (thus 1.6) gives a good agreement with the COP values stated by the compressor manufacturer as shown in Table 4.1. It is worth noting that the evaporator of the refrigerator was about -13 °C after 30 minutes of operation as illustrate in Figure 4.1 above.

**Table 4.1: COP Values of the selected compressor,
COP (ASHRAE)**

	W/W									
rpm \ °C	-30	-25	-23.3	-20	-15	-10	-5	0	5	10
2,000	1.10	1.25	1.31	1.42	1.61	1.82	2.06	2.31	2.57	2.84
2,500	1.07	1.19	1.24	1.34	1.53	1.74	1.97	2.23	2.50	
3,000	0.93	1.11	1.17	1.30	1.50	1.72	1.95	2.20		
3,500	0.89	1.03	1.09	1.23	1.44	1.68	1.91			

Source: (Danfoss, 2007)

Table 4.1 shows the COP of the VSDC compressor at various rotational speeds of the compressor and at different evaporator temperatures as documented by the manufacturer (Danfoss, 2007). Though the compressor performs differently at each speed, the optimisation exercise was done at a single compressor speed of 3500 RPM; this represents the optimum amount of refrigerant for the rest of the speeds (2000 RPM, 2500 RPM and 3000 RPM). This conclusion is justified since Binneberg, Kraus and Quack (2002) have documented previously that the optimum quantity of refrigerant in vapour compression refrigeration systems is independent of the rotational speed of a variable speed compressor.

4.2 PERFORMANCE CHARACTERISTICS OF THE SOLAR POWERED DC REFRIGERATOR AT VARYING COMPRESSOR SPEEDS

The performance of the developed stand-alone solar powered DC refrigerator has been evaluated at all the four speeds of the VSDC compressor viz; 3500 RPM, 3000 RPM, 2500 RPM and 2000 RPM. Evaporator temperature profile and the corresponding instantaneous power consumption of the refrigerator were measured over a period of four hours with a sampling space of one minute. Experiments were carried out with a fixed mass of refrigerant charge of 30 g and refrigerator thermostat set to maintain a “cut-in” and “cut-out” temperatures

of -5 °C and -20 °C respectively. The overall compressor efficiency was also assumed to be independent of the compressor speed.

To study the performance of the refrigerator at high temperature settings, all experiments were repeated for “cut-in” and “cut-out” temperatures of +5 °C and -5 °C by setting the thermostat knob to 1. Average power consumption of the refrigerator and the respective compressor run-time of the refrigerator operating at each of the speeds were used to determine the daily and annual energy consumption of the refrigerator operating at each speed of the VSDC compressor. A comparative analysis has been made about the possibility of some energy saving as a result of operating the refrigerator on low speeds instead of full capacity during part loading or high temperature settings. The following sections present the results obtained in the form of graphs indicating how the refrigerator performs at each speed of the VSDC compressor.

4.2.1. Evaporator Temperature Profile of the Solar Powered DC Refrigerator Operating at Low Temperature Settings (“cut out” Temperature of -20 °C) The performance of the refrigerator has been assessed at low evaporate temperature operating conditions. During these tests the thermostat knob of the refrigerator was set to 8. Evaporator temperature of the refrigerator was studied over a period of 4 hours for each of the four speeds of the VSDC compressor (3500 RPM, 3000 RPM, 2500 RPM and 2000 RPM). Figure 4.7 shows evaporator temperature profiles of the solar powered DC refrigerator operating at the various speeds of the VSDC compressor over a test period of four hours.

EVAPORATOR TEMPERATTURE VERSUS TIME

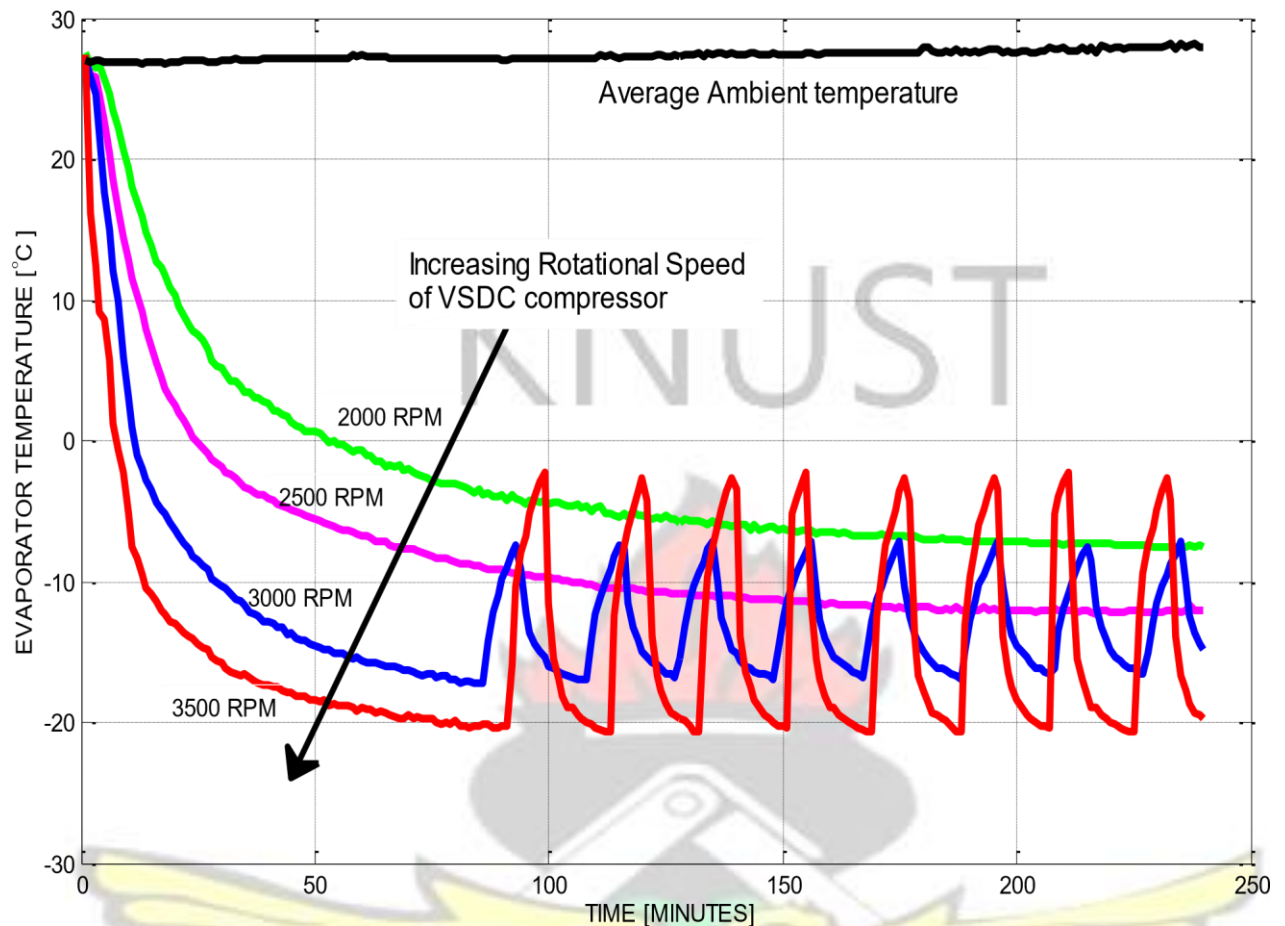


Figure 4.7: Evaporator Temperature Profile of the Solar Powered DC Refrigerator Operating at Low Back Pressure

From Figure 4.7 it is clear that the rotational speed of the compressor has a significant effect on the performance of the refrigerator (both pull down and cycling periods) at low thermostat settings.

The refrigerator when run at 3500 RPM and 3000 RPM pulls down from room temperature to -20 °C and -16 °C and cycles ON and OFF for the entire test period. On the contrary, operating the refrigerator at 2500 RPM and 2000 RPM results in a steady operation in which the refrigerator did not cycle but operated with a fairly constant by decreasing temperature. Similar results were obtained by Ekren et al. (2013) when they evaluated the performance of a VSDC

compressor on a 79 L domestic refrigerator. They observed that operating the refrigerator at low compressor speeds with low temperature settings (evaporator temperature of minus 25 °C) took 210 minutes before cycling.

Moreover, Figure 4.7 illustrates that the pull down time and average evaporator temperature of the refrigerator generally decrease with increasing rotational speed of the VSDC compressor. These results are in agreement with Ekren et al. (2013). It can also be observed that the refrigerator maintains average temperatures of -20 °C, -16 °C, -12 °C and -6 °C when operating at 3500 RPM, 3000 RPM, 2500 RPM and 2000 RPM respectively. This phenomenon can be attributed to increase in compressor capacity with increasing rotational speed of the VSDC compressor. Increasing the speed of a reciprocating compressor such as the one used in this study increases the mass flow rate of refrigerant through the VCRS resulting in increased rate of heat removal from the refrigerator cabinet hence the pattern shown above.

4.2.2. Power Consumption of the Solar Powered DC Refrigerator Operating at Low Temperature Settings (“cut-out” Temperature of -20 °C)

Figure 4.8 shows the corresponding instantaneous power consumption (W) of the refrigerator with the temperature profiles shown in Figure 4.7. The plot shows the power consumption versus time of the solar powered DC refrigerator with a VSDC compressor operating at 2000 RPM, 2500 RPM, 3000 RPM and 3500 RPM. Power consumption of the refrigerator was determined as the product of the current drawn by the refrigerator and the supplied voltage of the solar PV system.

POWER CONSUMPTION VERSUS TIME

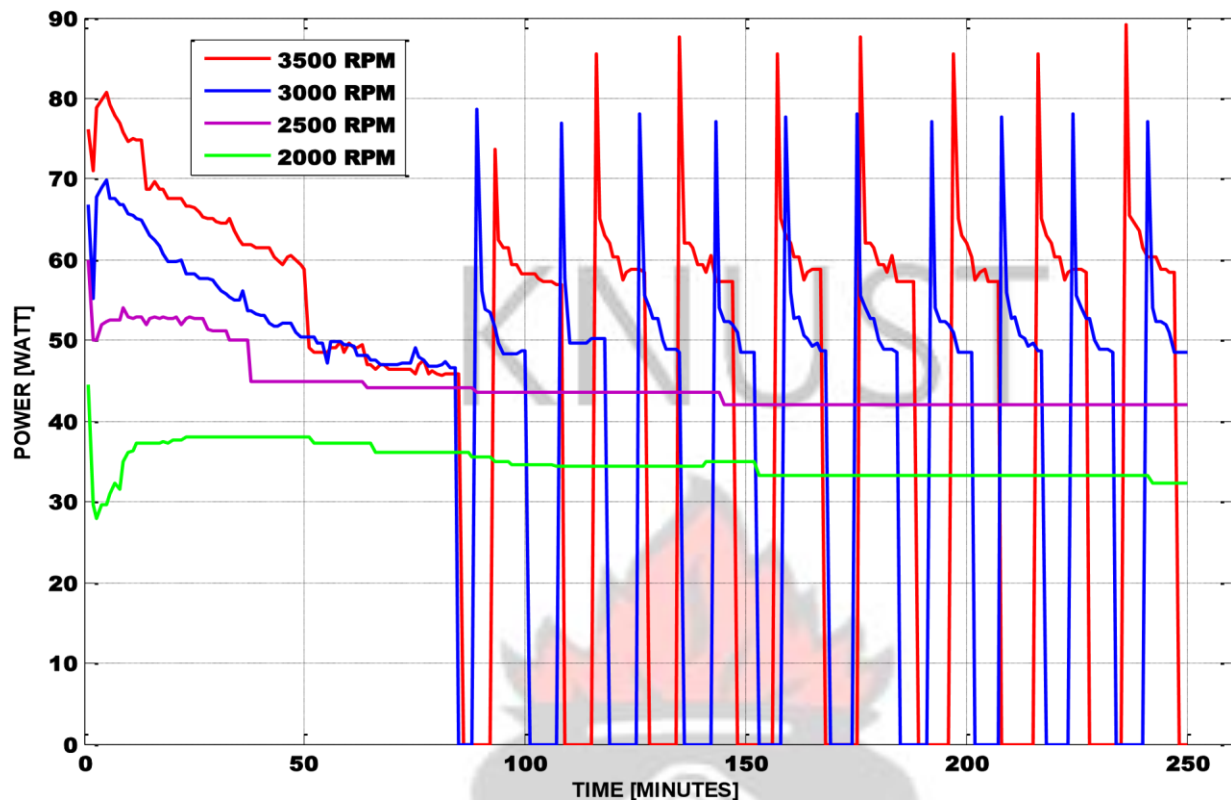


Figure 4.8: Instantaneous Power Consumption of the Solar Powered DC Refrigerator Operating at Low Temperature Settings

Figure 4.8 shows that the refrigerator draws average powers of 60 W, 50 W, 42 W and 33 W when operating at 3500 RPM, 3000 RPM, 2500 RPM and 2000 RPM respectively. Secondly, power consumption of the refrigerator is observed to be higher and unstable at the beginning of the experiment (thus the pull down period). These parameters turn to be stable after about one hour of continuous operation. Though stable throughout the experimental study, an average surge power of 1.5 times of the running/rated power were observed at the beginning of each ON cycle (applies to only 3500 RPM and 3000 RPM).

During the experimental study, it was observed that the voltage of the system stays fairly constant whiles the current drawn by the refrigerator changes intermittently to match the power consumption of the refrigerator. However, operating the refrigerator at rotation speeds of 2000

RPM and 2500 RPM resulted in fairly constant voltage and current after steady state was reached. The compressor was observed to be drawing an average current of 2.8 A and

3.5 A on the 12 volt system when operated at 2000 RPM and 2500 RPM respectively. This mode of operation gave a fairly constant power consumption of 33 W and 42W respectively after the system has stabilized. Therefore, operating the compressor at these speeds (2000 RPM and 2500 RPM) gave a continues mode of refrigeration which resulted in a gradual reduction of the evaporator temperature from room temperature to -8 °C and -12 °C respectively. Continuous of operation of the refrigerator in this mode resulted in the covering of the evaporator with ice. Figure 4.9 shows the evaporator of the refrigerator and the installed thermocouple before and after the experiment.

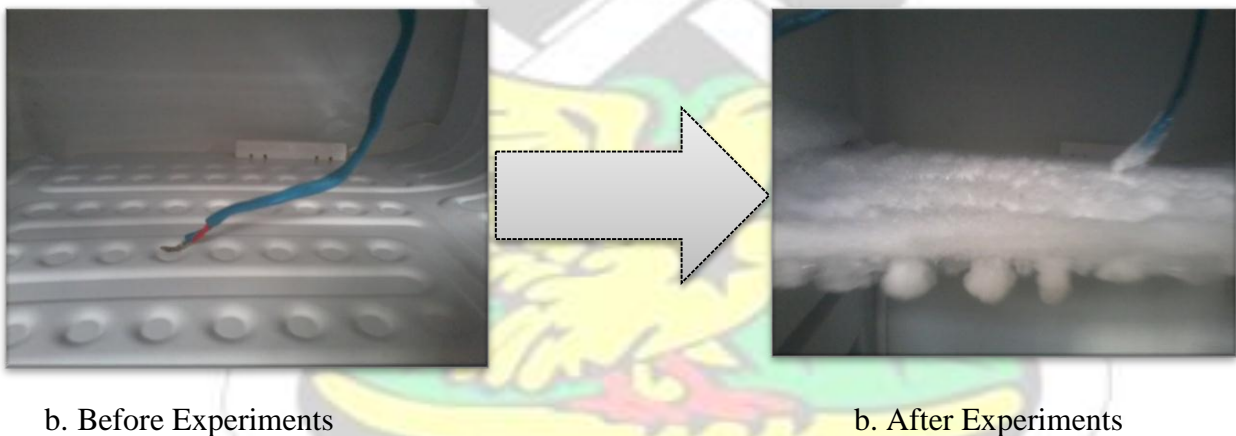


Figure 4.9: Formation of Ice by the Solar Powered DC Refrigerator Operating at Low Speeds

These results are in agreement with those obtained by Ekren et al. (2013) when they evaluated the performance of a variable speed DC compressor. In their study, they observed that the compressor did not cycle until 210 minutes of continuous operation. The authors did not state any reason for the delay in cycling. In the current research work, the compressor did not cycle after continue operation for over four hours. This can be attributed to low cooling capacities due to the low compressor speeds. Nonetheless, it can be observed from Figure 4.7 that

evaporator temperatures of the compressor operating at 2000 RPM and 2500 RPM are asymptotic about minus 20 °C. Therefore, one can state that the compressor is likely to cycle at a certain time (T_{∞}) when the evaporator temperature reaches minus 20 °C based on thermostat settings.

For this study, one can state that, operating the refrigerator with the two low compressor speeds (2000 RPM and 2500 RPM) at low temperature settings (“cut-out” temperature of 20°C) is ideal for freezing purpose; otherwise there will always be the need for manual defrosting of the refrigerator.

4.2.3. Evaporator Temperature Profile of the Solar Powered DC Refrigerator Operating at High Temperature Settings (“cut out” temperature of -5 °C)

Similar to the above analysis, the performance of the solar powered DC refrigerator has been evaluated for relatively high temperature settings. Experiments were conducted for all the speeds of the VSDC compressor by setting the thermostat knob to 1. This restricts the operation of the compressor to “cut-in” and “cut-out” temperatures of 5 °C and -5 °C respectively. Figure 4.10 shows the evaporate temperature profile of the refrigerator for the various rotational speeds of the VSDC compressor observed over four hours.

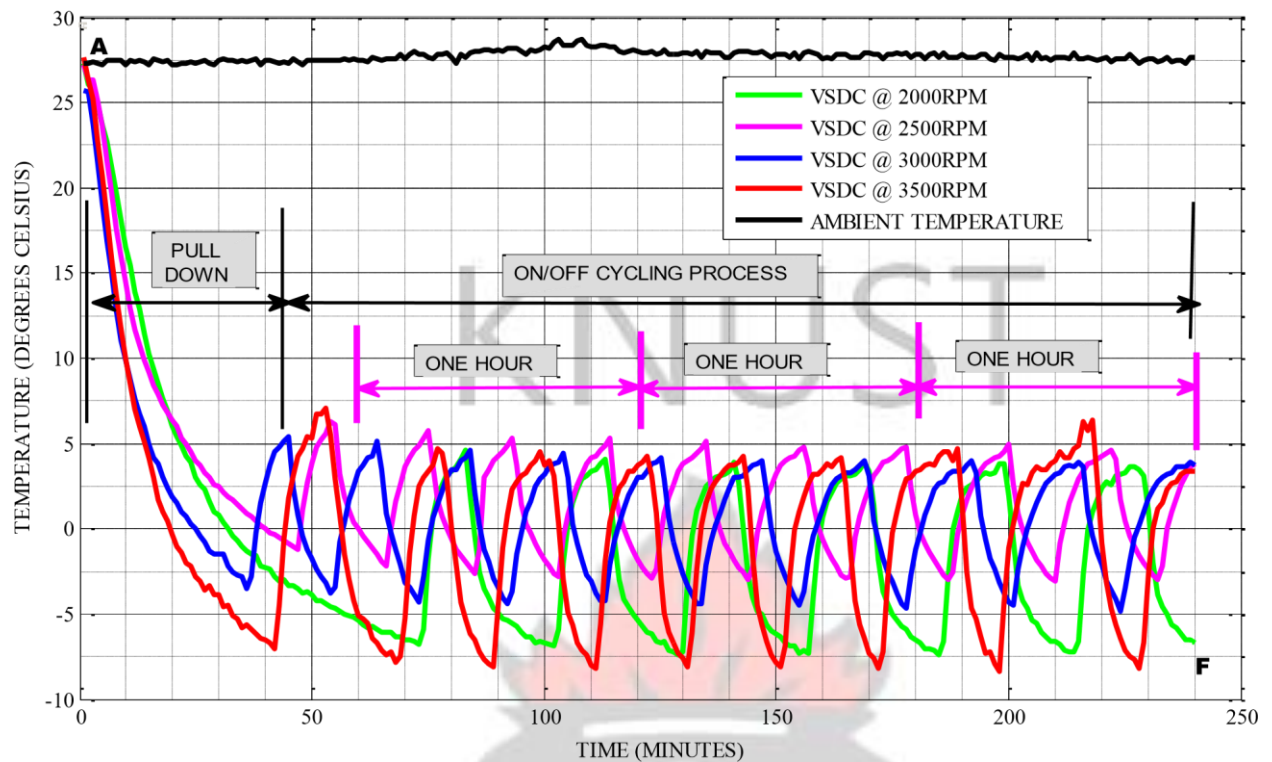


Figure 4.10: Pull Down and Cycling Characteristics of the Solar Powered DC Refrigerator operating at high temperature settings

Figure 4.10 indicates that the refrigerator pulls down for less than one hour (except operating the refrigerator at 2000 RPM) and cycles ON and OFF for the rest of the test period. It can also be determined that operating the refrigerator at 3500 RPM, 3000 RPM, 2500 RPM and 2000 RPM maintain average evaporator temperatures of -7°C , -4°C , -2.5°C and -6.5°C respectively. This therefore indicates that there is no significant difference in the performance (in terms of pull down and cycling characteristics) of the solar powered DC refrigerator operating at the various speeds of the VSDC compressor as far as high temperature settings is a concern. It can however be observed that refrigerator gives the lowest ON temperature of -8°C and -7°C when operated at 3500 RPM and 2000 RPM respectively as compared to -3°C and -5°C for 2500 RPM and 3000 RPM respectively. This study observed a change in pattern of performance; one would have expected the 2000 RPM to give the highest evaporator temperatures (positive) among the four speeds of the VSDC compressor. However, it happens to be providing the lowest ON temperatures after 3500 RPM. This mode of operation resulted

in longer ON and OFF cycles. To determine the energy consumption of the refrigerator at various speeds of the VSDC compressor in maintaining the above temperature profiles, the power consumption and average compressor run time were used. These are discussed in the following sections.

4.2.4. Power Consumption of the Solar Powered DC Refrigerator Operating at High Temperature Settings

Figure 4.11 shows a plot of the power consumption of the solar powered refrigerator operating at the various compressor speeds over a period of four hours at high temperature settings (“cut in” and “cut out” temperature of 5 °C and -5 °C).

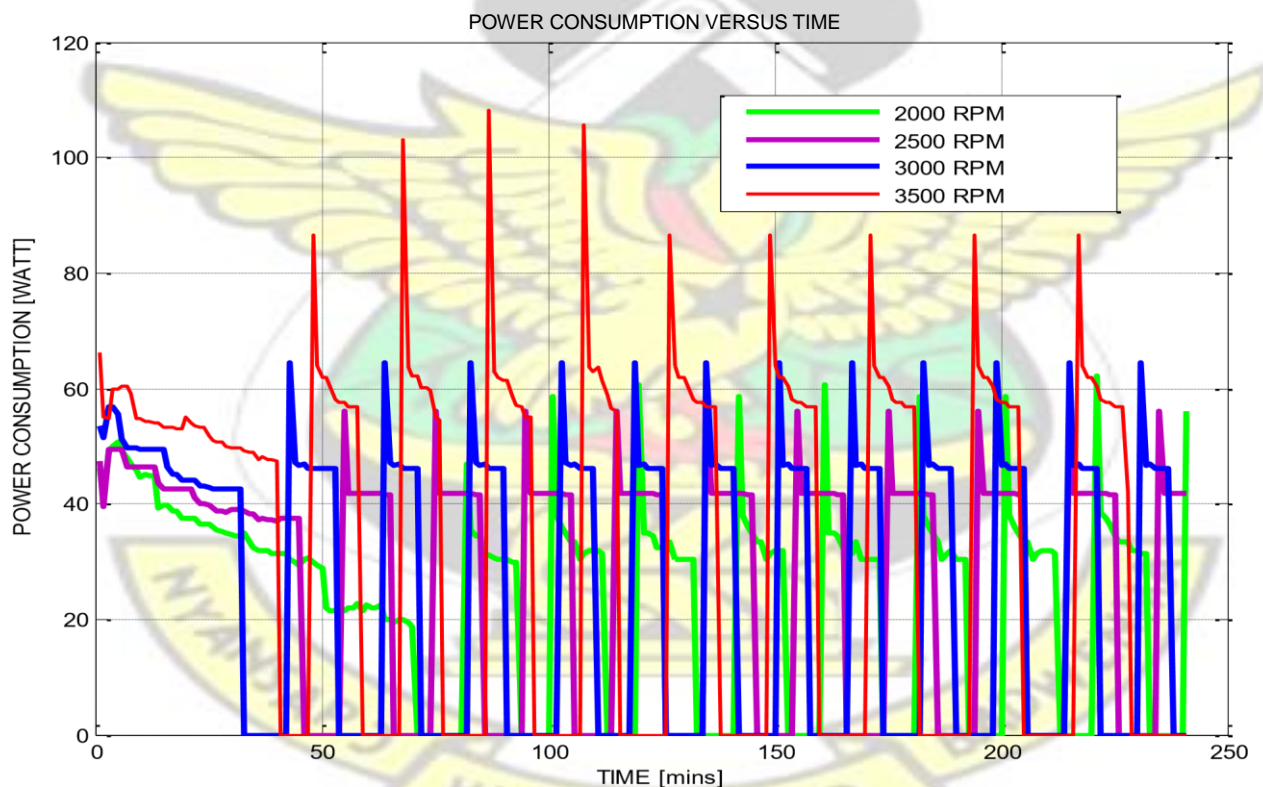
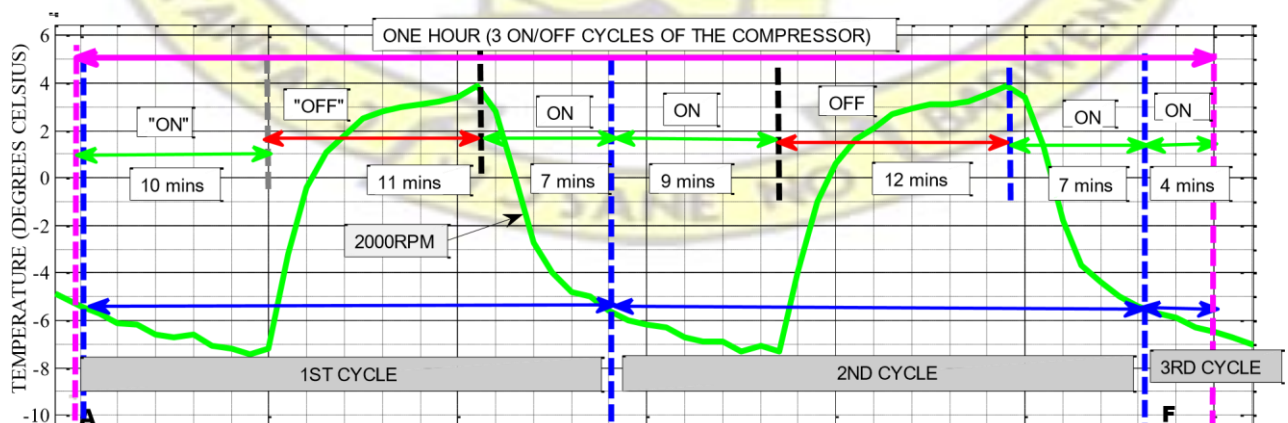


Figure 4.11: Power consumption of the solar powered DC refrigerator Operating at high temperature setting

Figure 4.11 confirms the already knowledge in literature that, decreasing the speed of the variable speed compressor decreases the corresponding power consumption of the refrigerator. The figure shows that the refrigerator draws the maximum rating/average power of 58 W when operated at the maximum speed of 3500 RPM. Similarly, operating the refrigerator at the lowest speed of 2000 RPM draws the minimum average power of 33 W. This phenomenon can be attributed to a reduction in mass flow rate, which translates into a reduction in compressor capacity. (Compressor speed and mass flow rate are related with equation 3.8 above). Therefore, to meet the cooling requirement of the refrigerator, the compressor was observed to be operating at higher run time than the other speeds (see Figure 4.10 above). The next section looks at the daily and annual energy consumption of the refrigerator operating at each of the speeds of the VSDC compressor.

4.2.5. Energy Analysis of the Solar Powered DC Refrigerator Operating at High Temperature Settings

This section presents an analysis of the annual energy consumption of the solar powered DC refrigerator operating at various speeds of the VSDC compressor. Annual energy consumption of a refrigerator was determined as a function of refrigerator power consumption and compressor's average run time per year. The run time per day of the VSDC compressor operating at the various speeds were determined by using their respective temperature profiles as illustrated in Figure 4.12 to Figure 4.15.



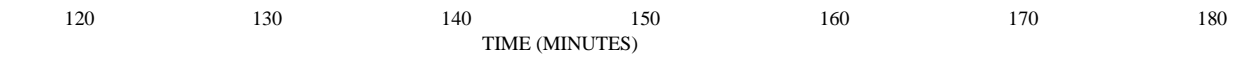


Figure 4.12: Compressor Run Time of the Solar Powered DC Refrigerator Operating at 2000 RPM

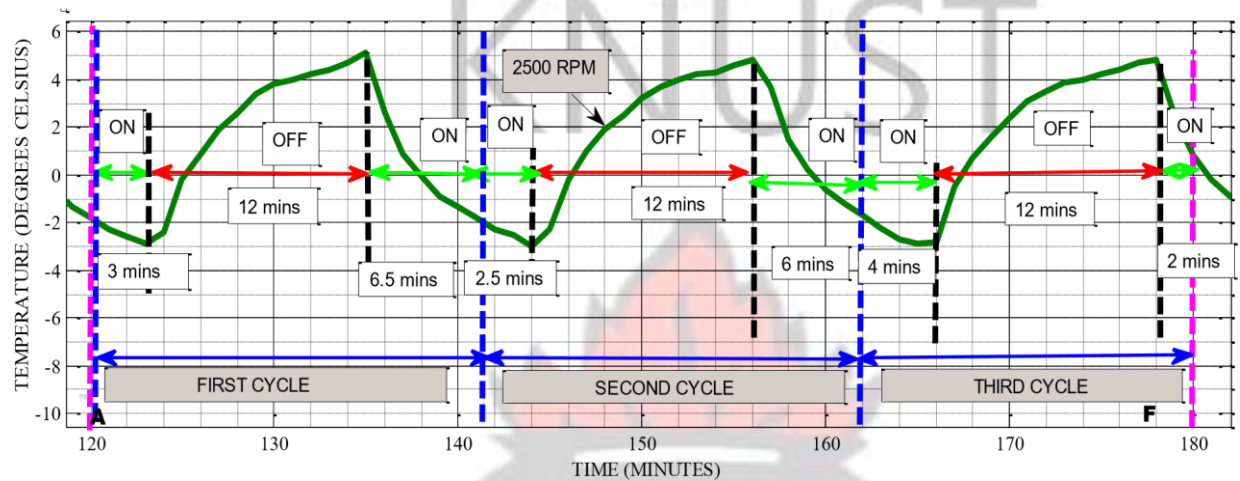


Figure 4.13 Compressor Run Time of the Solar Powered DC Refrigerator Operating at 2500RPM

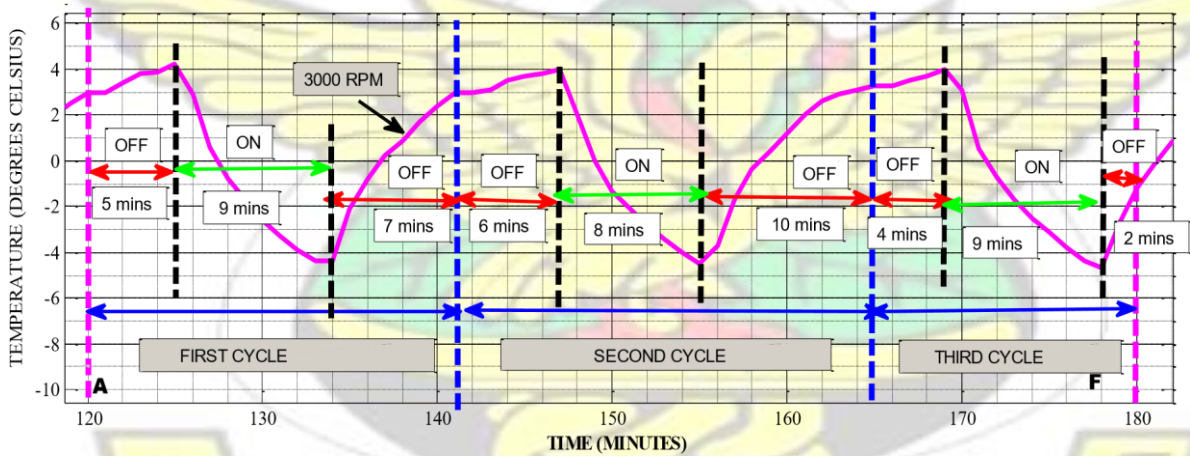


Figure 4.14 Compressor Run Time of the Solar Powered DC Refrigerator Operating at 3000RPM

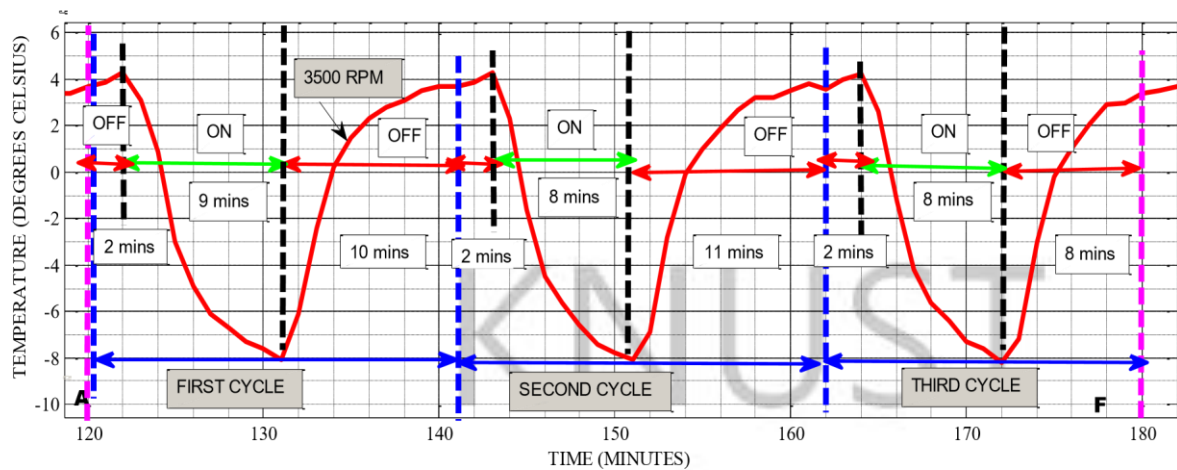


Figure 4.15 Compressor Run Time of the Solar Powered DC Refrigerator Operating at 3500RPM

From the above analysis, the average power consumption and the respective run time per day of the VSDC compressor operating at the various speeds were determined and presented in Figure 4.16 and Figure 4.17.

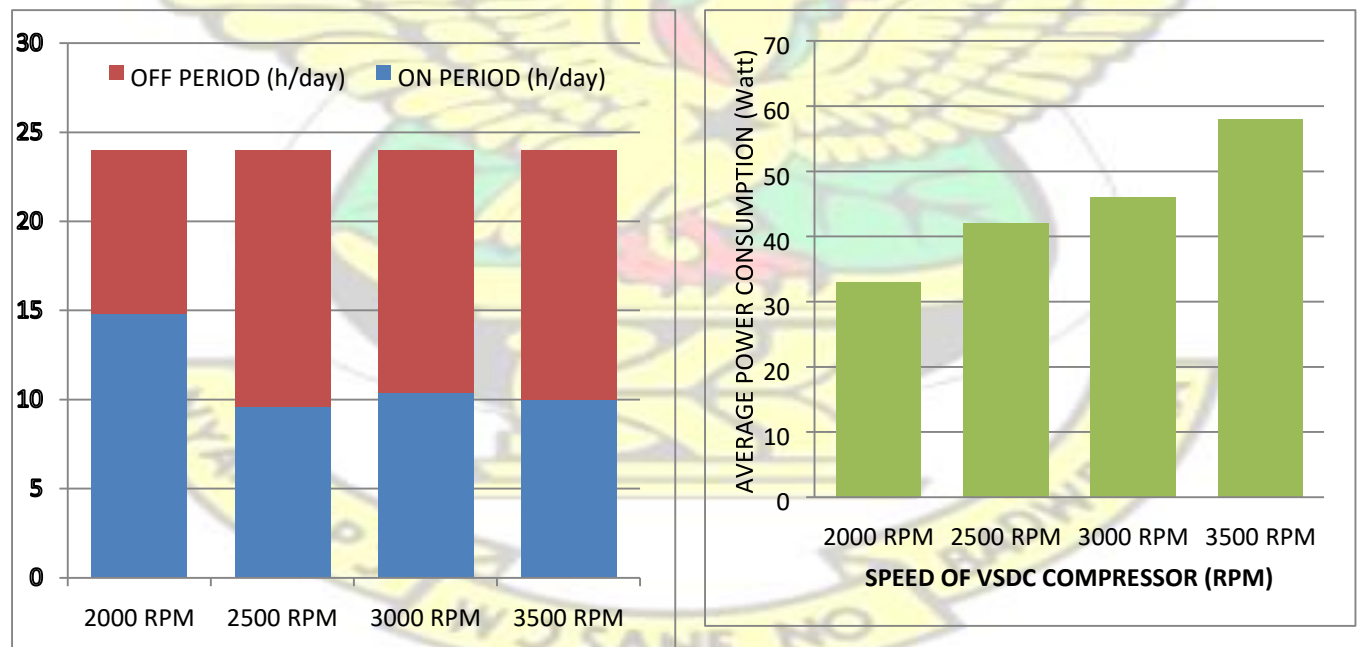


Figure 4.16: Compressor Run Time of the the Refrigerator Operating at Different Refrigerator Operating at Different Compressor

Figure 4.17: Average Power Consumption of Compressor Speeds Speeds

It can be determined from Figure 4.17 that operating the compressor at 2000 RPM instead of 3000 RPM has the potential of reducing the power consumption by 43%. However, the compressor was observed to make up for this low power consumption by operating with a higher compressor run time per day as illustrated in figure 4.16. It can be observed that the compressor run time increases from 10 hours a day to 14.8 hours a day when the refrigerator is operating at 2000 RPM instead of 3500 RPM. There is therefore the need to evaluate the daily energy consumption of the refrigerator, which is the product of refrigerator power consumption and the compressor run time per day. The daily and annual energy consumption of the solar powered DC refrigerator operating at the various speeds were therefore determined and present in figure 4.18 and figure 4.19. All calculations were based on 365 days in a year.

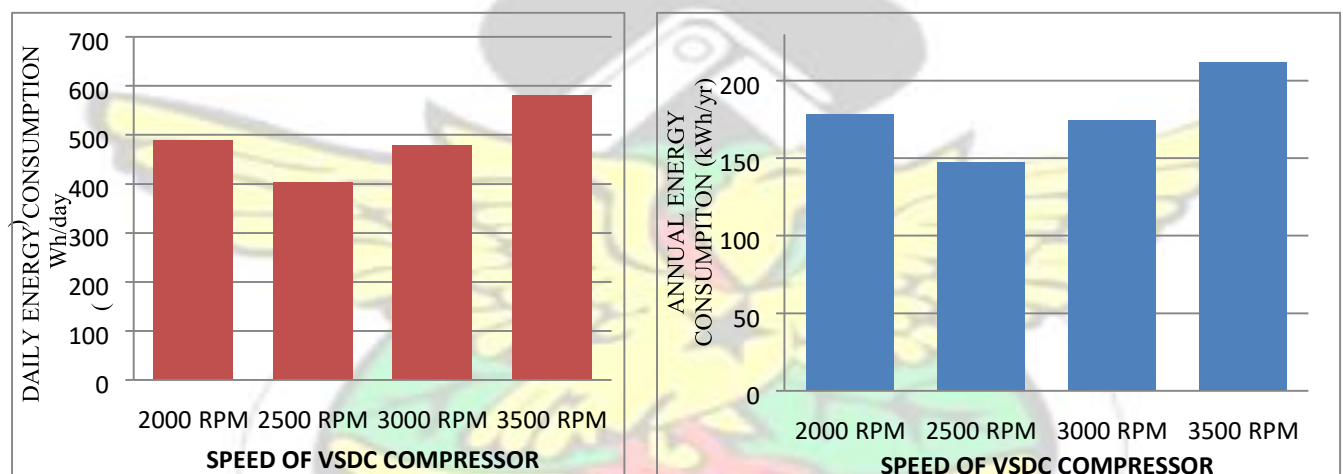


Figure 4.18 Daily Energy Consumption of Figure 4.19 Annual Energy Consumption of the the Solar Refrigerator Operating at Refrigerator Operating at Different Speeds Different Speeds

From Figure 4.18 and Figure 4.19 it can be seen that there is a significant energy reduction by operating the refrigerator at low compressor speeds at high thermostat settings (cut in and cut out temperatures of 5°C and -5°C). To examine the possible energy savings of operating the refrigerator at a lower speed other than the maximum speed, Figure 4.20 and Figure 4.21 were developed by using the performance of the refrigerator at maximum compressor speed as the base system.

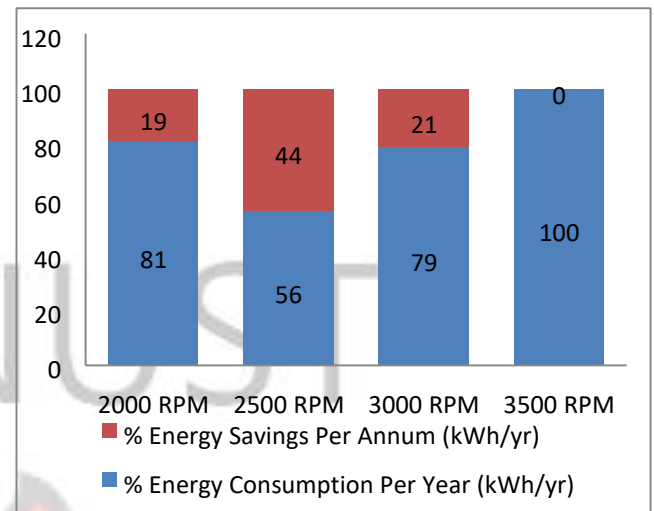
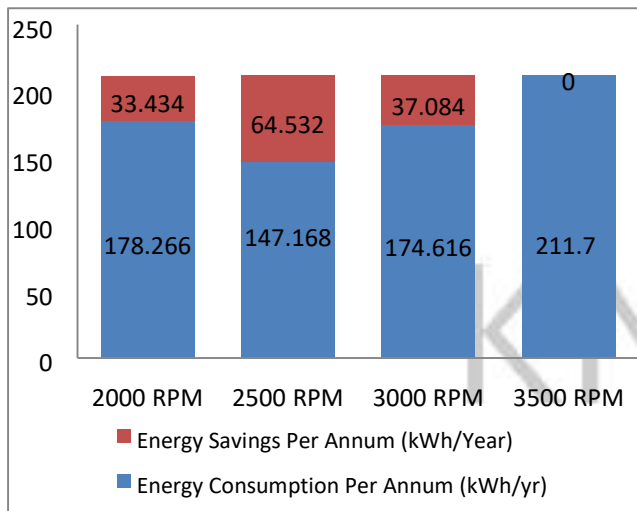


Figure 4.20 Energy Consumption and Energy Savings of the Refrigerator Operating at and Energy Savings of the DC Refrigerator Different Speeds Operating at Different Speeds

From the above analysis, it can be concluded that operating the refrigerator at 2000 RPM, 2500 RPM, 3000 RPM and 3500 RPM maintain average evaporator temperatures of -1.8°C , 0°C , 1.3°C and -2°C respectively. This results in an annual energy consumption of 178.3 kWh/year, 147 kWh/year, 175 kWh/year and 212 kWh/year respectively as shown in Figure 4.20.

Figure 4.21 on the other hand, shows the respective percentages energy consumption and energy savings by operating the refrigerator at lower compressor speeds instead of the maximum at part loading (high temperature settings). The entire analysis illustrates that by compromising on the insignificant evaporator temperature differences, the VSDC compressor can result in energy savings of 19 % to 44 % of the refrigerator's total energy consumption when operated at low speeds during part-loading or at high evaporator temperature settings.

4.2.6. Maximum Energy Consumption of the Solar Powered DC Refrigerator

The maximum energy consumption of the solar powered DC refrigerator is required for sizing the stand-alone solar PV refrigeration system. Power consumption and compressor run time of

the solar powered DC refrigerator operating at maximum speed of 3500 RPM were used for this analysis. Figure 4.22 shows the cabinet and evaporator temperature profiles of the solar powered DC refrigerator operating at the lowest evaporator temperature attained during the experimental study. This resulted in the average power consumption of 60 W.

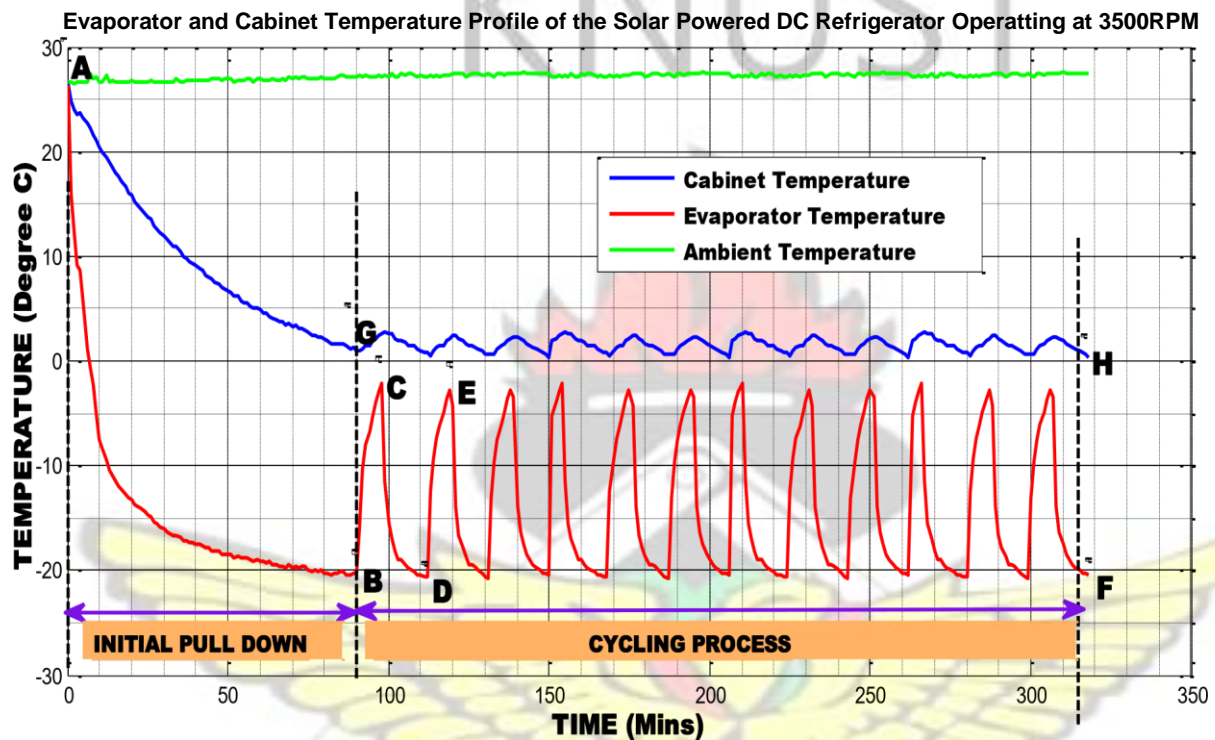


Figure 4.22: Temperature Profile of the Refrigerator Operating at 3500 RPM

To determine the daily energy consumption of the refrigerator, the maximum compressor run time per day of the refrigerator was determined from the ON/OFF cycle characteristic as illustrated in Figure 4.23.

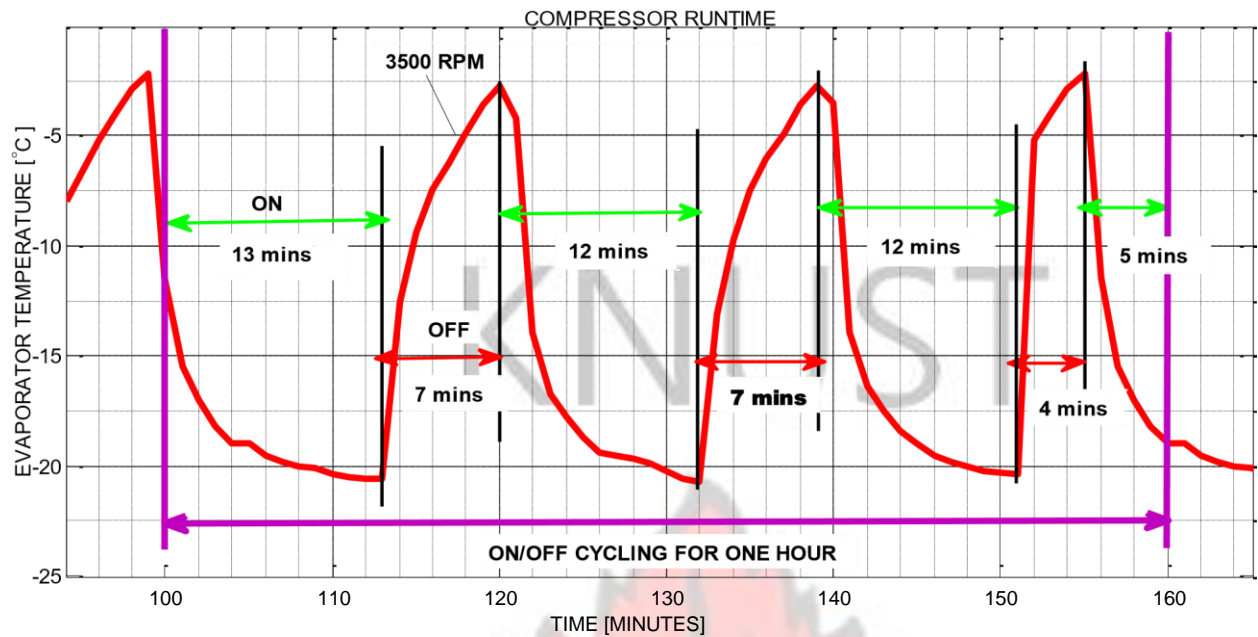


Figure 4.23: Compressor Run time of the refrigerator operating at 3500 RPM

From Figure 4.23 the run time of the compressor was determined to be 16 hours per day, therefore, with refrigerator power consumption of 60 W and an average compressor run time of 16 hours/day, the required sizes of the solar PV system were determined from Figure 3.7 and Figure 3.8 above and presented in Table 4.2.

Table 4.2: Sizes of the Solar Photovoltaic System

SOLAR PV COMPONENT	SIZE	REMARKS
Peak Wattage of Solar Panel	250 Wp	Maximum solar PV required using peak sun hours of 5.5
Battery Bank Capacity	100 AH	One Day of Autonomy with 80% DoD
Charge Controller	20	

4.3. PERFORMANCE COMPARISON OF THE SOLAR POWERED DC REFRIGERATOR AND A CONVENTIONAL AC REFRIGERATOR

This section presents the results of experiments conducted to study the performance characteristics of the solar powered DC refrigerator and an identical AC refrigerator. The performances of both refrigerators in terms of evaporator and cabinet temperature profile, refrigerator power consumption, coefficient of performance, and energy consumption have been studied. During these experiments the VSDC compressor was set to operate at the same

rotational speed as AC compressor (thus 3000 RPM). All experiments were conducted at the same thermostat settings and ambient conditions. Graphs indicating how the aforementioned performance indicators change with time for both refrigerators have been presented and discussed in the following sections.

4.3.1. Evaporator and Cabinet Temperature Characteristics of AC and Solar Powered DC Refrigerators

Evaporator and cabinet temperature profiles give an indication of how the refrigerator is cooling the refrigerator cabinet. Previously, air temperature distribution inside domestic refrigerators have been measured and analyzed worldwide as an indicator for performance of the refrigerator (Wong and James, 1988). In the current study, the evaporator and cabinet temperatures of both AC and solar powered DC refrigerators have been monitored over a period of four hours under the same experimental conditions. Figure 4.24 shows the cabinet and evaporator temperature profile of both refrigerators.

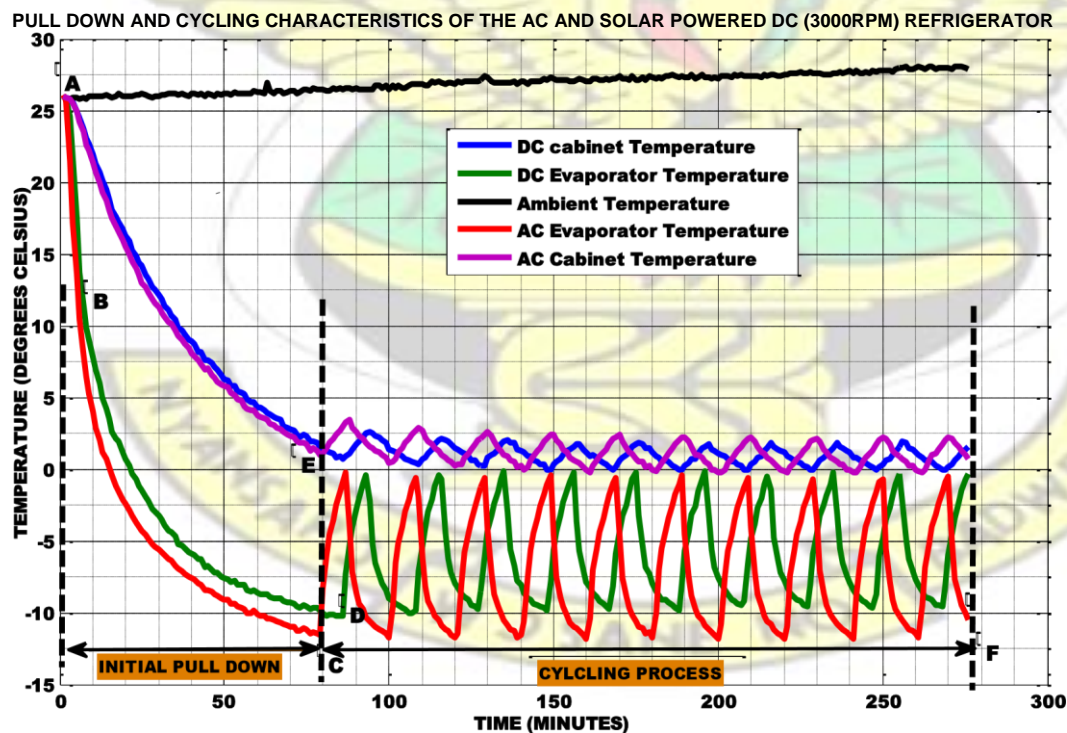


Figure 4.24: Pull Down and Cycling Characteristics of AC and Solar Powered DC Refrigerators (Both Operating at 3000 RPM)

From Figure 4.24 it is observed that evaporator temperatures of both refrigerators decreased from room temperature (26 °C) to a final temperature of about -12 °C for the AC refrigerator and -10 °C for the DC refrigerator (thus from point A to point C and D). As shown in the above figure, the AC and DC refrigerators completed pull down period within 80 and 84 minutes respectively. Both refrigerators then cycle ON and OFF for the rest of the test period. No significant temperature difference was observed between the AC and the solar powered DC refrigerator for the first 10 minutes of operation. However, the evaporator temperature of the AC refrigerator is observed to pull down 4 minutes faster than the DC refrigerator. It can also be observed that the AC refrigerator has about 2 °C lower cut out temperatures than the DC refrigerator. More importantly, both refrigerators were observed to maintain the same cabinet temperature profiles (thus; pull down and cycling characteristics) from beginning to the end of the experimental study. Both refrigerators maintained cabinet temperature of about 0 °C during the cycling process.

It can therefore be concluded that there is no significant difference in terms of evaporator and cabinet temperature characteristics when both refrigerators are operated at the same test conditions. The next section discusses the power consumption pattern of each refrigerator while maintaining the above temperature profile.

4.3.2. Power Consumption of AC and Solar Powered DC Refrigerators

Power consumptions of the AC refrigerator and the solar powered DC refrigerator have been studied for over four hours of continuous operation. Figure 4.25 shows the variation of instantaneous power consumption of both refrigerators versus time.

POWER CONSUMPTION OF AC AND DC REFRIGERATORS OPERATING AT 3000 RPM EACH

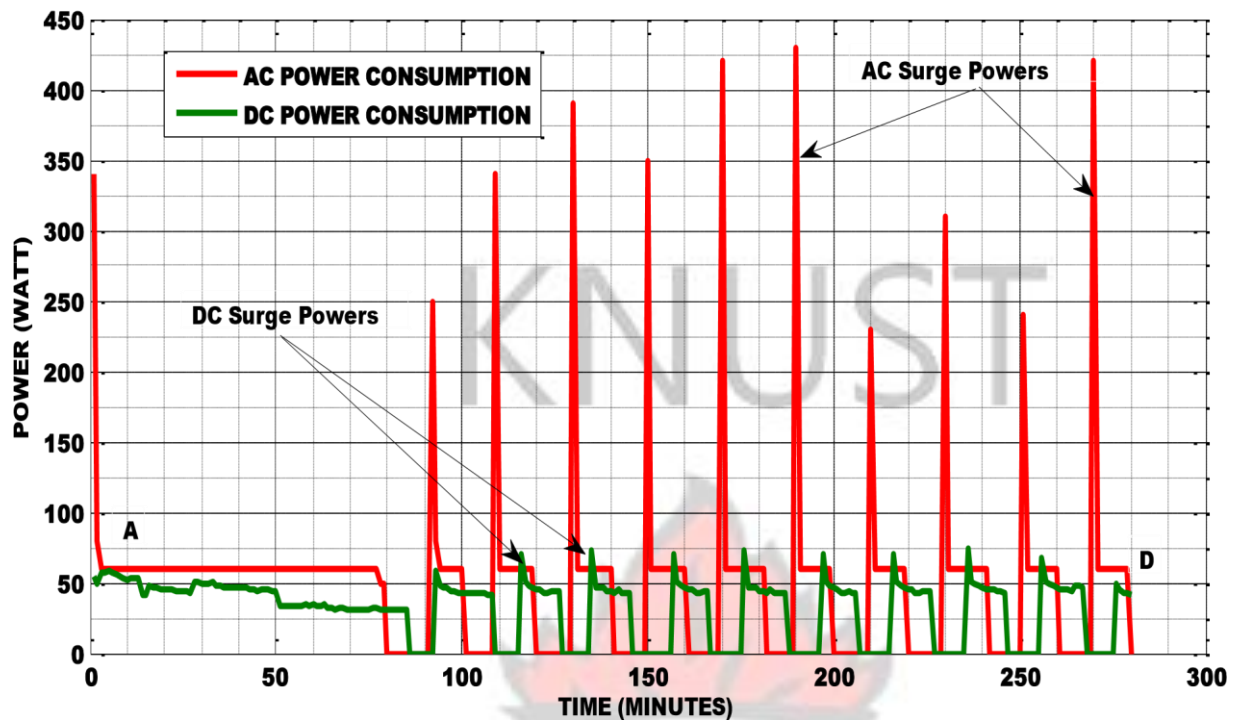


Figure 4.25: Comparing Power Consumption of the AC Refrigerator with the Solar Powered DC Refrigerator all Operating at 3000 RPM

From Figure 4.25 it is observed that the AC and solar powered DC refrigerators have running/rated powers of about 60 W and 48 W respectively. However, the AC refrigerator was found to operate with high surge powers in the magnitudes of 250 W to 425 W as compared to the relatively low surge powers of less than 75 W for the solar powered DC refrigerator. From Figure 4.25 it can be determined that the surge powers of the AC and DC refrigerators are about 7.1 and 1.5 times the rating power consumptions respectively. High surge powers as encountered by the AC refrigerator have two negative effects on the operation of the AC refrigeration system, especially when desired to power the refrigerator with a solar PV system via an inverter.

Firstly, high surge powers require higher capacity inverters to handle the required surge power of the AC compressor. High capacity power inverter means the high inverter cost and high energy conversion losses since both parameters are functions of the inverter capacity (wattage). This added up to the already high initial cost of the solar PV system makes this approach of providing refrigeration needs costly and unattractive.

Secondly, high surge powers imply higher battery bank capacity (Amp-Hour) requirement in order to accommodate the periodic high start-up powers of the AC compressor. Moreover, high surge power puts high stress on the battery bank/increase the cycles, thereby reducing the life span of the battery.

Contrary to the AC compressor, variable speed direct current compressors have high capacity start-up capacitors for smoothing up surge powers of the refrigerator. These compressors have been optimised for renewable energy and energy efficiency applications. During normal operation, the solar powered DC refrigerator was observed to be drawing an average current of 4 Amperes while operating on the 12 volt battery system. However, the current increased to about 6A during compressor start-up (surge current). The low running and surge powers make the DC refrigerator the best choice for stand-alone solar refrigeration as far as energy savings is concerned.

4.3.3. Energy Consumption of AC and Solar Powered DC Refrigerators

Energy consumption of a refrigerator is the product of refrigerator power consumption and the compressor run-time. For this study, the daily run time of each compressor was determined from the respective evaporator temperature characteristic graphs. Figure 4.26 and Figure 4.27 illustrate the ON and OFF periods of the compressors as extracted from Figure 4.24 above.

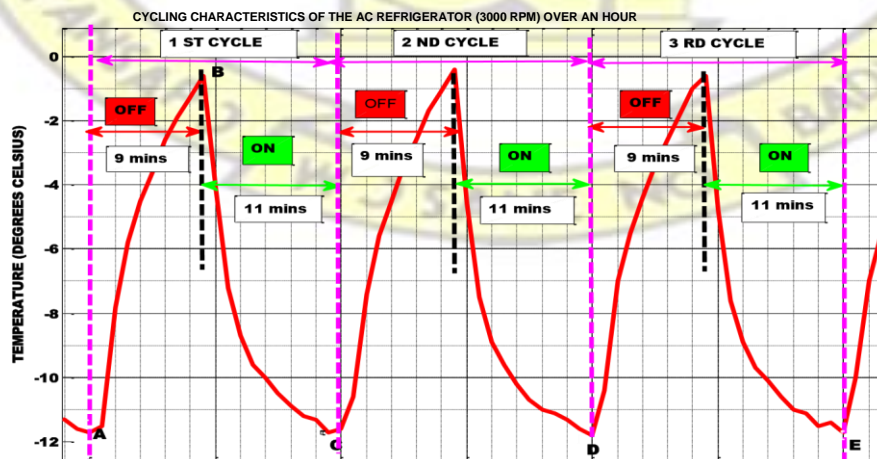


Figure 4.26: Compressor Run Time of AC Refrigerator

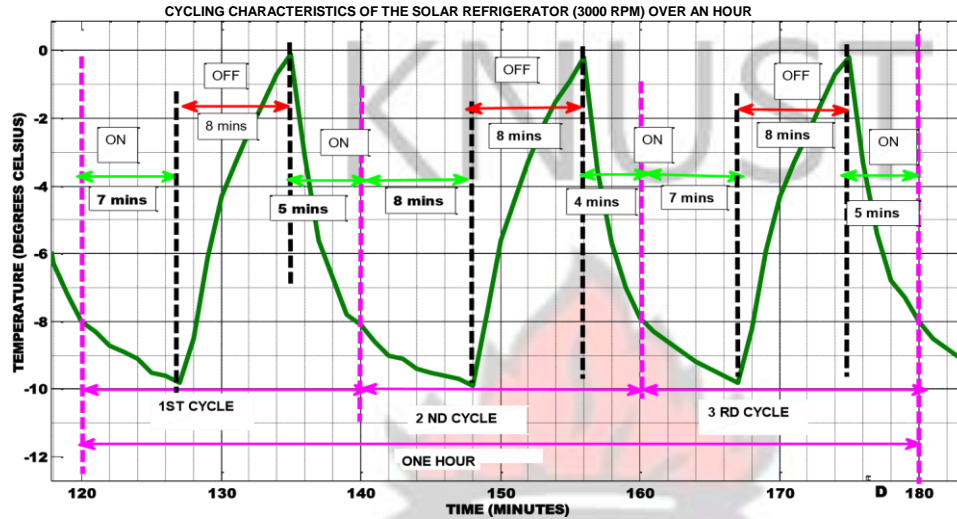


Figure 4.27 Compressor Run Time of the Solar Powered DC Refrigerator Operating at 3000 RPM

From Figure 4.26 and Figure 4.27, the daily run time of the AC and solar powered DC compressors were determined to be 13.2 and 14.4 hours/day respectively.

From the compressor run time and average power consumption, the daily, monthly and annual energy consumption of the three modes of powering refrigerators (as discussed in section 2.4.1) have been evaluated and presented in Table 4.3. The parameters were determined with equations Equation 3.17 to Equation 3.19 above.

In this analysis a third scenario has been considered, that is running a conventional AC refrigerator with a solar PV system via an inverter. The inverter considered was summed to be 90% efficient. Therefore, running the 60 W AC refrigerator with solar energy via the inverter would result in a power consumption of 66 W as used in Table 4.3.

Table 4.3: Energy Analysis of AC and Solar Powered Refrigerators

Parameter	Units	Conventional AC Refrigerator (Grid)	Solar AC Refrigerator via Inverter	Solar Powered DC Refrigerator Without an Inverter
Average power Consumption	[W]	60	66 [plus 10% inverter power]	48
Compressor Run Time Per-Day	[h/day]	13.2	13.2	14.4
Monthly Energy Consumption	[kWh/Month]	23.760	26.136	20.736
Annual Energy Consumption	[kWh/year]	285.12	313.63	248.83
Percentage increase in energy consumption as compared to the direct solar refrigeration	[%]	13	21	0

From Table 4.3, it is clear that converting a conventional AC refrigerator (which would have run on a solar PV system with an inverter) to a DC refrigerator powered by the solar PV system (without an inverter) has the potential of reducing the annual energy consumption by 21 %. Similarly, the analysis shows that converting a conventional AC refrigerator (which would have run on the national grid) to a stand-alone DC refrigerator (powered by the solar PV system without an inverter) has the potential of savings 13 % of the refrigerator's annual energy consumption.

4.3.4. Comparing the Coefficient of Performance of the Conventional and Solar Powered DC Refrigerator

Coefficient of performance is the single most important parameter that indicates how the actual performance of the entire refrigerator. In the current research work, the optimum COP of the solar powered DC refrigerator was determined to be 1.6 (W/W). According to (Baixue, 2009), the AC refrigerator has rated COP of 1.1 (W/W) at ASHRAE test conditions.

4.3.5. Economic Comparison of on AC Refrigerator and DC Refrigerator all Powered by Solar PV System

This section presents a comparative economic study of the AC refrigerator (with AC compressor) to the converted DC refrigerator (with DC compressor) all powered by a solar PV system. The AC refrigerator is powered with the solar PV system via an inverter whilst the DC refrigerator is powered directly from the solar PV system. Both systems have a 92 L internal volume.

The comparative study is based on the initial investment cost and the energy consumption of each refrigerator. Presented in Table 4.4 are the various variables used to determine the cost of each refrigerator. The experimentally determined power consumption and compressor run time for the DC and AC refrigerators were used for the computation. Based on the daily energy consumption, the required component sizes of the solar PV systems (solar panel and battery bank) were determined from Figure 4.28 and Figure 4.29.

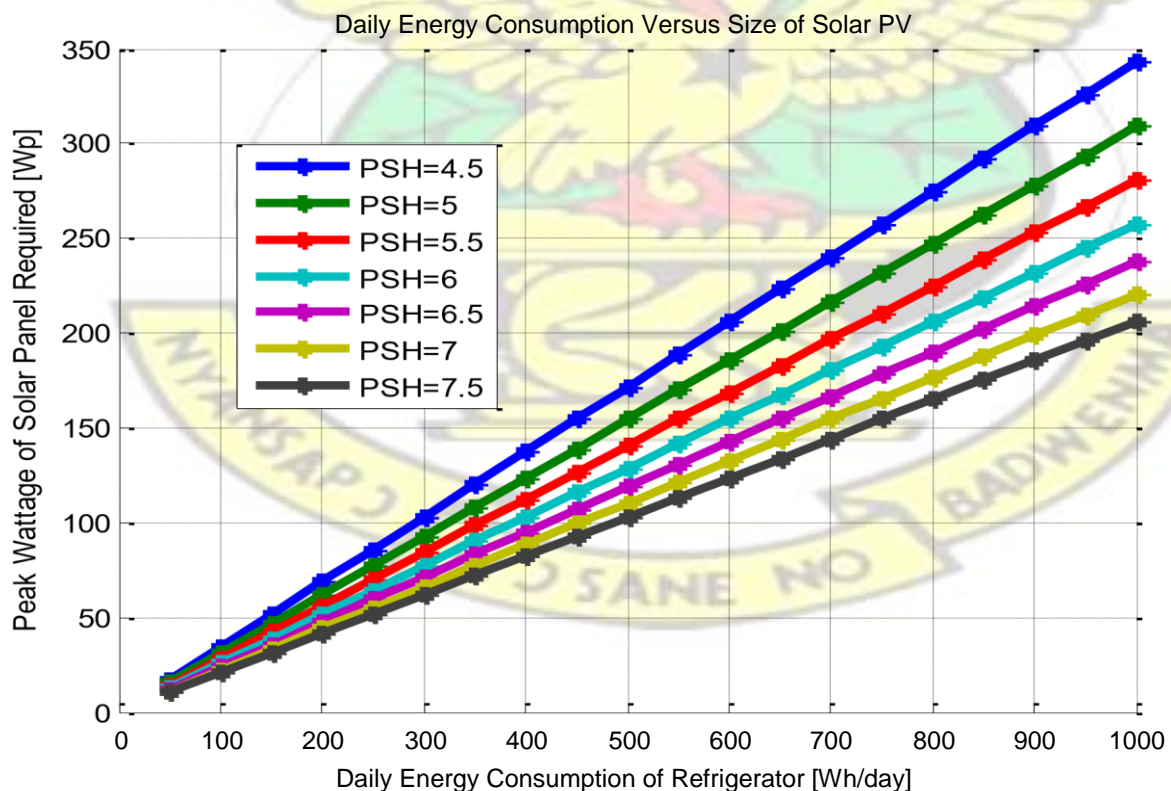


Figure 4.28: Daily Energy Requirement of the Refrigerator and Size of Solar Panel Required

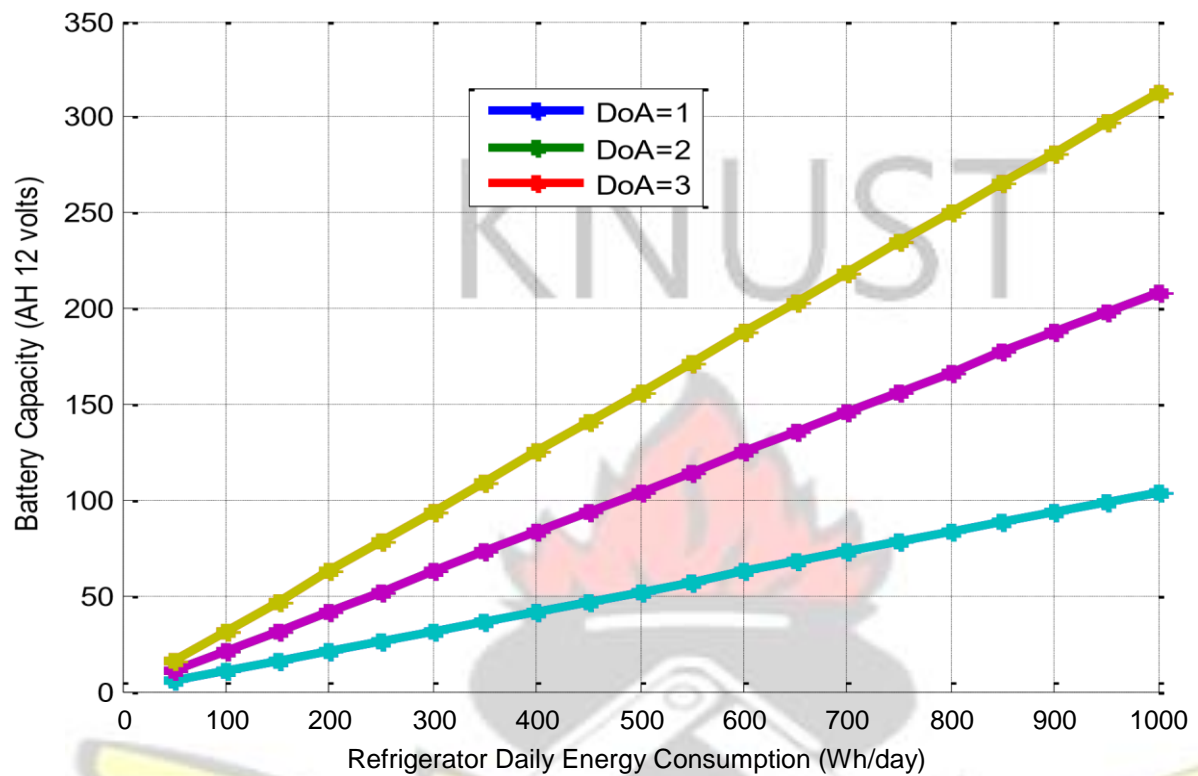


Figure 4.29: Daily Energy Requirement of Refrigerator versus Battery Capacity

Table 4.4: Economic Analysis of Direct Solar Refrigerator and Operating AC Refrigerator on Solar via an Inverter

ENERGY ANALYSIS	DC Refrigerator			AC Refrigerator			Remarks
Power Consumption	48 W			66 W			Both refrigerators operating at 3000 RPM
Compressor Run Time	14.4 h/day			13.2 h/day			
Daily Energy Consumption	691.2 Wh/day			871.2 Wh/day			
SOLAR PV SYSTEM	Calculated Size	Standard Size and Quantity	Cost	Calculated Size	Standard Size and Quantity	Cost	Unit cost
Sola PV	185 Wp	100 Wp X 2	1200	240 Wp	85 Wp X 3	1,530	6 GHS/Wp
Battery Bank	75 AH	100 AH X 1	900	90 AH	100 AH X 1	900	9 GHS/AH
Charge Controller	15.4 A	15 A X 1	75	21 A	25 A X 1	125	5 GHS/A
Cost of Refrigerator			N/A		420 W	978	2.33 GHS/Watt
Cost of Inverter			500			500	As at May, 2014
Cost of converting AC refrigerator to DC refrigerator			700			N/A	Cost of Compressor + ECU + others
Total Cost			3,375			4,033	

From Table 4.4 can be determined that running/operating the DC refrigerator has the potential of reducing the cost of the refrigeration system by 20 % compared to operating the AC refrigerator of the same size all running on solar PV system. Secondly, aside the 3000 RPM that has been

compared with the AC refrigerator, the variable speed compressor technology of the DC refrigerator offers the option of running the refrigerator at three other speeds as discussed in section 4.2 above.



CHAPTER 5 CONCLUSIONS AND RECOMMENDATIONS

A reliable and energy efficient approach of meeting refrigeration needs (both grid-connected and off-grid areas) is a major challenge for Ghana and most developing nations due to low energy access rate and unreliable power supply. Therefore, efficient and reliable technologies of providing refrigeration needs are very necessary.

In the current work, a 92 L stand-alone solar powered DC refrigerator operating with a variable speed direct current (VSDC) compressor has been developed as per the overall goal of this thesis. The DC refrigerator runs on an installed 170 Wp solar PV panel with a 100 AH battery bank without an inverter. By using the pull down time and coefficient of performance as the indicating factors, the refrigerator has been experimentally optimised with the correct quantity of refrigerant charge (30 g). A minimum evaporator temperature of $-20\text{ }^{\circ}\text{C}$ was achieved by the developed refrigerator (operating at 3500 RPM) within a pull down time of 70 minutes while consuming an average power of 60 W within an ambient temperature of $26 \pm 2.0\text{ }^{\circ}\text{C}$.

The effects of operating the refrigerator at the various speeds of the VSDC compressor (2000 RPM, 2500 RPM, 3000 RPM, and 3500 RPM) have been evaluated. The performance of the solar powered DC refrigerator has been experimentally compared with an identical domestic AC refrigerator operating on the national grid under the same test conditions. The findings and conclusions of the research work can be summarised as follows:

1. The research has developed the methodology of converting domestic refrigerator to serve as a solar powered DC refrigerator. This approach can be used to convert similar refrigerators for direct connection to renewable energy sources (such as solar) without an inverter.
2. To identify the optimum refrigerant required by the DC solar refrigerator, experiments were conducted at seven different quantities of refrigerant charges (18 g, 20 g, 25 g,

30 g, 35 g, 40g and 45 g). The design temperature and pull-down time set by International Standard Organisation (ISO) for small refrigerator were achieved with 20 g, 25 g, 30 g, 35 g, 40g and 45 g refrigerant charges, but they were early achieved with 30 g, 35 g, 40g and 45 g with a very close time interval. It was actually observed that increasing the refrigerant charge beyond 30 g did not have any significant change on the pull down time. On the other hand, the system was not able to achieve the minimum pull down temperature of -12°C when charged with 18 g after 90 minutes of continuous running. Only a minimum temperature of about -7°C was achieved. Secondly, the COP of the refrigerator increased from a minimum value of 1.3 W/W to a peak valued of 1.61 W/W when the refrigerant charge was varied from 18 g to 30 g. The COP remained virtually constant at 1.6 while the amount of refrigerant charge was increased from 30 g, 35 g to 40 g. A slight decrease in COP from the peak value of 1.6 to 1.58 was noticed as the amount of refrigerant charge is increased further to 45 g (possibly as a result of flooding of the evaporator).

The overall results revealed that the optimum performance of the refrigerator can be obtained with refrigerant charges of 30 g to 40 g. From these experimental results it is therefore worth concluding that the optimum charge of refrigerant required by the 92 L domestic refrigerator is about 30 g of refrigerant R134a

3. The performance of the solar powered DC refrigerator has been evaluated at various speeds of the VSDC compressor. The results show that operating the refrigerator at 2000 RPM, 2500 RPM, 3000 RPM and 3500 RPM maintains average evaporator temperatures of -6.5°C , -2.5°C , -4°C and -7°C while consuming average powers of 33 W, 42 W, 48 W and 60 W respectively. Compressor run times of 14.8 hours/day, 9.6 hours/day, 10.4 hours/day and 10 hours/day were noted for the refrigerator

operating at 2000 RPM, 2500 RPM, 3000 RPM and 3500 RPM respectively. This resulted in an annual energy consumption of 178.3 kWh/year, 147 kWh/year, 175 kWh/year and 212 kWh/year respectively. The experimental results and the energy analysis conducted revealed that by compromising on the insignificant evaporator temperature differences mentioned above, the refrigerator has the potential for saving about 19 % to 44 % of the refrigerator's total energy consumption when operated at low speeds during part loading or at high evaporator temperature settings ("cut-out" temperatures of -5°C).

On the other hand, the experimental results revealed that operating the refrigerator at compressor speeds of 2000 RPM and 2500 RPM with low thermostat setting ("cut-out" temperature settings of -20°C) results in a fairly constant temperature inside the refrigerator cabinet. Operating the refrigerator at 2000 RPM and 2500 RPM maintain constant temperatures of -7°C and -12°C respectively for the entire test period of four hours while consuming an average power of 33 W and 42 W continuously. This indicates that operating the refrigerator at either 2000 RPM or 2500 RPM during low temperature settings ("cut-out" temperature of -20°C) is ideal for freezing purpose; otherwise there will always be the need for manual defrosting of the refrigerator and higher daily energy consumption as compared to operating the refrigerator at 3000 RPM and 3500 RPM.

4. Experiments were conducted to compare the performance of the developed standalone solar powered DC refrigerator with a conventional/domestic AC refrigerator powered by the national grid. Performances of both refrigerators were measured in terms of evaporator temperature profile and refrigerator power consumption under the same test

conditions. Experimental results show that the AC refrigerator consumes average power of 60 W while maintain average cabinet and evaporator temperatures of 1 °C and -6 °C respectively. On the other hand, the DC refrigerator consumes 48 W power while maintaining average evaporator and cabinet temperatures of 1 °C and -5 °C respectively. Apart from the high power consumptions of the AC refrigerator, it has been identified that conventional refrigerators operating with an AC compressor produces higher surge powers in the magnitudes of about 250 W to 420 W representing 4 to 7.1 times their rated power as against the relatively low surge powers of about 1.5 times the rated power of the DC refrigerator.

5. An economic analysis was conducted to compare the cost of operating the direct solar refrigerator against running an AC refrigerator via an inverter. The results revealed that converting the AC refrigerator to DC has the potential of reducing the total cost of investment (refrigerator and solar, battery bank, charge controller, inverter, solar panel, etc.) by 20 %.

Based on the experiments conducted and the results obtained in the present work, the following recommendations are suggested:

1. For off-grid refrigeration purposes using solar PV systems as the energy source, it is more economical to convert the AC refrigerator to DC by following the methodology developed in this study instead of running the AC refrigerator on solar PV via an inverter.
2. Operating the solar powered DC refrigerator at either 2000 RPM or 2500 RPM during low temperature settings (“cut-out” temperature of -20 °C) is ideal for freezing purpose else there will always be the need for manual defrosting.

3. Further studies should be conducted on the developed solar refrigerator by using an Adaptive Energy Optimizing type of electronic control unit (example 101N0300 from Danfoss). This type of electronic control unit is capable of automatically adjusting the speed of the compressor to the required temperature in the refrigerator. This ensures that the right speed of the VSDC compressor is selected at the right time.
4. Future works on the developed refrigerator should be limited to refrigerant charges less than 80 g. During the experimental study it was realized that the compressor trips when charged beyond 80 g of refrigerant R134a (thus low side pressures greater than 1.2 bar).

REFERENCES

- Abhishek, S., & Karale, S. R. (2013). A review on Solar Powered Refrigeration and the Various Cooling Thermal Energy Storage (CTES) Systems. *International Journal of Engineering Research & Technology (IJERT)* Vol. 2 Issue 2, FebruaryVol. 2 Issue 2, February- 2013, 2278-0181 1.
- AHAM HRF-1, (2004). Energy Performance and Capacity of Household Refrigerators, Refrigerator-freezers and Freezers, *American National Standards Institute*, Washington - DC, USA,
- Ahiataku-Togobo, W. (2014). Development of Solar Energy In Ghana: Update and Progress. Kumasi: Ministry of Energy and Petroleum.
- AS/NZS 4474.1, (2007). Performance of Household Electrical Appliances - Refrigerating Appliances. Part 1: Energy Consumption and Performance. Part 2: Energy Labelling

and Minimum Energy Performance Standard Requirements, *Standards Association of New Zealand*, Wellington, New Zealand.

Aktacir, M. A. (2011). Experimental study of a multi-purpose PV-refrigerator system.

International Journal of Physical Sciences, 6(4), 746-757.

Akuffo, F. O., Edwin, I., Forson, F. K., Agbeko, K., Sunnu, A., & Brew-Hammond, A.

(2004). Solar Energy Resource Assessment for Ghana. *Journal of the Ghana Institution of Engineers* Vol. 2 (1) pp. 31-34.

Alanne, K., & Saari, A. (2006). Distributed energy generation and sustainable development.

Renew Sustain Energy Rev, 10(6), 539-58.

Apra, C., Mastrullo, R., & Renno, C. (2006). Experimental analysis of the scroll compressor performances varying its speed. *Applied Thermal. Engineering*(26), 983-992.

Apra, C., Mastrullo, R., & Renno, C. (2009). Determination of the compressor optimal working conditions. *Applied. Thermal. Engineering*(29), 199-1997.

Bacon, P. E. (1997). *Solar Powered Refrigerator for Developing Countries* . UK.

Baixue. (2009). *Compressor Catalogue* . Retrieved September 9, 2014, from Baixue R600a compressors : <http://wenku.baidu.com/view/e77606f9aef8941ea76e0575.html>

Bessler, & W. Hwang, F. B. (1980). Solar assisted heat pumps for residential use. . *ASHRAE Journal*, 59, 63.

Bilgili, M. (2011). Hourly simulation and performance of solar electric-vapor compression refrigeration system. *Solar Energy* 85, 2720–2731.

Binneberg, P., Kraus, E., & and Quack, H. (2002). Reduction In Power Consumption Of

Household Refrigerators By Using Variable Speed Compressors. *International Refrigeration and Air Conditioning Conference, Paper 615.*

- Bolaji, B., Akintaro, A., Alamu, O., & Olayanju, T. (2012). Design and Performance Evaluation of a Cooler Refrigerating System Working with Ozone Friendly Refrigerant. 6(25-32).
- Bjork Erik and Bjorn Palm, (2006), Refrigerant mass charge distribution in a domestic refrigerator, Part I: Transient conditions. *Applied Thermal Engineering* 26 829–837
- Brew-Hammond, A., Edjekumhene, I., & Amadu, M. B. (2001). Preserving and enhancing public benefits under power sector reform: the case of Ghana. *Energy for Sustainable Development* , Kumasi Institute of Technology and Environment (KITE), P.O. Box 6534, Kumasi, Ghana, V(2 1).
- Btek Renewable Energy. (2000). *sizing battery bank*. Retrieved 7 12, 2014, from <http://www.btekenergy.com/documents/215.html>
- Cengel, A. Y., & Boles, M. A. (2006). *Thermodynamics: An Engineering Approach* (5th ed.). McGraw-Hill.
- Chatuverdi, S., & Abazeri, M. (1987). Transient simulation of a capacity modulated, directexpansion solar-assisted heat pump. *Solar Energy* (39), 1421–1428.
- Concorde, B. C. (2006). Retrieved 8 20, 2014, from www.concordebattery.com/otherpdf/sunextenderbatterysizingtips.pdf
- Dadzie, F. Y. (2008). *Design of a grid connected photovoltaic system for KNUST and economic and environmental analysis of the designed system*. Mphil Thesi, KNUST, Kumasi, Ghana.
- Danfoss. (2007). *Danfoss VSDC Compressors*. Retrieved January 24, 2014, from Danfoss Compressors: Available at <http://www.danfoss.com/BusinessAreas/RefrigerationAndAirConditioning>

Danfoss, V. (2003). *VTZ variable-speed compressors*. Retrieved August 20, 2014, from www.danfoss.com/NR/rdonlyres/B52465AC.../0/CC071GB0903.pdf

Datta, S. P., Das, P. K., & Mukhopadhyay, S. (2014). Effect of Refrigerant Charge, Compressor Speed and Air Flow Through the Evaporator on the Performance of an Automotive Air Conditioning System. *International Refrigeration and Air Conditioning Conference. Paper 1470*. Kharagpur, India.

Dmitriyev, V., & Pisarenko, V. (1984). Determination of optimum refrigerant charge for domestic refrigerator units. *Int J. Refrigeration*, 7(3), 178–180.

Ekren, O., Serdar, C., Brad, N., & Ryan, K. (2013). Performance evaluation of a variable speed DC compressor. *International journal of refrigeration*, 36, 745-757.

Ekren, O., Yilanci, A., Cetin, E., & Ozturk, H. K. (2011). Experimental Performance Evaluation of a PV-Powered Refrigeration System. *Electronics And Electrical Engineering*(8), 114.

Embraco, S., Development, C. R., G, M., Schwarz, & Leader, V. G. (2001). *Variable Capacity Compressors, a new dimension for refrigeration engineers to explore*.

Energy Commission. (2012). *Sustainable Energy For All Action Plan*. Accra: Energy Commission.

Essandoh-Yeddu, J. (1994). *Performance study of solar photovoltaic refrigerator systems in Ghana*. Accra, Ghana: Ministry of Energy and Mines.

Farzard, M., & O'Neal, D. (1994). The effect of improper refrigerant charging on the performance of a residential heat pump with fixed expansion devices (capillary tube and short tube orifice). *The 29th Intersociety Energy-Conversion Engineering Conference, Part 2*. California.

- Grace, I. N., Data, D., & Tassou, S. A. (2005). Sensitivity of refrigeration system performance to charge levels and parameters for on-line leak detection. *Applied Thermal Engineering* 25, 557–566.
- Houcek, J., & Thedford, M. (1984). research into a new method of refrigeration charging and the effects of improper charging. *Proceedings of the First Annual Symposium on Efficient Utilization of Energy in Residential and Commercial Buildings*. Texas A&M University, TX.
- ISO. (1991). (International Standard Organisation) Household Refrigerating Applications (Refrigerators/Freezers) Characteristics and Test Methods,.
- JIS C 9801, (2006) Japanese Industrial Standard, Household Electric Refrigerators, Refrigerators-freezers and Freezers, *Japanese Standards Association*, Tokio, Japan,
- Kaplanis, S., & Papanastasiou, N. (2006). The study and performance of a modified conventional refrigerator to serve as a PV powered one. *Renewable Energy* (31), 771– 780.
- Kim, D., & Ferreira, I. (2008). Solar refrigeration options—a state-of-the-art. *International journal of refrigeration*, 3-15, 31.
- Kim, J. W., & Lee, J. (2000). Performance Prediction for the Design of a Variable Speed Compressor. *International Compressor Engineering Conference*, 1362.
- Klein, S., & Alvarado, F. (2001). EES - Engineering Equation Solver, Version 6.264. F-Chart Software www.fchart.com.
- Kuang, Y., Sumathy, K., & Wang, R. (2003). Study on a direct expansion solar-assisted heat pump water heating system. *International of Energy Research* 27, 531–548.

Kuijpers, L., Janssen, M., & Verboven, P. (1988). The influence of the refrigerant charge on the functioning of small refrigerating appliances,. *94*, 813–828.

McCarney, S., Joanie, R., Juliette, A., Kristina, L., & John, L. (2013). Using solar-powered refrigeration for vaccine storage where other sources of reliable electricity are inadequate or costly. *Vaccine*(31), 6050– 6057.

McCormick, B. (1986). *Homebrew Low Voltage DC Refrigeration*. Retrieved August 21, 2014, from Alternative Energy: <http://www.ibiblio.org/london/alternativeenergy/homepower-magazine/archives/16/16pg48.txt>

Miller, V. B., Ramde, E. W., Jr, R. T., & Schaefer, L. A. (2011). Hydrokinetic power for energy access in rural Ghana. *Renewable Energy* (36), 671-675.

Ministry of Energy. (2010). *Medium-Term National Development Policy Framework: Ghana Shared Growth and Development Agenda (Gsgda), 2010-2013, Volume I*. Accra: Ministry of Energy.

Modi, A., Anirban, C., Bhavesh, V., & Jyotirmay, M. (2009). Performance analysis of a solar photovoltaic operated domestic refrigerator. *Applied Energy* 86 , 2583–2591.

MoME. (1998). *Solar Map of Ghana*. Accra: Ministry of Mines and Energy, Ghana.

NABCEP. (2009, APRIL). *Study Guide For Photovoltaic System Installers*. Retrieved 09 2, 2014, From North American Board Of Certified Energy Practitioners: Available at <Http://Www.Nabcep.Org/>

- Nyarko-Kumi, E. (2012, November). Technical and Economic Analysis of a 1MW Gridconnected Solar Photovoltaic Power System at KNUST- Kumasi. Kumasi, Ghana/ West Africa.
- Obeng, G. Y., & Hans-Dieter, E. (2009). *Solar PV rural electrification and energy-poverty: A review and conceptual*. Technology Consultancy Centre Kwame Nkrumah Univ. of Science & Technology Kumasi, Center for Development Research (ZEF), University of Bonn.
- Otanicar, T., Robert, A. T., & Phelan, P. E. (2012). Prospects for solar cooling – An economic and environmental assessment. *Solar Energy*(86), 1287–1299.
- Philipp, J., Kraus, E., & Meyer, A. (1996). Presentation of a Test Rig To Record Mass Flow Rate, Pressures and Temperatures of a Household Refrigerator During On/Off Cycling Mode. *Proc. of the 1996 International Refrigeration Conference at Purdue. West Lafayette, Indiana: IIR*, pp. 477 – 482.
- Polar Power. (N/A). *Polar Power*,. Retrieved 9 1, 2014, from <http://www.polarpowerinc.com/info/operation20/operation23.htm>
- Qureshi, T. Q., & Tassou, S. A. (1995). REVIEW PAPER: Variable-Speed Capacity Control In Refrigeration Systems. *Applied Thermal Engineering*, Vol. 16, No. 2, pp. 103-113,.
- Saidur, R., Rahim, N., & Hasanuzzaman, M. (2009). A review on compressed-air energy use and energy savings. *Renewable and Sustainable Energy Reviews*(14), 1135–53.
- Sarbu, I., & Sebarchievici, C. (2013). Review Review of solar refrigeration and cooling systems. *Energy and Buildings* 67, 286–297.
- Shankar, R. R., Nawaz, I., & Ankur, K. (2012). Energy Efficient Solar Refrigeration System. *VSRD International Journal of Mechanical, Auto. & Prod. Engg*, 2(1), 1-8.

Sheldrake, T. (1991). Introducing variable speed drives. *Building Services*, 25-32.

Solar Choice. (2000). Retrieved 6 13, 2014, from <http://www.solarchoice.net.au/blog/queensland-solar-panels-compare-solar-systemprices/>

Solar Energy International. (2004). *Photovoltaics: Design and Installation Manual*. Canada: New Society Publishers.

Srichai, P. R., & Bullard, C. W. (1997, July). Two-Speed Compressor Operation in a Refrigerator/Freezer. *Air Conditioning and Refrigeration Center Technical Report121*.

Suberu, M. Y., Mustafa, M. W., & Bashir, N. (2013). Power sector renewable energy integration for expanding access to electricity in sub-Saharan Africa. *Renewable and Sustainable Energy Reviews*(25), 630–642.

Suntech. (2007, April). Retrieved 04 14, 2014, from www.fibat.ro/energie_neconv/panouri_ibc_solar/6.pdf

SWERA, S. a. (2003). Solar and Wind Energy Resource Assessment, Ghana

Thomachan, A., & Kattakayam, S. K. (2000). Thermal performance characterization of a photovoltaic driven domestic refrigerator. *International Journal of Refrigeration* (23), 190-196.

WHO. (1988). World Health Organization. Standard equipment specifications and test procedures expanded programme on immunization. *EPI Technical Series No. 5*.

Wong, A. K., & James, R. W. (1988). Capacity control of a refrigeration system using a variable-speed compressor. 63-8(9).

Yesilata, B., & Isiker, Y. (2006). Experimental analyses of a refrigerator system worked by

Photovoltaic power. *J. Eng. Mach.*(558), 54-60.

Yusof, T. M., & Yusoff, A. R. (2011, 7). *Analisis For Optimum Refrigerant Charge Of A Mini Bar Refrigerator Using Experimental Method*. Retrieved 02 20, 2015, from http://www.researchgate.net/publication/232066870_Analisis_For_Optimum_Refrigerant_Charge_Of_A_Mini_Bar_Refrigerator_Using_Experimental_Method

